

**ELECTRODEPOSITION OF TIN AND TIN
CHALCOGENIDES FROM TIN (II) METHANESULFONATE
SOLUTION**

KOAY HUN LEE

**THESIS SUBMITTED IN FULFILLMENT OF THE
REQUIREMENTS FOR THE DEGREE OF
DOCTOR OF PHILOSOPHY**

**DEPARTMENT OF CHEMISTRY
FACULTY OF SCIENCE
UNIVERSITY OF MALAYA
KUALA LUMPUR**

2014

UNIVERSITI MALAYA

ORIGINAL LITERARY WORK DECLARATION

Name of Candidate: **KOAY HUN LEE** I/C/Passport No: **760923-71-5277**
Registration/Matric No.: **SHC060036**
Name of Degree: **DOCTOR OF PHILOSOPHY**

Title of Project Paper/Research Report/Dissertation/Thesis ("this Work"):

"ELECTRODEPOSITION OF TIN AND TIN CHALCOGENIDES FROM TIN (II) METHANESULFONATE SOLUTION"

Field of Study: **ELECTROCHEMISTRY AND MATERIAL SCIENCE**

I do solemnly and sincerely declare that:

- (1) I am the sole author/writer of this Work,
- (2) This Work is original,
- (3) Any use of any work in which copyright exists was done by way of fair dealing and for permitted purposes and any excerpt or extract from, or reference to or reproduction of any copyright work has been disclosed expressly and sufficiently and the title of the Work and its authorship have been acknowledged in this Work,
- (4) I do not have any actual knowledge nor do I ought reasonably to know that the making of this work constitutes an infringement of any copyright work,
- (5) I hereby assign all and every rights in the copyright to this Work to the University of Malaya ("UM"), who henceforth shall be owner of the copyright in this Work and that any reproduction or use in any form or by any means whatsoever is prohibited without the written consent of UM having been first had and obtained,
- (6) I am fully aware that if in the course of making this Work I have infringed any copyright whether intentionally or otherwise, I may be subject to legal action or any other action as may be determined by UM.

(Candidate Signature)

Date:

Subscribed and solemnly declared before,

Witness's Signature

Date:

Name **DR. WAN JEFREY BASIRUN**

Designation **PROFESSOR**

Abstract

There were many researches had been done by scientists on electro-deposition of tin and tin chalcogenide thin films. Most of them were using SnCl_2 , Sn(EDTA) , Sn(OH)_2 , SnSO_4 and so on. But, there are not many studies have been done on the tin sulfoselenide (SnSSe) which is the derivative of the tin thin films. Therefore, an alternative for the tin ion source is tin (II) methanesulfonate to fabricate the tin and tin chalcogenide thin films. The process of electrodeposition of tin and tin chalcogenide thin films on the copper substrate by using a solution of tin (II) methanesulfonate ($(\text{CH}_3\text{SO}_3)_2\text{Sn}$ (50 wt. % in H_2O), sodium thiosulfate ($\text{Na}_2\text{S}_2\text{O}_3$), sodium selenite (Na_2SeO_3) and methane sulfonic acid ($\text{CH}_3\text{SO}_3\text{H}$) is described. The chemical bath contained 0.01M tin (II) methanesulfonate, 0.01M sodium thiosulfate, 0.01M sodium selenite (Na_2SeO_3), and 40ml of methane sulfonic acid ($\geq 99.5\%$) are prepared. Cyclic voltammetry (CV) experiments are conducted using potentiostat and galvanostat to study the reduction and oxidation potential. The CV experiments are conducted under different potential. The electrodeposition of Sn, SnS and SnSSe are observed and described. The characterization of the coated tin and tin chalcogenide thin films on the copper substrate were studied by using EDAX, SEM, AFM, XRF and XRD. The results of the characterization are studied.

The electrodeposition of tin from tin (II) methanesulfonate solution with 1-butyl-1-methylpyrrolidinium trifluoro methanesulfonate (BMPOTF) ionic liquid at varying concentration was studied under the room temperature. Cyclic Voltammetry served to characterize the electrochemical behaviour of tin reduction and oxidation. The diffusion coefficient of stannous ions in the mixture of BMPOTF ionic liquid and MSA

based electrolyte obtained via Randles-Sevcik was approximately $2.11 \times 10^{-7} \text{cm}^2$. Electroplating on copper panel was conducted under different current densities to determine BMPOTF based tin plating solution current efficiency. Mixture of BMPOTF and MSA based tin plating solution gave current efficiency as high as 99.9%. The deposit morphology of the mixture BMPOTF and MSA based tin coated substrates was observed by using EDX and SEM. A dense, fine and polygonal grain structure was obtained. Voltammetry and chronoamperometry for the electrodeposition of tin from tin (II) methanesulfonate mixed with ionic liquid and methane sulfonic acid at room temperature was studied. Cyclic voltammetry shows redox waves of tin (II), which proves that the electrodeposition of tin from tin (II) methanesulfonate is a diffusion-controlled process. The diffusion coefficient of tin (II) ions in the solvent mixture showed good agreement from both voltammetry and chronoamperometry results. The diffusion coefficient of tin (II) in the mixture was much smaller than in aqueous solution, and it depends on the anion of the ionic liquid.

Abstrak

Terdapat banyak penyelidikan telah dilakukan oleh ahli sains terhadap elektrodeposisi filem nipis tin dan tin chalkogenid. Kebanyakan adalah menggunakan SnCl_2 , Sn(EDTA) , Sn(OH)_2 , SnSO_4 dan lain-lain. Tetapi, tidak banyak kajian telah dilakukan terhadap tin sulfoselenide (SnSSe) iaitu sebagai terbitan untuk filem nipis tin. Oleh itu, sebagai pilihan untuk sumber ion tin ialah tin (II) methanesulfonate untuk fabrikasi filem nipis tin dan tin chalkogenid. Proses elektrodeposisi filem nipis tin dan tin chalkogenid terhadap substrat tembaga dengan menggunakan campuran cecair tin (II) methanesulfonate ($(\text{CH}_3\text{SO}_3)_2\text{Sn}$ (50 wt. % in H_2O), natrium thiosulfate ($\text{Na}_2\text{S}_2\text{O}_3$), natrium selenite (Na_2SeO_3) dan asid methane sulfonic ($\text{CH}_3\text{SO}_3\text{H}$) telah diselidik. Campuran cecair kimia yang mengandungi 0.01M tin (II) methanesulfonate, 0.01M natrium thiosulfate, 0.01M natrium selenite (Na_2SeO_3), dan 40ml asid methane sulfonic ($\geq 99.5\%$) telah disedia. Eksperimen kitaran voltammetri telah dilakukan dengan menggunakan potensiostat dan galvanostat untuk mengkaji potensi reduksi dan oksidasi. Eksperimen kitaran voltammetri telah dilakukan dengan potensi berlainan. Elektrodeposisi Sn, SnS dan SnSSe telah dikaji dan diselidik. Pencirian saduran filem nipis tin dan tin chalkogenid terhadap substrat tembaga telah dikaji dengan menggunakan EDAX, SEM, AFM, XRF and XRD. Hasil pencirian telah dikaji.

Elektrodeposisi tin dari campuran cecair tin (II) methanesulfonate yang mengandungi 1-butyl-1-methylpyrrolidinium trifluoro methanesulfonate (BMPOTF) cecair ionik dengan kepekatan berlainan telah dikaji pada suhu bilik. Kitaran Voltammetri adalah sebagai pencirian kelakuan elektrokimia reduksi dan oksidasi tin. Pekali penyebaran ion tin di dalam campuran berasas cecair ionik BMPOTF dan MSA

elektrolit dicapai melalui persamaan Randles-Sevcik ialah menghampiri $2.11 \times 10^{-7} \text{cm}^2$. Penyaduran tin terhadap panel tembaga telah dilakukan di bawah kepadatan elektrik berlainan untuk menentukan efisien elektrik dalam penyaduran tin dengan menggunakan campuran cecair berasas BMPOTF. Campuran cecair yang berasas BMPOTF dan MSA telah memberi efisien electric setinggi 99.9%. Morfologi endapan tin pada substrat tembaga dari cecair campuran yang berasas BMPOTF dan MSA telah dikaji dengan menggunakan EDX dan SEM. Suatu struktur bijiran polygonal yang padat dan teliti telah dicapai. Voltammetri dan kronoamperometri bagi elektrodposisi tin dari campuran tin (II) methanesulfonate dengan cecair ionik dan asid methane sulfonic pada suhu bilik telah dikaji. Kitaran voltammetri menunjukkan aliran redoks untuk tin (II) telah membuktikan elektrodposisi tin dari tin (II) methanesulfonate ialah suatu proses kawalan difusi. Pekali penyebaran ion tin (II) di dalam campuran pelarut membuktikan kedua-dua hasil penyelidikan dari voltammetri dan kronoamperometri adalah tepat dan teliti. Pekali penyebaran tin (II) di dalam campuran cecair adalah bergantung pada anion cecair ionik.

Acknowledgements

I would like to express my greatest thankful, gratitude and appreciation to my Ph.D supervisor, Professor Dr. Wan Jefrey Basirun for his supervision and guidance in my Ph.D research works. At the same time, I would like to thank Dr. Mehdi, Dr. Reza and Mr. Yang Kok Kee as the members of Dr. Wan Jefrey Basirun's Electrochemistry Research Team for the assistance and supports.

Also, I would like to thank Malaysia Toray Science Foundation for providing the research grant and funding for my research works. This material is based upon work supported by the Malaysia Toray Science Foundation.

Koay Hun Lee

6th June 2014

TABLE OF CONTENTS

	Page Number
Abstract	ii
Abstrak	iv
Acknowledgements	vi
Table of Contents	vii
List of Figures	x
List of Tables	xiii
List of Symbols and Abbreviations	xiv
List of Appendices	xv
 Chapter 1 : General Introduction	
1.1 Introduction	1
1.2 Objectives	6
 Chapter 2 : Literature Review	
2.1 General Literature Review	8
 Chapter 3 : Methodology and Experimental Methods	
3.1 Electrodeposition of Tin using Tin (II) Methanesulfonate from a mixture of Ionic Liquid and Methane Sulfonic Acid.	12
3.2 Diffusion Coefficient of Tin (II) Methanesulfonate in Ionic Liquid and Methane Sulfonic Acid (MSA) Solvent.	14
3.3 Metal Substrates Pretreatment	15
3.4 Preparation of Mixture Solutions	15
3.5 Cyclic Voltammetry (CV) Experiments	16
3.6 Fabrication Methods	17

Chapter 4 : Results and Discussion

Part I: Results and Discussion for Electrodeposition of Tin by using Tin (II) Methanesulfonate from a mixture of Ionic Liquid and Methane Sulfonic Acid.

4.1	Voltammetry	19
4.2	Chronoamperometry	21
4.3	Bulk Electrodeposition	25

Part II: Results and Discussion for Electrodeposition of Tin from Tin (II) Methanesulfonate and Methane Sulfonic Acid Solution.

4.4	Cyclic Voltammetry Characterization for Sn Thin Films	30
4.5	Energy Dispersive X-Ray (EDX) characterization for Sn Thin Films.	31
4.6	X-ray Diffraction (XRD) characterization for Sn Thin Films.	34

Part III: Results and Discussion for Electrodeposition of Tin Sulfide from Tin (II) Methanesulfonate and Methane Sulfonic Acid Solution.

4.7	Cyclic Voltammetry Characterization.	38
4.8	Energy Dispersive X-Ray (EDX) characterization.	39
4.9	Scanning Electron Microscopy (SEM) Characterization.	43
4.10	X-ray Diffraction (XRD) Characterization.	44
4.11	Atomic Force Microscopy (AFM) Characterization.	48
4.12	Comparative Discussion.	51

Part IV: Results and Discussion for Electrodeposition of Tin Sulfoselenide from Tin (II) Methanesulfonate and Methane Sulfonic Acid Solution.

4.13	Cyclic Voltammetry Characterization for SnSSe Thin Films.	55
4.14	Energy Dispersive X-Ray (EDX) Characterization for SnSSe Thin Films.	56
4.15	Scanning Electron Microscopy (SEM) Characterization for SnSSe Thin Films.	62
4.16	X-ray Diffraction (XRD) Characterization for SnSSe Thin Films.	63

4.17	Atomic Force Microscopy (AFM) Characterization of SnSSe Thin Films.	68
------	---	----

Chapter 5: Conclusion

5.1	Conclusion	76
-----	------------	----

	References	77
--	-------------------	----

	Appendices	83
--	-------------------	----

List of Figures

		Page Number
Figure 4.1	Cyclic voltammogram at 0.05 V/s for solution X M ($(\text{CH}_3\text{SO}_3)_2\text{Sn}$, A=0M , B=0.1M, C=0.2M, D=0.3M, E=0.4M, F=0.5M.	20
Figure 4.2	Effect of Sn^{2+} concentration on peak current density.	21
Figure 4.3	Effect of tin (II) concentration on peak current density.	22
Figure 4.4	Chronoamperometry of current I/A vs time/s , stepped at -0.9 V vs Ag/AgCl at various concentrations.	22
Figure 4.5	Cottrell plots, I/A vs $t^{-1/2}$ for chronoamperometry in Fig. 4.4 , stepped to - 0.9 V vs Ag/AgCl.	23
Figure 4.6	SEM (3500 times magnification) and EDX spectrum of tin electrodeposited from 0.5 M tin (II) methanesulfonate solution at 1 A dm ⁻² .	27
Figure 4.7	SEM (3500 times magnification) and EDX spectrum of tin electrodeposited from 0.1 M tin (II) methanesulfonate solution at 7 A dm ⁻² .	28
Figure 4.8	SEM (3500 times magnification) and EDX spectrum of tin electrodeposited from 0.5 M tin (II) methanesulfonate solution at 7 A dm ⁻² .	28
Figure 4.9	The cyclic voltammogram for electro-deposition of Sn at the scan rate of 0.02 V/s.	30
Figure 4.10	EDX characterization for electro-deposition of Sn on Copper Substrate at the potentials of (a) -1.30V, (b) - 1.40V, (c) -1.50V, (d) -1.60V, (e) -1.70V and (f) - 1.80V.	33
Figure 4.11	XRD characterization for electro-deposition of Sn on Copper Substrate at the potentials of (a) -1.30V, (b) - 1.40V, (c) -1.50V, (d) -1.70V.	35
Figure 4.12	The cyclic voltammogram for electro-deposition of SnS at the scan rate of 0.05 V/s.	38
Figure 4.13	EDX characterization for electro-deposition of SnS on Copper Substrate at the potentials of (a) -0.15V, (b) - 0.25V, (c) -0.35V, (d) -0.50V, (e) -1.00V and (f) -	40

1.20V.

Figure 4.14	SEM characterization for electro-deposition of SnS on Copper Substrate at the potentials of (a) -0.15V, (b) -0.25V, (c) -0.35V, (d) -0.50V, (e) -1.00V and (f) -1.20V.	44
Figure 4.15	XRD characterization for electro-deposition of SnS on Copper Substrate at the potentials of (a) -0.15V, (b) -0.25V, (c) -0.35V, (d) -0.50V, (e) -1.00V and (f) -1.20V.	45
Figure 4.16	AFM characterization for electro-deposition of SnS on Copper Substrate at the potential of -0.35 V.	48
Figure 4.17	AFM characterization for electro-deposition of SnS on Copper Substrate at the potential of -0.50 V.	49
Figure 4.18	AFM characterization for electro-deposition of SnS on Copper Substrate at the potential of -1.00 V.	50
Figure 4.19	SnS direct band gap determination for deposition potential of -0.35V.	52
Figure 4.20	XRD characterization for electro-deposition of SnS on Copper Substrate at the potential of -0.35 V.	53
Figure 4.21	Citation from Ogah E. Ogah and Guillaume Zoppi paper - XRD spectra of SnS layers deposited.	54
Figure 4.22	The cyclic voltammogram for electro-deposition of SnSSe at the scan rate of 0.05 V/s.	55
Figure 4.23	EDX characterization for electro-deposition of SnSSe on Copper Substrate at the potentials of (a) -0.15V, (b) -0.25V, (c) -0.35V, (d) -0.45V, (e) -0.55V and (f) -0.65V (g) -0.75V (h) -0.85V.	57
Figure 4.24	SEM characterization for electro-deposition of SnSSe on Copper Substrate at the potentials of (a) -0.15V, (b) -0.25V, (c) -0.35V, (d) -0.45V, (e) -0.55V, (f) -0.65V, (g) -0.75V and (h) -0.85V.	63
Figure 4.25	XRD characterization for electro-deposition of SnSSe on Copper Substrate at the potentials of (a) -0.15V, (b) -0.25V, (c) -0.35V, (d) -0.45V, (e) -0.55V, (f) -0.65V, (g) -0.75V and (h) -0.85V.	64
Figure 4.26	AFM characterization for electro-deposition of SnSSe on Copper Substrate at the potential of -0.15 V.	68

Figure 4.27	AFM characterization for electro-deposition of SnSSe on Copper Substrate at the potential of -0.25 V.	69
Figure 4.28	AFM characterization for electro-deposition of SnSSe on Copper Substrate at the potential of -0.35 V.	70
Figure 4.29	AFM characterization for electro-deposition of SnSSe on Copper Substrate at the potential of -0.45 V.	71
Figure 4.30	AFM characterization for electro-deposition of SnSSe on Copper Substrate at the potential of -0.55 V.	72
Figure 4.31	AFM characterization for electro-deposition of SnSSe on Copper Substrate at the potential of -0.65 V.	73
Figure 4.32	AFM characterization for electro-deposition of SnSSe on Copper Substrate at the potential of -0.75 V.	74
Figure 4.33	AFM characterization for electro-deposition of SnSSe on Copper Substrate at the potential of -0.85 V.	75

List of Tables

		Page Number
Table 4.1	Tin (II) diffusion coefficient from literature.	24
Table 4.2	Current efficiencies of tin electrodeposition obtained at different tin (II) concentrations.	26

List of Symbols and Abbreviations

Symbols and Abbreviations	Name
BMPOTF	1-butyl-1-methyl-pyrrolidinium trifluoro-methanesulfonate
MSA	methane sulfonic acid
Tin (II) MS	tin (II) methanesulfonate
Sn	tin
S	sulfur / Sulphur
SnS	tin sulfide
SnSSe	tin sulfo-selenide
Ag/AgCl	argentum chloride reference electrode
SCE	saturated calomel reference electrode
R.E.	reference electrode
C.E.	counter electrode
W.E.	working electrode
XRF	X-Ray Fluorescent Technique
EDAX	Energy Dispersive X-Ray Technique
SEM	Scanning Electron Microscopy
XRD	X-Ray Diffraction Technique
AFM	Atomic Force Microscopy
CV	Cyclic Voltammetry

List of Appendices

Appendix A:

Paper Published in ISI Journal : Advanced Materials Research

Appendix B:

Paper Published in ISI Journal : Metallurgical and Materials Transactions B

Chapter 1 : General Introduction

1.1 Introduction :

Tin and tin chalcogenides thin films are very important in industrial application, for instance tin is important in industrial tin plating and tin chalcogenides can be used as solar cell materials. This research focused on the deposition of tin and tin chalcogenides on copper substrate by using electrochemical deposition method (ECD).

Electrochemical deposition method (ECD) is very common to be used because of it is a simple and economically viable technique, and this method produces good quality thin films for device application ^[5,6]. In the ECD method, preparation of chemical bath is very important. This is to ensure feasibility of tin and tin chalcogenides deposition and also in order to obtain good quality thin films. Therefore, composition of the chemical bath is essential part of this work.

Electrochemical deposition is an electroplating process of a metal coating or semiconducting ions electrochemically deposited on a conducting surface. Usually, electrochemical deposition or electroplating are used to prevent surface corrosion on the substrate, for the aesthetic appearance, to design for the special surface properties and to engineer for the mechanical surface properties.

An electrochemical deposition system (ECD) usually contains electrolytes aqueous solution or also known as chemical bath. Basically, anode and cathode are dipped into chemical bath containing required metal ions.

During ECD process, positive ions or cations are deposited at negative terminal or cathode, and negative ions or anions are deposited at positive terminal or anode.



In this research, electrochemical bath consists of tin (II) methanesulfonate and methanesulfonic acid (MSA) mixture of solution. Tin source was from tin (II) methanesulfonate whereas sulfur source was from natrium thiosulfate and selenium source was from natrium selenite. In the deposition of tin, ionic liquid was used as an additive to the chemical bath. Ionic liquid was used in the electrodeposition of tin in order to obtain good morphology of the thin film's surface. The ionic liquid used was 1-butyl-1-methylpyrrolidinium trifluoro methanesulfonate (BMPOTF).

Problems associated with preparation of good chemicals bath for the electrochemical deposition of tin and tin chalcogenides thin films are:

- (i) The chemicals source must be suitable. Tin (II) methanesulfonate and natrium thiosulfate are very suitable chemicals sources, easily releasing Sn^{2+} ion and also sulfur is easily reduced from $\text{S}_2\text{O}_3^{2-}$ through electrochemical deposition.

- (ii) The chemicals bath must be homogeneous. Acid is required in the chemicals bath because acid can be used to dissolve any undissolved chemicals to make the chemicals bath more homogeneous. Strong inorganic acid such as HCl, H_2SO_4 and HNO_3 are not suitable, because these acids can cause corrosion problems on copper substrate during electrochemical deposition. Therefore, methanesulfonic acid is very suitable to be used as solvent in the preparation of the chemical bath.
- (iii) Gas evolution. Evolution of chlorine gas might interfere with the electrochemical deposition process of tin when SnCl_2 is used as the tin source. Therefore, tin (II) methanesulfonate is very suitable to be used as an alternative tin source in fabrication of SnS thin films.
- (iv) Corrosion of substrate during electrochemical deposition process. Chemical bath containing tin (II) methanesulfonate, methanesulfonic acid (MSA) and sodium thiosulfate mixture of solutions is very suitable because it does not corrode copper substrate during electrochemical deposition process.
- (v) Methanesulfonic acid was used in the preparation of chemical bath in this work because it can function as an antioxidant in the chemical bath for the laboratory scale preparation of SnS thin films. Sn^{2+} can be easily oxidized into Sn^{4+} , therefore, methanesulfonic acid is very important to be used to prevent oxidation of Sn^{2+} into Sn^{4+} .

Other benefits of tin electroplating from methanesulfonic acid bath outlined in this research are (1) environmentally friendly method of fabrication of tin chalcogenide tin

films; (2) cost effective; (3) application in electroplating industries; (4) potential application in solar cell industries.

Tin chalcogenide thin films are advanced material which consist of tin element combined with other metal or non-metal elements such as SnS and SnSSe whereby they can be deposited on metal substrate like copper plate, titanium plate and glass substrate like Indium Tin Oxide (ITO) glass.

The research on tin chalcogenide thin films is important due to its application in semiconductor, solar cells and batteries industries.

Many related research have been done in Malaysia and abroad on tin (Sn) thin film and its application. But, source of tin (Sn) are SnCl_2 , SnSO_4 , $\text{Sn}(\text{CO}_3)$, which at most cases are unsuitable, because SnCl_2 produces Cl_2 gas, SnSO_4 produces SO_2 , SO_3 gas and H_2SO_4 , $\text{Sn}(\text{CO}_3)$ produces CO and CO_2 gas which can be dissolved in water to give $\text{H}_2(\text{CO}_3)$. When it comes to release of gas, it complicates the whole electrodeposition process and pH of the electrolyte can be changed. Whereas for electrodeposition of thin films derived from tin, $\text{Sn}(\text{OH})_2$ is unsuitable because $\text{Sn}(\text{OH})_2$ react with other metal ion to produce unwanted precipitation of metal oxides.

Currently, most of the researchers use SnCl_2 , but SnCl_2 produces Cl_2 gas during the process of electrochemical deposition of tin (Sn) element. The Cl_2 gas produced at

first is not environmental friendly, secondly, Pt rod or Pt wire which performed as counter electrode is sensitive to Cl_2 gas. PtCl_2 can be formed when the Pt metal come into contact with chlorine gas.

In semiconductor industries, electroplating of tin is essentially by using methanesulfonic acid (MSA) as medium of solution and solvent. But, very few research have been done on the tin derivatives thin films by using mixture solution of tin (II) methanesulfonate and methanesulfonic acid. Examples for tin chalcogenide tin films are SnS and SnSSe thin films.

Also, mixture of tin (II) methanesulfonate and methanesulfonic acid is commonly used in industrial tin plating. There are very few studies on fabrication of tin chalcogenide thin films by using chemical bath containing mixture of tin (II) methanesulfonate and methanesulfonic acid. For instance, tin sulfide (SnS) thin film fabrication which was done previously, mostly by using tin chloride or tin sulfate as precursor chemicals. But, in this research, method of tin sulfide thin film fabrication by using chemical bath containing mixture of tin (II) methanesulfonate and methanesulfonic acid was investigated.

Therefore, tin (II) methanesulfonate was used in this research instead of tin chloride. It is more environmentally friendly than SnCl_2 .

Medium of solution would be methanesulfonic acid and water. Methanesulfonic acid (MSA) is environmentally friendly unlike most tin precursor chemicals. Tin derivatives thin films were fabricated by using potentiostat and galvanostat. Cyclic Voltammetry (CV) was performed to study reduction and oxidation potentials. The CV experiments were conducted under different potentials and scan rates. The thin films can be electrodeposited on copper, titanium and ITO glass substrates. Then, the electrodeposition of the tin derivatives thin films was observed, and most optimum conditions of their controlling parameters which produce these semiconductor thin films were identified. Characterization of the coated tin derivatives thin films was studied by using EDAX, SEM, XRD and AFM. Results of characterization were analyzed. These tin derivatives thin films have potential to be applied as semiconductor advance materials, optoelectronics materials, solar energy cells and battery materials.

1.2 Objectives:

Research objectives are (1) to deposit tin thin film on copper substrate by using chemical bath of tin (II) methanesulfonate solution mixture containing ionic liquid BMPOTF; (2) to investigate diffusion coefficient of chemical bath of tin (II) methanesulfonate solution mixture containing ionic liquid BMPOTF ; (3) to deposit tin, tin sulfide and tin sulfoselenide on copper substrate by using chemical bath of tin (II) methanesulfonate solution mixture; (4) to investigate feasibility of the chemical bath of tin (II) methanesulfonate solution mixture to deposit tin and tin chalcogenide thin film at different potentials.

Research focus is to investigate feasibility of using tin (II) methanesulfonate and methanesulfonic acid to electrodeposit the tin and tin chalcogenides thin film, respectively the tin (Sn) thin film, tin sulfide (SnS) thin film and tin sulfoselenide (SnSSe) thin film. The research is focused on method of fabrication and composition of the chemical bath for electrodeposition of tin and tin chalcogenide thin films. The fabrication method basically is using electroplating method with chemical bath containing tin (II) methanesulfonate and methanesulfonic acid. This research is to prove that tin and tin chalcogenide thin films which are Sn, SnS and SnSSe thin films can be fabricated and electrochemically deposited by using tin (II) methanesulfonate and methanesulfonic acid mixture of solution.

Chapter 2 : Literature Review

2.1 General Literature Review :

Tin and its alloys can be electrodeposited from various electrolytes such as aqueous fluoroborate, sulfate and methanesulfonate solutions. The sulfate electrolyte is generally adopted as a first choice of plating electrolyte due to its low cost and long history. The fluoroborate bath is used when high current density is required. The methanesulfonate based electrolyte is favored for its environmental benefits and it facilitates higher stannous ion saturation solubility with a low oxidation rate to stannic ions^[1].

However, hydrogen evolution reaction often occurs in the aqueous based electrolyte electrodeposition resulting in profound effect on current efficiency and quality of the tin deposits. As a result, different additives may be needed to suppress such difficulties. In contrast, a fundamental advantage of using ionic liquid electrolytes in electroplating is that, since these are non-aqueous solutions, there is negligible hydrogen evolution during electroplating and the coatings possess superior mechanical properties compared to the pure metal. Hence essentially crack-free, more corrosion resistant deposits are possible. This may allow thinner deposits to be used, thus reducing overall material and power consumption^[2].

Electrodeposition in ionic liquids was rarely studied in the past. In 1992, Wilkes and Zaworotko reported the first air and moisture stable imidazolium based ionic liquid with either tetrafluoroborate or hexafluorophosphate as anions. Then, several, liquids

consisting of 1-ethyl-3-methylimidazolium, 1,2-dimethyl-3-propylimidazolium, or 1-butyl-1-methyl-pyrrolidinium cations with various anions, such as tetrafluoroborate (BF_4^-), tri-fluoro-methanesulfonate (CF_3SO_3^-), bis (tri-fluoro-methanesulfonyl) imide $[(\text{CF}_3\text{SO}_2)_2\text{N}]^-$ & tris (tri fluoro methanesulfonyl) methide $[(\text{CF}_3\text{SO}_2)_3\text{C}]^-$, were found and received much attention because of low reactivity against moisture ^[3-4].

Few studies were reported on the electrodeposition of tin (II) in ionic liquids. The first was done by Hussey and Xe ^[5] in an AlCl_3 mixed in 1-methyl-3-ethyl imidazolium chloride melt. W. Yang et. al. ^[6] has done tin and antimony electrodeposition in 1-ethyl-3-methylimidazolium tetrafluoroborate, and N. Tachikawa et. al. ^[7] has done electrodeposition of tin (II) in a hydrophobic ionic liquid, 1-n-butyl-1-methylpyrrolidinium bis (trifluoromethylsulfonyl) imide.

In view of the advantages of the air and water stable ionic liquids, this research reported the results on the tin electrodeposition from a mixture of an ionic liquid, 1-butyl-1-methyl-pyrrolidinium trifluoro-methanesulfonate, (BMPOTF) with tin (II) methanesulfonate in methane sulfonic acid (MSA).

Tin and alloys of tin has been electrodeposited from electrolytes of tin (II) salts such as the fluoroborate and sulfate. Both the anions have certain advantages over the other, but a new tin (II) salt, which is based on methanesulfonate anion, is gathering interest because of its environmental low toxicity and its low oxidation rate to stannic ions.^[1]

The use of ionic liquid in smaller laboratory-scale electrodeposition was proven to be an effective solvent to reduce the effect of hydrogen evolution reaction; thus, essentially it is crack free and better quality. In addition, reduced overall material and power consumption were also reported.^[8]

Many scientists had reported on the importance of the SnS thin films as solar cell materials application. M. Ichimura and K. Takeuchi reported that SnS has a bandgap around 1.0 – 1.3 eV and the p-type conductivity which is suitable to be used as absorption layer in solar cell ^[32]. SnS has a direct bandgap of 1.3 eV and indirect bandgap of 1.0 eV ^[31]. Therefore, SnS has good electrical and optical properties and also its constituent elements are inexpensive and environmental friendly. Robert W. Miles and Ogah E. Ogah reported that SnS is amphoteric such that a range of solar cell structures using SnS as an absorber layer can be envisioned ^[33]. There are many methods of SnS thin films fabrication done by other scientists, for instance conventional thermal evaporation and electron beam evaporation were experimented by Tanusevski et al. ^[34] and Ogah et al. ^[35], respectively. Thin films of SnS can be also obtained by many other techniques, such as vacuum evaporation ^[36], electron beam deposition ^[37], chemical vapor transport ^[38], and spray pyrolysis ^[39]. The optical band gaps for the films vary from 1.0 to 1.3 eV depending on the deposition technique and method of measurement. However, although there are many fabrication methods for SnS, but they all had the same application as solar cell material.

Electrochemical deposition (ECD) is a widely used coating method because of it is a simple and economically viable technique, and this method produces good quality

thin films for device application ^[34,35]. In the chemical bath deposition system for SnS, SnCl₂ is normally used as Sn source and different reagents are used as S sources. For instance, R. Mariappan and T. Mahalingam reported SnS fabrication from the SnCl₂.2H₂O as the tin source by using electrochemical deposition method ^[42].

Chapter 3 : Methodology and Experimental Methods

3.1 Electrodeposition of Tin using Tin (II) Methanesulfonate from a mixture of Ionic Liquid and Methane Sulfonic Acid.

The electrochemical behavior of tin reduction and oxidation was studied in water and air stable ionic liquid 1-butyl-1 methyl-pyrrolidinium trifluoro-methanesulfonate, (BMPOTF) which was purchased from Merck. Component of tin methanesulfonate solution was 55% of tin (II) methanesulfonate (CH_3SO_3)Sn , 30% of H_2O and 15% of $\text{CH}_3\text{SO}_3\text{H}$. Component of ionic liquid 1-butyl-1 methyl-pyrrolidinium trifluoro-methanesulfonate, (BMPOTF) was 98% assay (electrophoresis), 1% of H_2O and less than 0.1% of halides.

The experiments were carried out using a conventional 3-electrode cell. The working electrode was a copper rod with a diameter of 4 mm and an exposed area of 0.1257 cm^2 . Before each experiment, the pre-treatment of the copper rod was as follows: wet grinding with SiC type abrasive paper grade 100, 1000 and 1200 to a mirror finish. Cleaning 10 minutes in ethanol and then de-scaled with 10% Methane Sulfonic Acid (10%) and final rinsing in de-ionized water. The counter electrode was a platinum wire with 4 cm length and 0.1 mm diameter. The working electrode potentials reported herein were measured versus a Ag/AgCl reference electrode.

For the electroplating experiments, copper panels with dimension 2 cm x 2 cm were used as the substrate for tin electrodeposition. Before each experiment, the pretreatment of the copper panels were as follows: Cleaning 10 minutes in ethanol and

then de-scaled with 10% methane sulfonic acid (10%) and final rinsing in de-ionized water. Precautionary measures were taken to eliminate oxygen from the system by bubbling high purity nitrogen through the solution prior to the experiments for 3 minutes.

The electrochemical experiments were carried out using an Autolab PGSTAT 30 Potentiostat/Galvanostat. All experiments were conducted at room temperature, 29 +/- 1 °C in a mixture of BMPOTF ionic liquid and MSA based tin methane sulfonate salts. Tin methanesulfonate, $(\text{CH}_3\text{SO}_3)_2\text{Sn}$ was added in the desired amounts. No organic additives were mixed in the solutions in this study. The electrolyte volume for the mixture was fixed at 15 mL in these experiments. Scanning Electron Microscopy (SEM) was model Philips XL 30 and Energy Dispersive X-Ray Analysis (EDX) was using EDAX Analyzer Genesis was used in the surface studies of these deposits.

3.2 Diffusion Coefficient of Tin (II) Methanesulfonate in Ionic Liquid and Methane Sulfonic Acid (MSA) Solvent

The water and air stable ionic liquid BMPOTF (>98 pct purity) and tin (II) methanesulfonate $(\text{CH}_3\text{SO}_3)_2\text{Sn}$ were purchased from Merck (Whitehouse Station, NJ). The experiments were carried out using a conventional three-electrode cell. The working electrode was a copper rod with diameter of 4 mm with an exposed area of 0.1257 cm^2 . Before each experiment, the copper rod was subjected to wet grinding with a SiC-type abrasive paper grade 100, 1000, and 1200 to obtain a smooth finish, followed by cleaning for 10 minutes in ethanol and then descaling with 10-pct MSA (10 pct) and final rinsing in deionized water. The counter electrode was a platinum wire with 4 cm length and 0.1 mm diameter. The working electrode potentials reported herein were measured vs a saturated Ag/AgCl reference electrode. Oxygen was eliminated from the system by bubbling nitrogen gas through the solution for 3 minutes prior to each experiment. The weight percentage composition of the tin (II) methanesulfonate used in this study was 55% of tin (II) methanesulfonate $(\text{CH}_3\text{SO}_3)_2\text{Sn}$, 30% of H_2O and 15% of methanesulfonic acid $\text{CH}_3\text{SO}_3\text{H}$.

All experiments were conducted at room temperature, $302 \text{ K} \pm 1 \text{ K}$ ($29^\circ\text{C} \pm 1^\circ\text{C}$) in a mixture of BMPOTF ionic liquid and MSA where tin methanesulfonate $(\text{CH}_3\text{SO}_3)_2\text{Sn}$ was diluted, in desired amounts with pure MSA and ionic liquid with a ratio of 1:1, to obtain a final solution of 0.1 M to 0.5 M Tin (II) methanesulfonate. The electrochemical experiments were carried out using an Autolab PGSTAT 30 Potentiostat/Galvanostat (Eco Chemie, Utrecht, Netherlands). No organic additives were mixed in the solutions in this study. The scanning electron microscope (SEM)

used in the surface studies of these deposits was Philips XL 30 (Philips, Amsterdam, The Netherlands), and the energy dispersive X-ray analysis (EDX) machine used was the EDAX Analyzer Genesis (EDAX Inc., Mahwah, NJ).

3.3 Metal Substrates Pretreatment

Pretreatment for copper metal substrates was important in order to remove any impurities and metal oxides on the surface of the copper metal substrates.

The metal substrates were rinsed with pure acid solution like sulfuric acid and phosphoric acid, to remove impurities which can be dissolved in the acid solution. The ionic impurities were dissolved in the acidic condition.

Then, the metal substrates were rinsed with methanol and absolute ethanol, this was to remove impurities which can be dissolved in the methanol and ethanol solvents. The organic impurities were dissolved in the methanol and ethanol.

The pretreated metal substrates were dried in oven. Then, the pretreated metal substrates were prepared.

3.4 Preparation of Mixture Solutions

Preparation of mixture solution for Sn thin films fabrication

A volume of 100 ml of 0.01M tin (II) methanesulfonate was prepared. The precipitate appeared was dissolved with 40 ml of methanesulfonic acid ($\geq 99.5\%$) in

order to obtain homogenized solution. Then, pH of the solution was determined by using pH meter.

Preparation of mixture solution for SnS thin films fabrication

100 ml of 0.01M tin (II) methanesulfonate and 0.01M sodium thiosulfate ($\text{Na}_2\text{S}_2\text{O}_3$) are prepared. The precipitate appeared was dissolved with 40 ml of methanesulfonic acid ($\geq 99.5\%$) in order to obtain homogenized solution. Then, pH of the solution was determined by using pH meter.

Preparation of mixture solution for SnSSe thin films fabrication

100 ml of 0.01M tin (II) methanesulfonate, 0.01M sodium thiosulfate ($\text{Na}_2\text{S}_2\text{O}_3$), 0.01M sodium selenite (Na_2SeO_3) are prepared. The precipitate appeared was dissolved with 40 ml of methanesulfonic acid ($\geq 99.5\%$) in order to obtain homogenized solution. Then, pH of the solution was determined by using pH meter.

3.5 Cyclic Voltammetry (CV) Experiments

Cyclic voltammetry experiments were done by using a potentiostat / galvanostat. Purpose of the cyclic voltammetry experiments was to obtain oxidation and reduction potentials for the researched materials. Anodic and cathodic scans were performed for the research materials. From the reduction potentials observed, best and most optimum conditions for electrodeposition of Sn, SnS and SnSSe thin films were determined.

3.6 Fabrication Methods

Fabrication of Sn Thin Films

Mixture of solution containing 100 ml of 0.01M tin (II) methanesulfonate prepared was transferred to the electrochemical cell. Then the apparatus device was set up where the counter electrode (platinum electrode), reference electrode (SCE electrode) and working copper substrate were properly connected to the potentiostat & galvanostat and the chemical bath.

Then, Sn thin films were deposited on the substrates at various reduction potentials. The Sn thin films were deposited on copper substrate under different potentials, they were -1.30V, -1.40V, -1.50V, -1.60V, -1.70V and -1.80V.

The electrodeposited Sn thin films were put in oven for one hour. Sn thin films were fabricated.

Fabrication of SnS Thin Films

Mixture of solution containing 100 ml of 0.01M tin (II) methanesulfonate and 0.01M sodium thiosulfate ($\text{Na}_2\text{S}_2\text{O}_3$) prepared was transferred to the electrochemical cell. Then the apparatus device was set up where the counter electrode (platinum electrode), reference electrode (SCE electrode) and working copper substrate were properly connected to the potentiostat & galvanostat and the chemical bath.

Then, SnS thin films were deposited on the substrates at various reduction potentials. The SnS thin films were deposited on copper substrate under different potentials, they were -0.15V, -0.25V, -0.35V, -0.50V, -1.00V and -1.20V.

The electrodeposited SnS thin films were put in oven for one hour. SnS thin films were fabricated.

Fabrication of SnSSe Thin Films

Mixture of solution containing 100 ml of 0.01M tin (II) methanesulfonate, 0.01M sodium thiosulfate ($\text{Na}_2\text{S}_2\text{O}_3$), 0.01M sodium selenite (Na_2SeO_3) prepared was transferred to the electrochemical cell. Then the apparatus device was set up where the counter electrode (platinum electrode), reference electrode (SCE electrode) and working copper substrate were properly connected to the potentiostat & galvanostat and the chemical bath.

Then, SnSSe thin films were deposited on the substrates at various reduction potentials. The SnSSe thin films were deposited on copper substrate under different potentials, they were -0.15V, -0.25V, -0.35V, -0.45V, -0.55V, -0.65V, -0.75V and -0.85V.

The electrodeposited SnSSe thin films were put in oven for one hour. SnSSe thin films were fabricated.

Chapter 4 : Results and Discussion

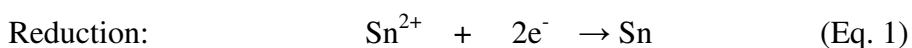
Part I: Results and Discussion for Electrodeposition of Tin by using Tin (II)

Methanesulfonate from a mixture of Ionic Liquid and Methane Sulfonic Acid.

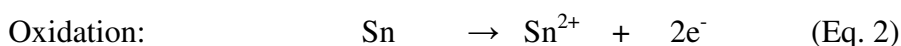
4.1 Voltammetry

Figure 4.1 shows the voltametric response for BMPOTF with different tin concentration. Cyclic voltammetry experiments were swept from 0 to -1.0 V vs. Ag/AgCl, and the sweep direction was reversed. The potential sweep rate was set at 0.05 Vs^{-1} throughout the experiments. Increasing tin (II) concentration produces a stronger reduction and oxidation peak. A single reduction and oxidation peak were observed in the cyclic voltammetry of tin deposition and dissolution at a copper substrate, where these peaks were absent when done with only the ionic liquid without the $(\text{CH}_3\text{SO}_3)_2 \text{Sn}$ in MSA.

The forward sweep from 0 to -1V vs. Ag/AgCl shows a reduction peak for tin deposition corresponding to a two-electron step:



On reversing the potential sweep from -1.0V to 0V vs. Ag/AgCl, a single stripping peak was observed confirming the two-electron oxidation of metallic to stannous ions via the reverse reaction:



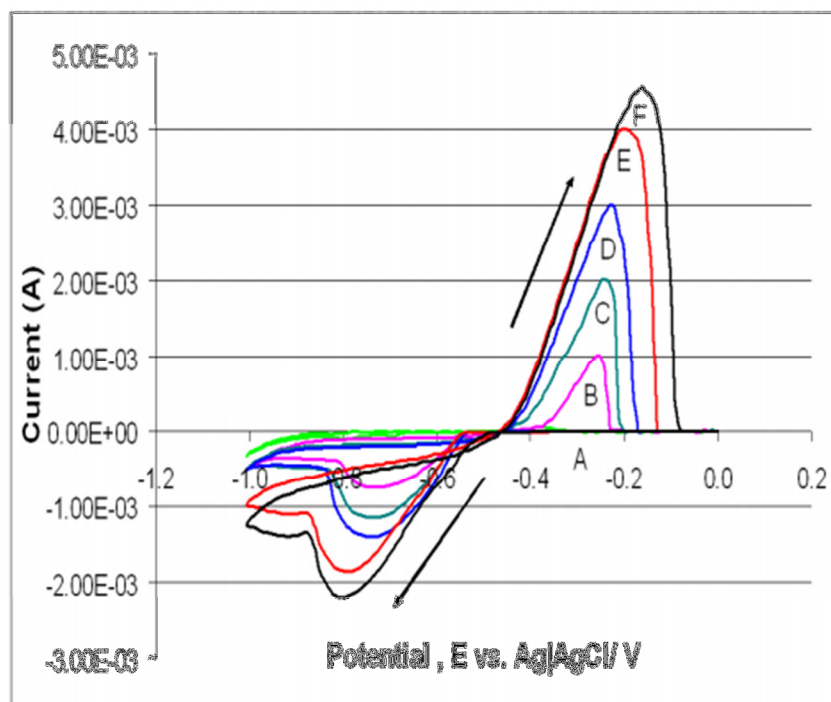


Figure 4.1 : Cyclic voltammogram at 0.05 V/s for solution X M $(\text{CH}_3\text{SO}_3)_2\text{Sn}$, A=0M , B=0.1M, C=0.2M, D=0.3M, E=0.4M, F=0.5M .

The relation between the peak current density, J_p and the concentration of the electroactive species in solution can be given by the Randles-Sevcik equation:

$$J_p = 2.69 \times 10^5 Z^{1.5} D^{0.5} \nu^{0.5} c \quad (\text{Eq. 3})$$

Where J_p is the peak current density, Z is the number of electrons involved in the electrode process, D is the diffusion coefficient of stannous ions, ν is the potential sweep rate and c is the concentration of stannous ions.

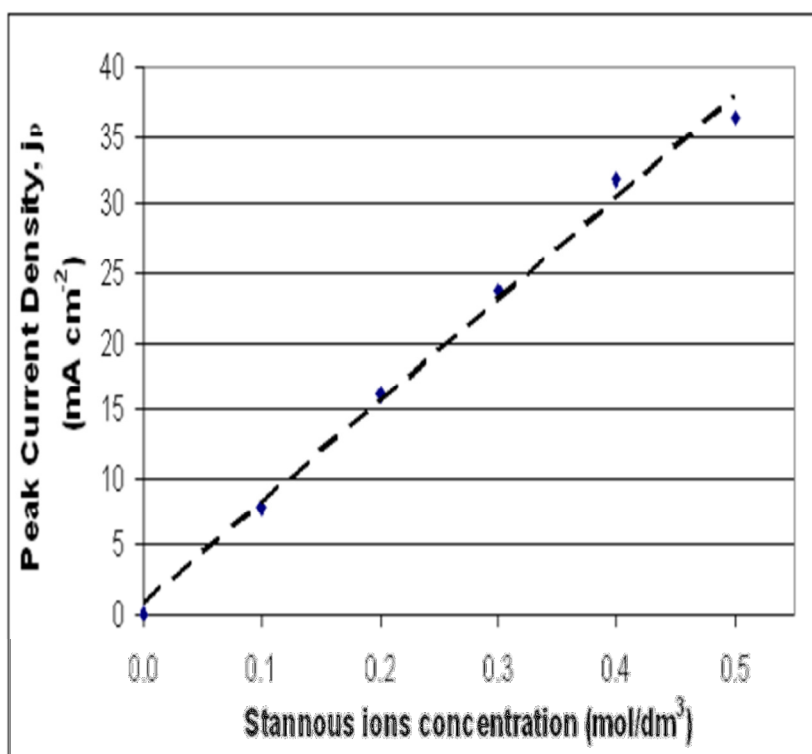


Figure 4.2 : Effect of Sn^{2+} concentration on peak current density.

4.2 Chronoamperometry

Figure 4.3 shows chronoamperometry of of current I/A vs time/s, stepped at – 0.9 V for 0.1 M to 0.5 M of tin (II). For chronoamperometry, the relation between the current I/A and the time/s can be given by the Cottrell equation ^[10]

$$I = \frac{n F A D^{\frac{1}{2}} c}{\pi^{\frac{1}{2}} t^{\frac{1}{2}}} \quad (\text{Eq. 4})$$

where n is the number of electrons involved in the electrode process, A is the area of electrode, D is the diffusion coefficient of tin (II) ions, F is the Faraday constant, t is the time in s, and c is the concentration of tin (II) ions.

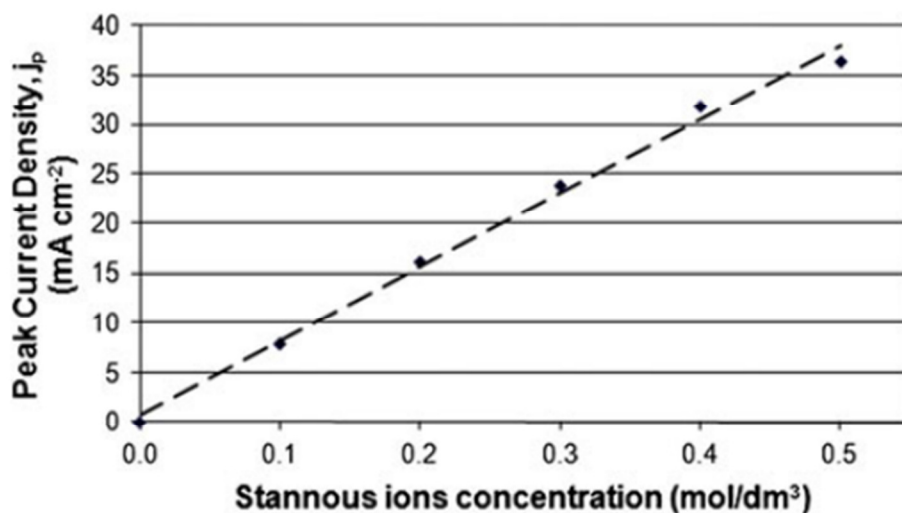


Figure 4.3 : Effect of tin (II) concentration on peak current density.

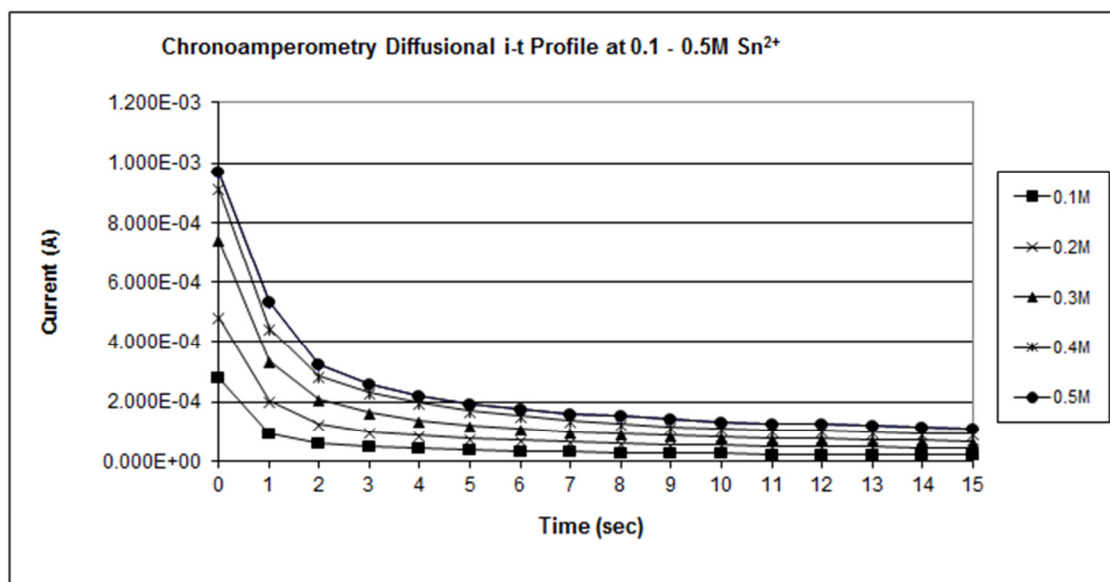


Figure 4.4 : Chronoamperometry of current I/A vs time/s , stepped at -0.9 V vs $Ag/AgCl$ at various concentrations.

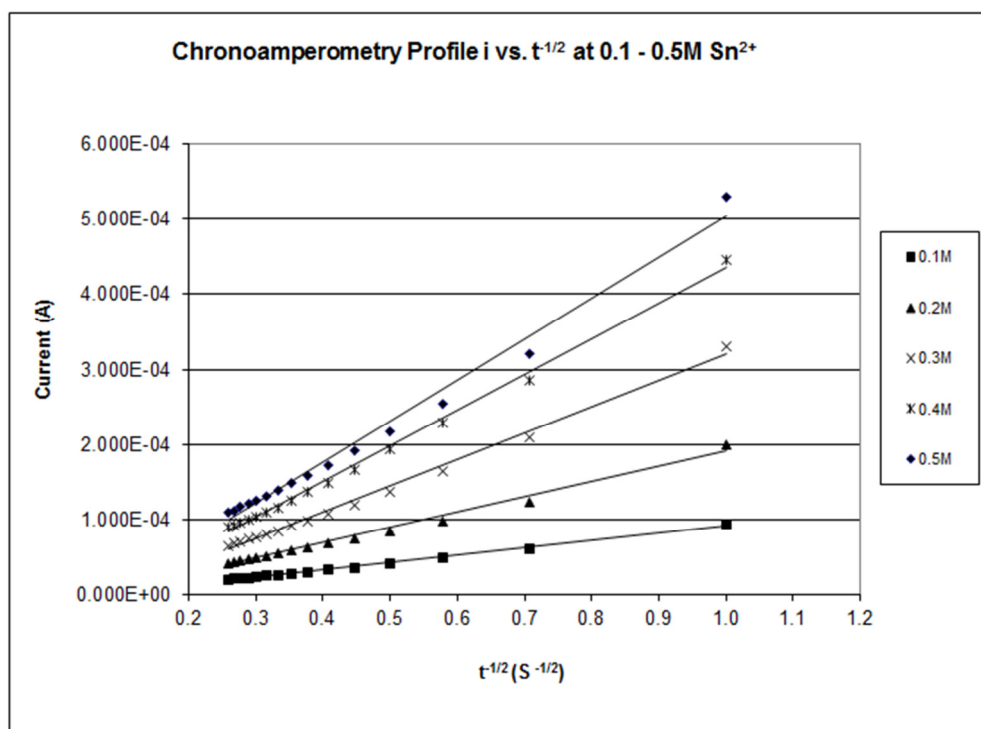


Figure 4.5 : Cottrell plots, I/A vs $t^{-1/2}$ for chronoamperometry in Fig. 4.4 , stepped to -0.9 V vs Ag/AgCl.

The results in Figure 4.3 show clearly that the electro-reduction of tin (II) in the mixture of ionic liquid and MSA solvent is diffusion controlled, which permits the Diffusion constant to be calculated from Cottrell plots in Figure 4.5. The average diffusion coefficient calculated for all concentration used within 0.1 to 0.5 M was $2.5 \times 10^{-7} \text{ cm}^2 \text{ s}^{-1}$ and is comparable with the voltammetry experiments.

From the graph in Fig. 4.2, the diffusion coefficient of stannous ions in BMPOTF ionic liquid is approximately $2.11 \times 10^{-7} \text{ cm}^2 \text{ s}^{-1}$. Table 4.1 gives the diffusion coefficients of tin (II) in various types of ionic liquids.

Table 4.1 : Tin (II) diffusion coefficient from literature.

Solvent	Ref.	Tin (II) Dif. coefficient $D/\text{cm}^2 \text{ s}^{-1}$
Aqueous	[1]	6.5×10^{-6}
1-ethyl-3-methylimidazolium tetrafluoroborate	[6]	6.1×10^{-7}
1- <i>n</i> -butyl-1-methylpyrrolidinium bis (trifluoromethylsulfonyl) imide	[7]	1.0×10^{-7}
AlCl_3 with 1-Methyl-3-Ethyl Imidazolium chloride	[5]	5.3×10^{-7}
1-Butyl-1-Methylpyrrolidinium Trifluoro-Methanesulfonate	This work	2.11×10^{-7}

The dependency of the Diffusion coefficient to the viscosity and the radius of the diffusing species can be explained by the Stoke-Einstein equation, $D = kT / 6 \pi \eta r$ where k = Boltzmann constant, T = Kelvin temperature, η = viscosity of the solvent, r = dynamic radius of the diffusing species. Hussey et. al. ^[5] found that the Tin (II) exists as SnCl_4^{2-} in AlCl_3 with 1-methyl-3-ethyl imidazolium chloride ionic liquid and the low values of the diffusion coefficient was due to the increased viscosity of the ionic liquid. They also suggest that there is some degree of association between the tin (II) with chloroaluminate ions such as AlCl_4^- and Al_2Cl_7^- , which contribute to the low value of the diffusion coefficient ^[5].

W. Yang et. al. ^[6] used tetrafluoroborate, BF_4^- based ionic liquid, where the diffusion coefficient was higher than calculated from the chloroaluminate ionic liquid by Hussey. From the Stoke-Einstein equation, it can be seen that the smaller tin (II) tetrafluoroborate species will contribute to a slightly higher diffusion coefficient value for the tin (II) species.

Studies using trifluoromethylsulfonyl imide ionic liquids from Tachikawa et. al.^[7] and this work using trifluoromethylsulfonate ionic liquid gave smaller diffusion coefficient for the tin (II) species. It can be suggested that the complexation between the tin (II) with trifluoromethylsulfonate and trifluoromethylsulfonyl imide, which is larger than the chloride ion and the tetrafluoroborate ion, has increased the radius of the tin (II) species in solution. This contributes to the lower diffusion coefficient compared to the chloride and tetrafluoroborate based ionic liquids in the works of Hussey and Tachikawa.

4.3 Bulk Electrodeposition

Electroplating on copper surface (2 cm x 2 cm) was carried out to estimate the plating current efficiency for tin electrodeposition from tin (II) methanesulfonate dissolved in BMPOTF with MSA as the solvent.

Scanning electron microscopy and EDX were used to examine the surface morphology and analyze the elemental compositions of the electrodeposits. The current efficiency is defined as the proportion of the current that is used in the specified reaction: The unused portion in this process is considered a waste. Thus, the current efficiency for metal deposition ϕ is defined as the ratio of the experimental mass of electrodeposition to the theoretical mass of electrodeposition. Thus,

$$\phi (pct) = \frac{Mass (experimental)}{Mass (theoretical)} \times 100 \quad (Eq. 6)$$

The efficiencies are not always 100 % as hydrogen evolution, oxygen reduction, and solvent decomposition can occur at the cathode.^[5,10] The Faraday's law

$$Q = I \times t \quad (\text{Eq. 7})$$

$$m = \frac{Q M}{F n} \quad (\text{Eq. 8})$$

where m is the theoretical mass of the substance produced at the electrode (in grams), Q is the total electric charge that passed through the solution (in coulombs), n is the number of the electron transferred in the electron transfer step, $F = 96,485 \text{ C mol}^{-1}$ is Faraday's constant, and M is the molar mass of tin (in g mol^{-1}).

Table 4.2 : Current efficiencies of tin electrodeposition obtained at different tin (II) concentrations.

Current Density (A dm^{-2})	Tin(II) Concentration (M)				
	0.1	0.2	0.3	0.4	0.5
1.0	99.58	99.58	98.90	98.23	94.84
2.0	99.92	98.23	98.23	97.89	87.73
3.0	99.81	96.42	98.00	97.78	81.07
4.0	99.24	98.74	97.89	97.04	72.65
5.0	99.58	98.63	97.01	96.87	66.25
6.0	99.70	97.66	96.87	95.97	61.65
7.0	98.71	97.55	96.29	94.55	58.26

Table 4.2 shows the current efficiencies obtained from experiments using current densities from 1 A dm^{-2} (ASD) to 7 ASD for various concentrations of tin (II) from 0.1 M to 0.5 M in ionic liquids solutions. From the results, increasing current densities for higher concentrations of tin (II) such as 0.4 M and 0.5 M gave decreasing current efficiencies for tin deposition. From the solution preparation, 0.5 M has the highest water content, and at these conditions, the hydrogen evolution reaction from the presence of water becomes prominent and decreases the current efficiency for the tin deposition. The deposits became dull and less reflecting in appearance because of the porous nature of the surface as can be observed in Figure 4.8.

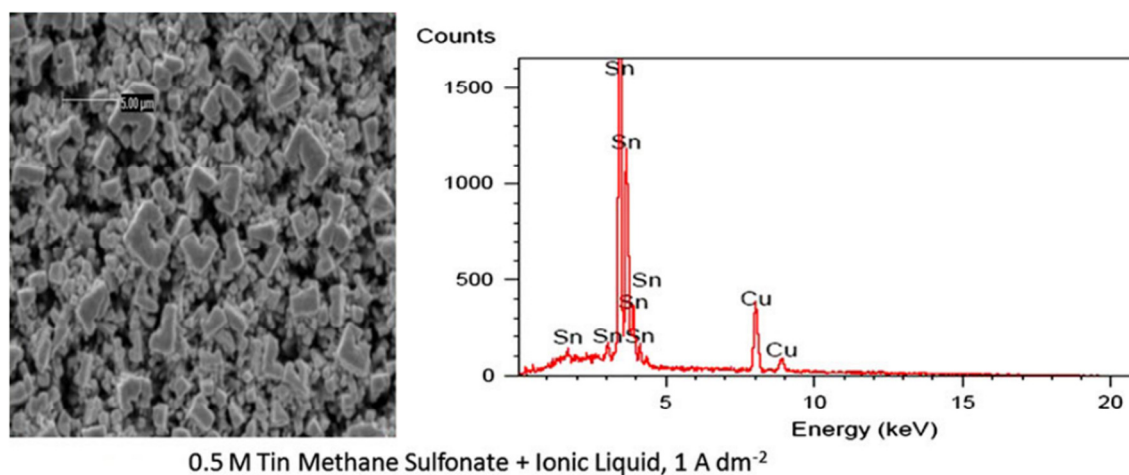


Figure 4.6 : SEM (3500 times magnification) and EDX spectrum of tin electrodeposited from 0.5 M tin (II) methanesulfonate solution at 1 A dm^{-2} .

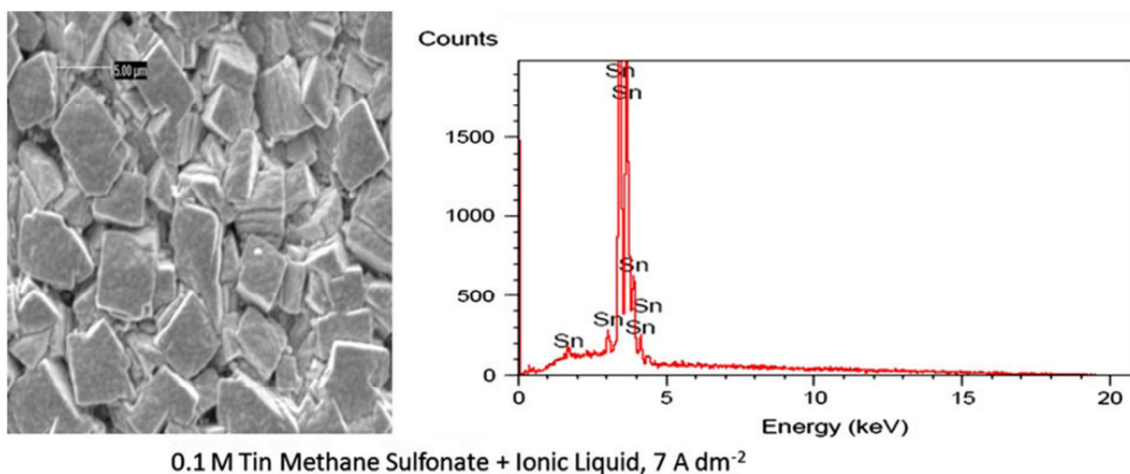


Figure 4.7 : SEM (3500 times magnification) and EDX spectrum of tin electrodeposited from 0.1 M tin (II) methanesulfonate solution at 7 A dm⁻².

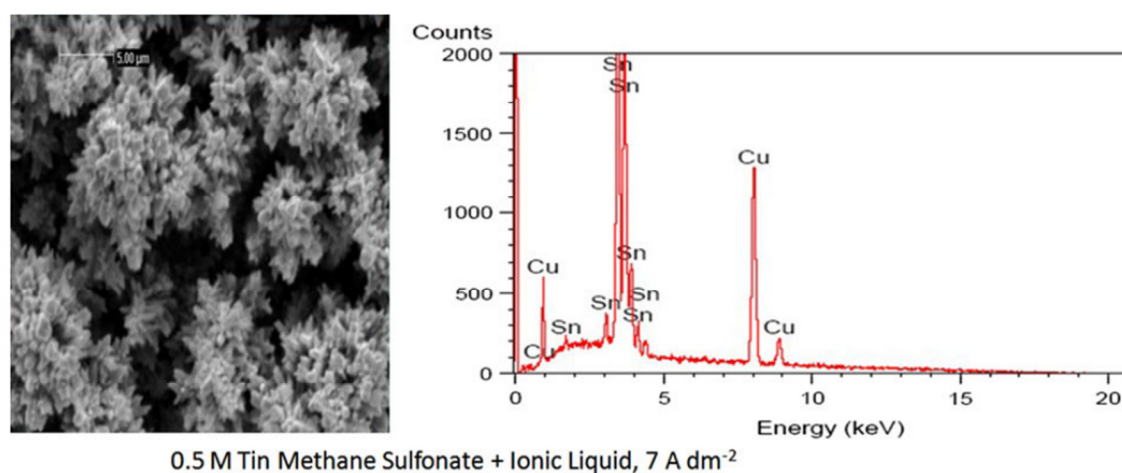


Figure 4.8 : SEM (3500 times magnification) and EDX spectrum of tin electrodeposited from 0.5 M tin (II) methanesulfonate solution at 7 A dm⁻².

Scanning electron microscopy from Figure 4.6 through Figure 4.8 were at 3500 times magnification reveal that the deposits became less compact, less dense, and more porous for higher current densities and higher concentrations of tin (II). The poor

quality of deposits with increasing amount of tin (II) concentration is expected as higher concentrations of tin (II) prepared from the stock solution contained slightly more percentage of water compared with lower tin (II) concentrations, thus facilitating the hydrogen evolution process. As for the poor quality of deposit with increasing current density, the increase in current density will result in the increase toward negative potentials where the hydrogen evolution reaction and solvent decomposition are more dominant than metal electro-deposition. This behavior is quite similar with previous works involving platinum,^[10,11] nickel^[12,13] and nickel-cobalt alloy.^[14,15] The poor quality and porous nature of the deposits can be also observed in the EDX results in Figures 4.6 and Figure 4.8. The copper element was present in the EDX spectrum at the tin-plated surface when analyzed under 20 keV EDX as shown in Figures 4.6 and Figure 4.8 when done with higher current densities of 7 A dm^{-2} and higher tin (II) concentration of 0.5 M of tin (II), which shows copper peaks from the copper substrate, because of the porous nature of the deposits.

Part II: Results and Discussion for Electrodeposition of Tin from Tin (II)

Methanesulfonate and Methane Sulfonic Acid Solution.

4.4 Cyclic Voltammetry Characterization for Sn Thin Films

Cyclic voltammetry (CV) is used to investigate electrochemical properties of an analyte in solution. It is a type of potentiodynamic electrochemical measurement. Cyclic voltammogram is the result of cyclic voltammetry experiment. In cyclic voltammogram, current versus potential graph is plotted. The cyclic voltammogram has the information of REDOX potentials for the researched analytes. The cyclic voltammetry experiment was performed by cathodic scan followed by anodic scan to achieve a cycle of REDOX activities of the researched analytes.

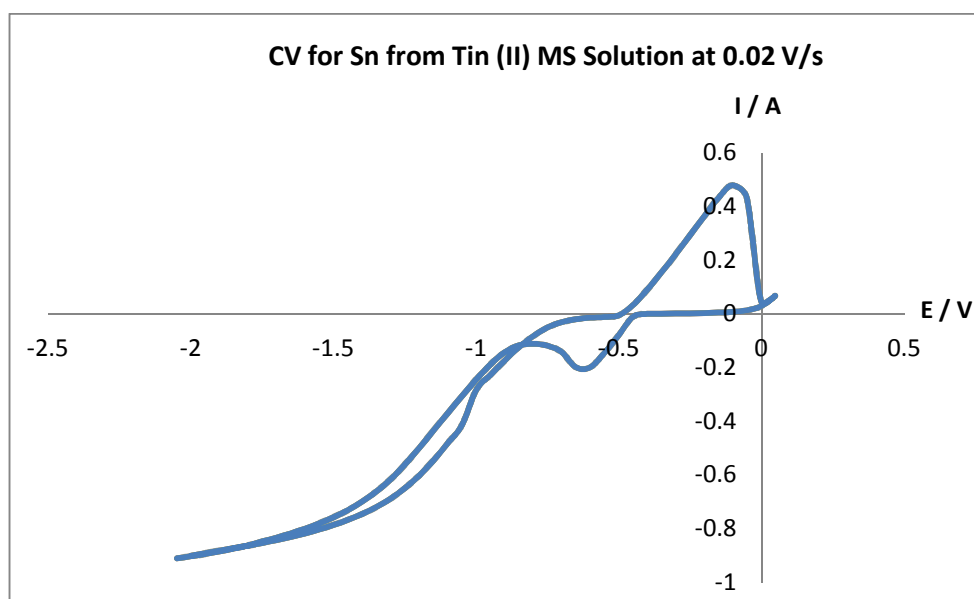


Figure 4.9 : The cyclic voltammogram for electro-deposition of Sn at the scan rate of 0.02 V/s.

The Figure 4.9 shows the cyclic voltammogram for the solution of 100ml of 0.01M tin (II) methanesulfonate (50%w/v) and 40ml methane sulfonic acid ($\geq 99.5\%$). Reference electrode used was SCE electrode, counter electrode used was platinum wire, and copper substrate was working electrode. The scan rate was 0.02 V/s. From the cyclic voltammogram result, the reduction potential peak to form Sn solid, E_{pc} is -0.60V, where the cathodic peak current I_{pc} is -0.20A. The oxidation potential peak to form Sn^{2+} , E_{pa} is -0.10V, where the anodic peak current, I_{pa} is 0.47A. The Sn thin films were deposited on the copper substrate under different potentials, they are -1.30V, -1.40V, -1.50V, -1.60V, -1.70V and -1.80V.

4.5 Energy Dispersive X-Ray (EDX) characterization for Sn Thin Films

Elemental analysis and chemical characterization of thin film samples can be performed by Energy Dispersive X-Ray spectroscopy (EDX). It is because each element has unique atomic structure which can be reflected as unique set of peaks on the X-ray spectrum. Thus, the elemental composition also can be measured by EDX method. (SEM-EDX machine LEICA S440 was used in this study).

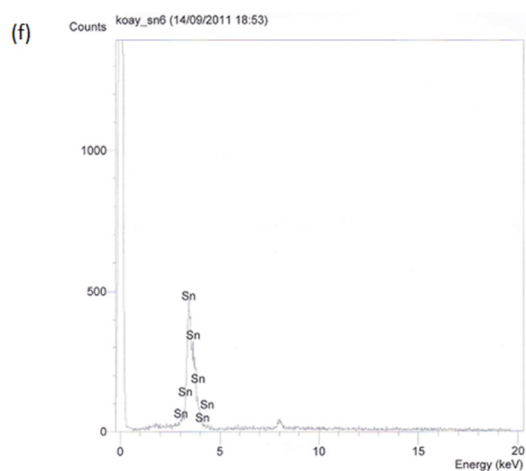
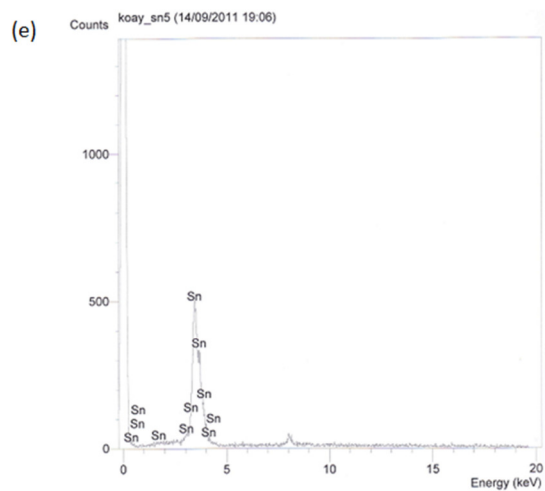
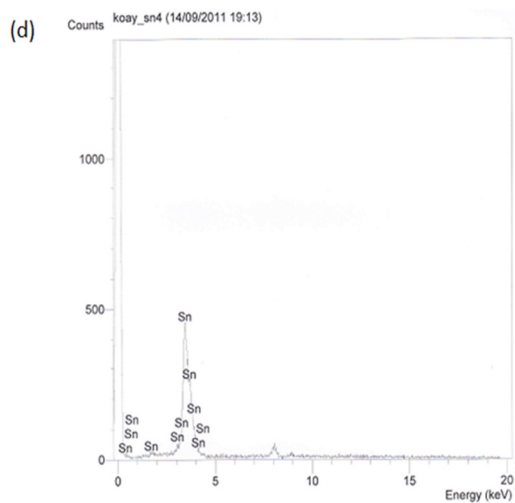
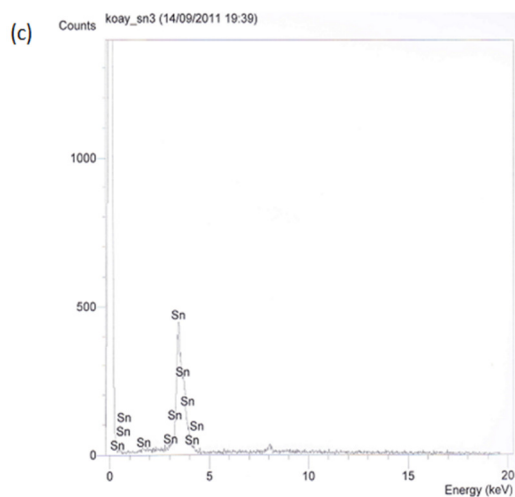
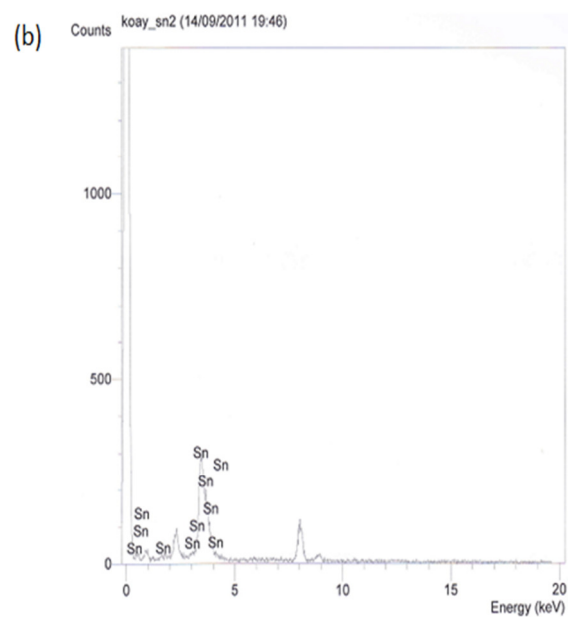
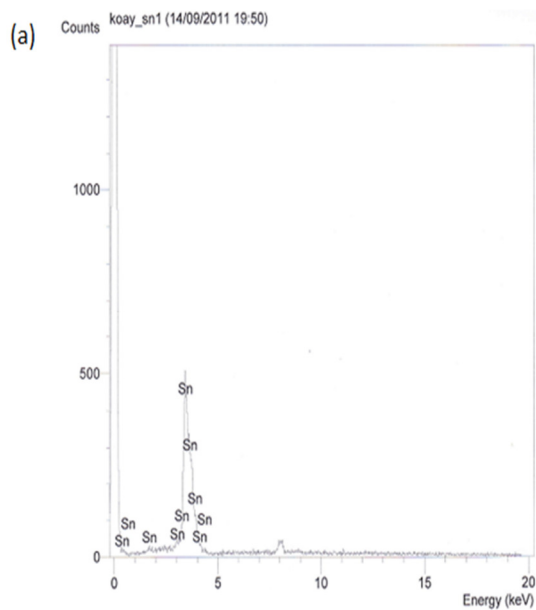


Figure 4.10: EDX characterization for electro-deposition of Sn on Copper Substrate at the potentials of (a) -1.30V, (b) -1.40V, (c) -1.50V, (d) -1.60V, (e) -1.70V and (f) -1.80V.

The EDX results shown in Figure 4.10 (a) prove that the Sn thin film can be deposited on the copper substrate at the potential of -1.30V. The tin element is the only element deposited from the tin (II) methanesulfonate solution at the potential of -1.30V.

The EDX results shown in Figure 4.10 (b) prove that the Sn thin film can be deposited on the copper substrate at the potential of -1.40V. The tin element is the only element deposited from the tin (II) methanesulfonate solution at the potential of -1.40V.

The EDX results shown in Figure 4.10 (c) prove that the Sn thin film can be deposited on the copper substrate at the potential of -1.50V. The tin element is the only element deposited from the tin (II) methanesulfonate solution at the potential of -1.50V.

The EDX results shown in Figure 4.10 (d) prove that the Sn thin film can be deposited on the copper substrate at the potential of -1.60V. The tin element is the only element deposited from the tin (II) methanesulfonate solution at the potential of -1.60V.

The EDX results shown in Figure 4.10 (e) prove that the Sn thin film can be deposited on the copper substrate at the potential of -1.70V. The tin element is the only element deposited from the tin (II) methanesulfonate solution at the potential of -1.70V.

The EDX results shown in Figure 4.10 (f) prove that the Sn thin film can be deposited on the copper substrate at the potential of -1.80V. The tin element is the only element deposited from the tin (II) methanesulfonate solution at the potential of - 1.80V .

4.6 X-ray Diffraction (XRD) characterization for Sn Thin Films

The XRD results indicate that, the tin thin film deposited on the copper substrate has the body-centered tetragonal lattice. The XRD results attained is compared with the JCPDS data with the JCP catalog number of [JCP2.2CA: 01-086-2264] (ICSD number: 040037). The XRD radiation source is $\text{CuK}\alpha 1$ and the lambda value is 1.54056 Å. The d-spacing is obtained by diffractometer techniques performed by XRD machine. The XRD results are characterized according to the Bragg's law and Bragg's equation, $2d\sin\theta = n\lambda$, where θ is the angle of incident angle and scattering angle for XRD radiation, d is the value of the spacing distance between the lattice, lambda is the wavelength of the radiation and n is the integer number.

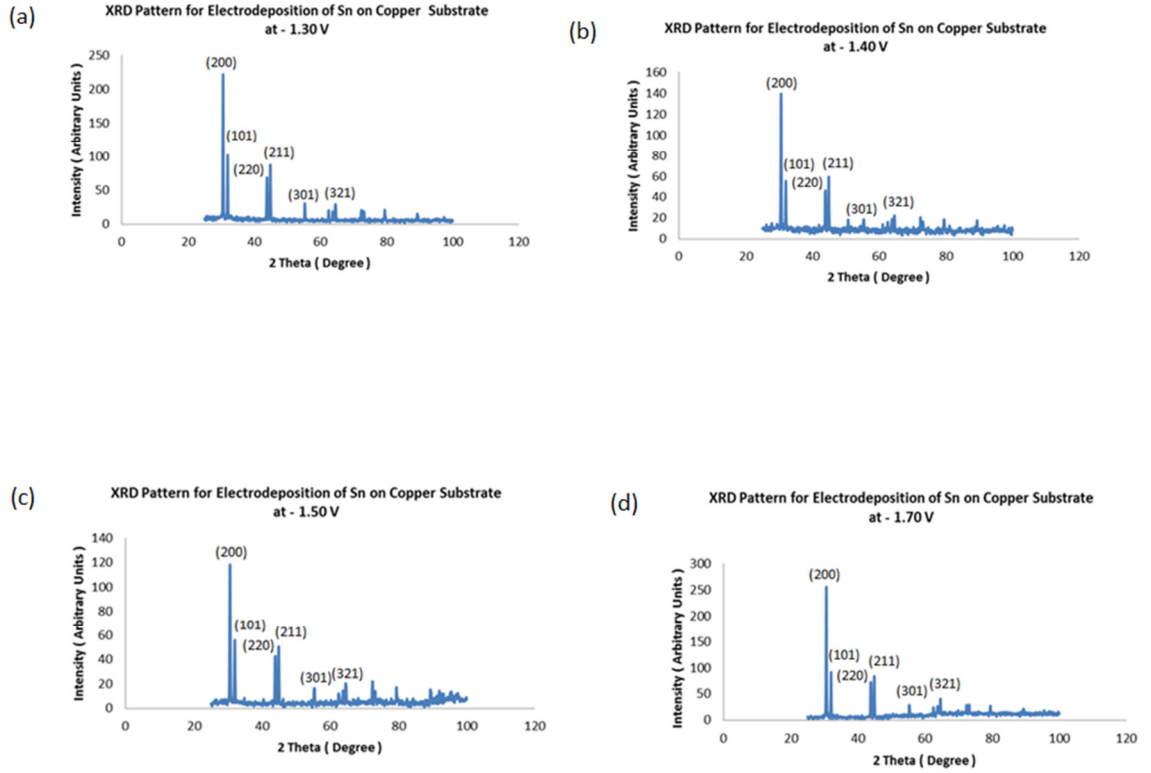


Figure 4.11: XRD characterization for electro-deposition of Sn on Copper Substrate at the potentials of (a) -1.30V, (b) -1.40V , (c) -1.50V, (d) -1.70V.

Figure 4.11 (a) indicates that the Sn thin film deposited on the copper substrate at the potential of -1.30V has the d-spacing value of 2.91530 \AA at the strongest intensity. The Miller Indices value at the strongest intensity is (200). The incident angle for the radiation, θ at the strongest intensity is 15.321° . The second strongest intensity happened at the d-spacing of 2.79400 \AA . The Miller Indices value at the second strongest intensity is (101). The incident angle for the radiation, θ at the second strongest intensity is 16.0035° . The third strongest intensity happened at the d-spacing of 2.01674 \AA . The Miller Indices value at the second strongest intensity is (211). The incident angle for the radiation, θ at the third strongest intensity is 22.4545° . The fourth strongest intensity happened at the d-spacing of 2.06140 \AA . The Miller Indices value at the second strongest

intensity is (220). The incident angle for the radiation, θ at the fourth strongest intensity is 21.9425° . Therefore, the tin thin film deposited on the copper substrate at the potential of -1.30V has the body-centered tetragonal lattice.

Figure 4.11 (b) indicates that the Sn thin film deposited on the copper substrate at the potential of -1.40V has the d-spacing value of 2.91530 \AA at the strongest intensity. The Miller Indices value at the strongest intensity is (200). The incident angle for the radiation, θ at the strongest intensity is 15.321° . The second strongest intensity happened at the d-spacing of 2.79400 \AA . The Miller Indices value at the second strongest intensity is (101). The incident angle for the radiation, θ at the second strongest intensity is 16.0035° . The third strongest intensity happened at the d-spacing of 2.01674 \AA . The Miller Indices value at the third strongest intensity is (211). The incident angle for the radiation, θ at the third strongest intensity is 22.4545° . The fourth strongest intensity happened at the d-spacing of 2.06140 \AA . The Miller Indices value at the fourth strongest intensity is (220). The incident angle for the radiation, θ at the fourth strongest intensity is 21.9425° . Therefore, the tin thin film deposited on the copper substrate at the potential of -1.40V has the body-centred tetragonal lattice.

Figure 4.11 (c) indicates that the Sn thin film deposited on the copper substrate at the potential of -1.50V has the d-spacing value of 2.91530 \AA at the strongest intensity. The Miller Indices value at the strongest intensity is (200). The incident angle for the radiation, θ at the strongest intensity is 15.321° . The second strongest intensity happened at the d-spacing of 2.79400 \AA . The Miller Indices value at the second strongest intensity is (101). The incident angle for the radiation, θ at the second strongest intensity

is 16.0035° . The third strongest intensity happened at the d-spacing of 2.01674 \AA . The Miller Indices value at the third strongest intensity is (211). The incident angle for the radiation, θ at the third strongest intensity is 22.4545° . The fourth strongest intensity happened at the d-spacing of 2.06140 \AA . The Miller Indices value at the fourth strongest intensity is (220). The incident angle for the radiation, θ at the fourth strongest intensity is 21.9425° . Therefore, the tin thin film deposited on the copper substrate at the potential of -1.50V has the body-centred tetragonal lattice.

Figure 4.11 (d) indicates that the Sn thin film deposited on the copper substrate at the potential of -1.70V has the d-spacing value of 2.91530 \AA at the strongest intensity. The Miller Indices value at the strongest intensity is (200). The incident angle for the radiation, θ at the strongest intensity is 15.321° . The second strongest intensity happened at the d-spacing of 2.79400 \AA . The Miller Indices value at the second strongest intensity is (101). The incident angle for the radiation, θ at the second strongest intensity is 16.0035° . The third strongest intensity happened at the d-spacing of 2.01674 \AA . The Miller Indices value at the third strongest intensity is (211). The incident angle for the radiation, θ at the third strongest intensity is 22.4545° . The fourth strongest intensity happened at the d-spacing of 2.06140 \AA . The Miller Indices value at the fourth strongest intensity is (220). The incident angle for the radiation, θ at the fourth strongest intensity is 21.9425° . Therefore, the tin thin film deposited on the copper substrate at the potential of -1.70V has the body-centred tetragonal lattice.

Part III: Results and Discussion for Electrodeposition of Tin Sulfide from Tin (II) Methanesulfonate and Methane Sulfonic Acid Solution.

4.7 Cyclic Voltammetry Characterization

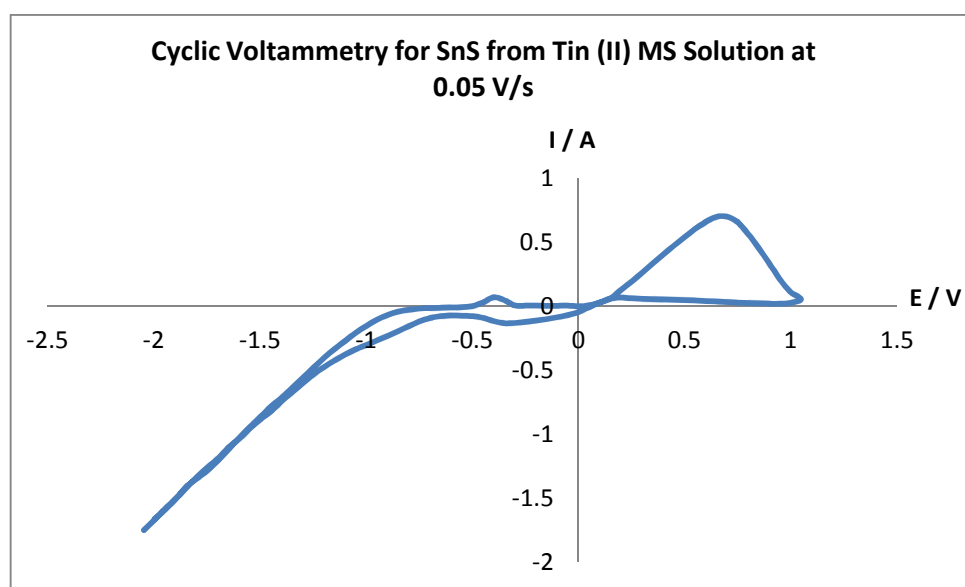
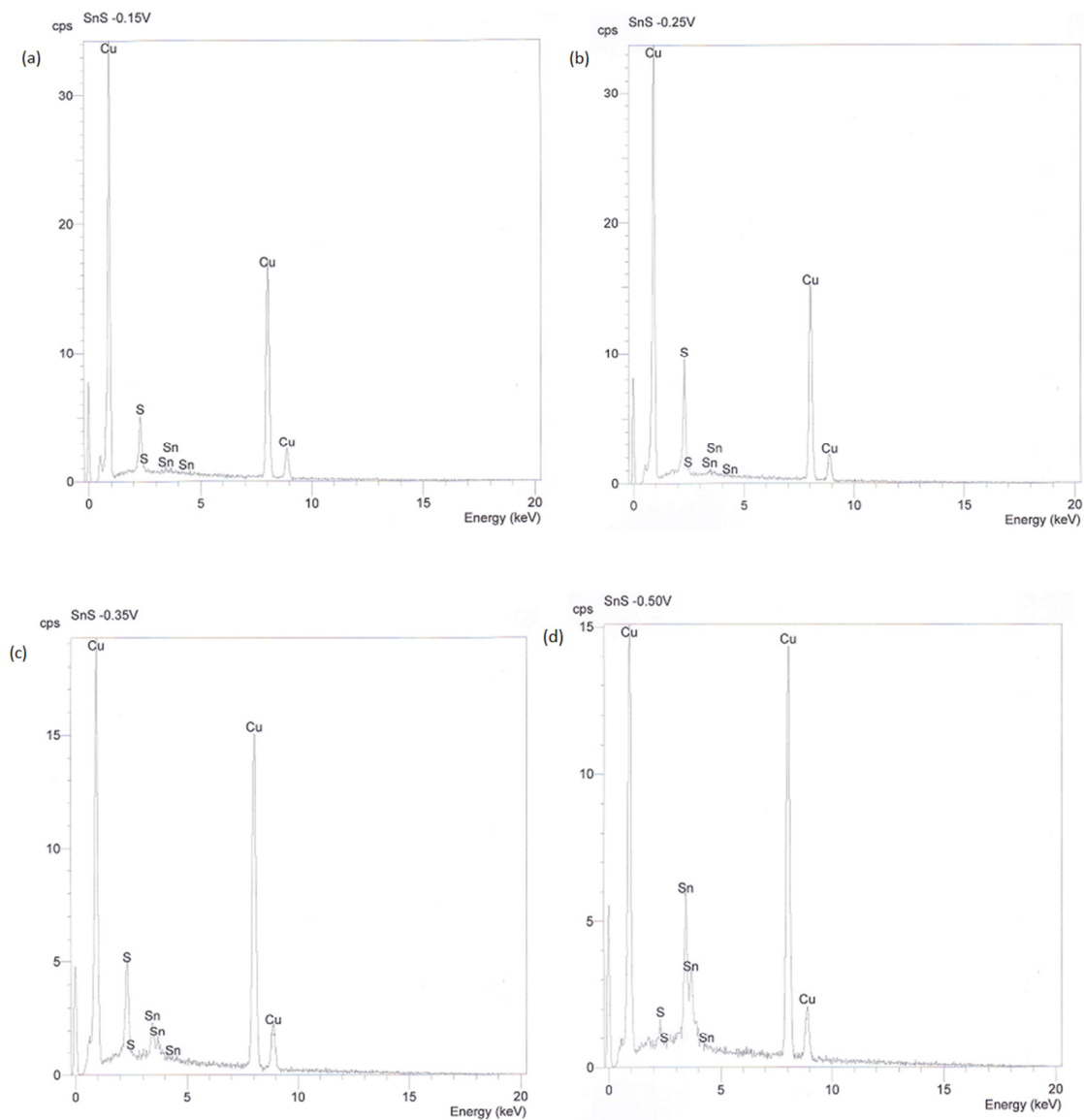


Figure 4.12: The cyclic voltammogram for electro-deposition of SnS at the scan rate of 0.05 V/s.

The Figure 4.12 showed the cyclic voltammogram result for the solution containing 100ml of 0.01M tin (II) methanesulfonate (50%w/v), 0.01M $\text{Na}_2\text{S}_2\text{O}_3$ and 40ml Methane Sulfonic Acid ($\geq 99.5\%$). Reference electrode used was SCE electrode, counter electrode used was platinum wire, and copper substrate was the working electrode. The scan rate was 0.05 V/s. From the cyclic voltammogram result, considering the negative potential region, the reduction potential peak to form SnS thin film, E_{pc} is -0.29V, where the cathodic peak current, I_{pc} is -0.13A. The oxidation potential peak, E_{pa} is -0.44V, where the anodic peak current, I_{pa} is 0.029A.

4.8 Energy Dispersive X-Ray (EDX) characterization



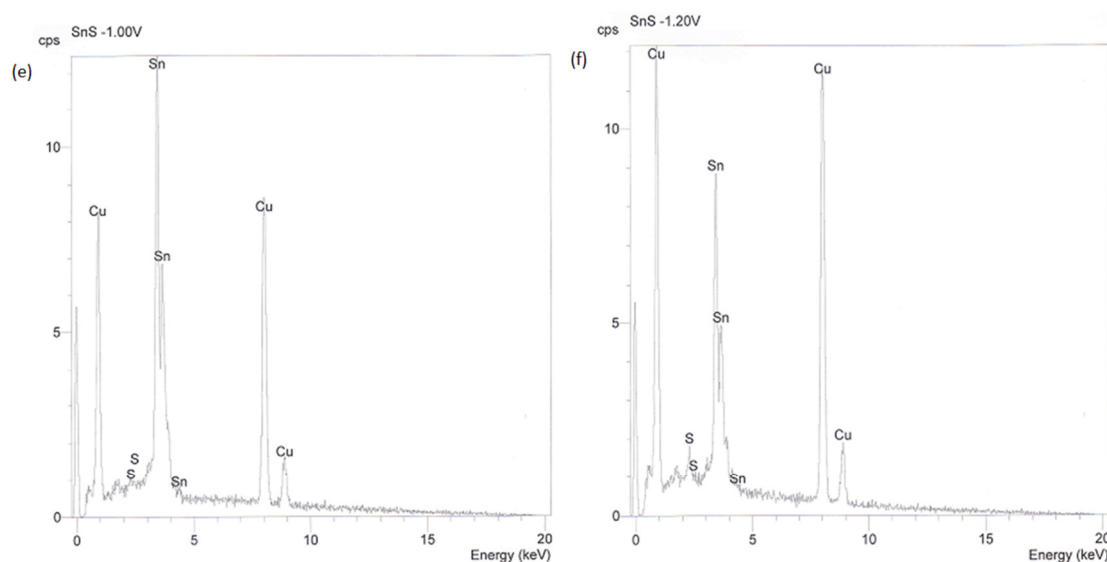


Figure 4.13: EDX characterization for electro-deposition of SnS on Copper Substrate at the potentials of (a) -0.15V, (b) -0.25V, (c) -0.35V, (d) -0.50V, (e) -1.00V and (f) -1.20V.

The EDX results shown in Figure 4.13 (a) proves that the SnS thin film can be deposited on the copper substrate at the potential of -0.15V by using tin (II) methanesulfonate solution containing natrium thiosulfate ($\text{Na}_2\text{S}_2\text{O}_3$). The tin and sulfur elements are the elements deposited on the copper substrate from the tin (II) methanesulfonate solution containing natrium thiosulfate ($\text{Na}_2\text{S}_2\text{O}_3$) at the potential of -0.15V. The element weight percentage is shown in the ratio of Sn : S equals to 27.57 : 72.43. In term of element weight percentage, the SnS thin film deposited at the potential of -0.15V containing 27.57% of Sn and 72.43% of S. Therefore, for the deposition of SnS at the potential of -0.15V, the sulfur element has higher element percentage than the tin element.

The EDX results shown in Figure 4.13 (b) proves that the SnS thin film can be deposited on the copper substrate at the potential of -0.25V by using tin (II) methanesulfonate solution containing natrium thiosulfate ($\text{Na}_2\text{S}_2\text{O}_3$). The tin and sulfur elements are the elements deposited on the copper substrate from the tin (II) methanesulfonate solution containing natrium thiosulfate ($\text{Na}_2\text{S}_2\text{O}_3$) at the potential of -0.25V. The element weight percentage is shown in the ratio of Sn : S equals to 15.92 : 84.08. In term of element weight percentage, the SnS thin film deposited at the potential of -0.25V containing 15.92% of Sn and 84.08% of S. Therefore, for the deposition of SnS at the potential of -0.25V, the sulfur element has higher element percentage than the tin element.

The EDX results shown in Figure 4.13 (c) proves that the SnS thin film can be deposited on the copper substrate at the potential of -0.35V by using tin (II) methanesulfonate solution containing natrium thiosulfate ($\text{Na}_2\text{S}_2\text{O}_3$). The tin and sulfur elements are the elements deposited on the copper substrate from the tin (II) methanesulfonate solution containing natrium thiosulfate ($\text{Na}_2\text{S}_2\text{O}_3$) at the potential of -0.35V. The element weight percentage is shown in the ratio of Sn : S equals to 58.82 : 41.18. In term of element weight percentage, the SnS thin film deposited at the potential of -0.35V containing 58.82% of Sn and 41.18% of S. For the electrodeposition of SnS at the potential of -0.35V, the element percentage is very close for Sn element and S element. Therefore, the electrodeposition potential of -0.35V is very suitable for the fabrication of SnS thin film on copper substrate by using tin (II) methanesulfonate mixture of solutions.

The EDX results shown in Figure 4.13 (d) proves that the SnS thin film can be deposited on the copper substrate at the potential of -0.50V by using tin (II) methanesulfonate solution containing natrium thiosulfate ($\text{Na}_2\text{S}_2\text{O}_3$). The tin and sulfur elements are the elements deposited on the copper substrate from the tin (II) methanesulfonate solution containing natrium thiosulfate ($\text{Na}_2\text{S}_2\text{O}_3$) at the potential of -0.50V. The element weight percentage is shown in the ratio of Sn : S equals to 96.30 : 3.70. In term of element weight percentage, the SnS thin film deposited at the potential of -0.50V containing 96.30% of Sn and 3.70% of S. Therefore, for the deposition of SnS at the potential of -0.50V, the tin element has higher element percentage than the sulfur element.

The EDX results shown in Figure 4.13 (e) proves that the SnS thin film can be deposited on the copper substrate at the potential of -1.00V by using tin (II) methanesulfonate solution containing natrium thiosulfate ($\text{Na}_2\text{S}_2\text{O}_3$). The tin and sulfur elements are the elements deposited on the copper substrate from the tin (II) methanesulfonate solution containing natrium thiosulfate ($\text{Na}_2\text{S}_2\text{O}_3$) at the potential of -1.00V. The element weight percentage is shown in the ratio of Sn : S equals to 99.47 : 0.53. In term of element weight percentage, the SnS thin film deposited at the potential of -1.00V containing 99.47% of Sn and 0.53% of S. Therefore, for the deposition of SnS at the potential of -1.00V, the tin element has higher element percentage than the sulfur element.

The EDX results shown in Figure 4.13 (f) proves that the SnS thin film can be deposited on the copper substrate at the potential of -1.20V by using tin (II)

methanesulfonate solution containing sodium thiosulfate ($\text{Na}_2\text{S}_2\text{O}_3$). The tin and sulfur elements are the elements deposited on the copper substrate from the tin (II) methanesulfonate solution containing sodium thiosulfate ($\text{Na}_2\text{S}_2\text{O}_3$) at the potential of -1.20V. The element weight percentage is shown in the ratio of Sn : S equals to 97.66 : 2.34. In term of element weight percentage, the SnS thin film deposited at the potential of -1.20V containing 97.66% of Sn and 2.34% of S. Therefore, for the deposition of SnS at the potential of -1.20V, the tin element has higher element percentage than the sulfur element.

4.9 Scanning Electron Microscopy (SEM) Characterization

Images of sample can be obtained by using Scanning Electron Microscopy (SEM). The focused beam of electrons from SEM interacts with the electrons of the samples to produce signals which can be detected and interpreted because the signals carries the information of surface images of the samples. The surface images for the SnS thin films deposited were obtained by performing the SEM analysis. The SnS thin films are crystalline and with the variety of shapes and grain sizes at different reduction potentials. The SEM micrographs for the SnS thin films which was obtained at different deposition potentials are shown below. The SEM images below indicate that, at the deposition potentials of -0.15V, -0.25V and -0.35V, the nanowire shapes of the thin films are obtained. At the deposition potentials of -0.50V, the surface of the thin films has granules. At the deposition potentials of -1.00V, the granules are folded together in the dendritic growth. Whereas, at the deposition potentials of -1.20V, many granules are on the surface of the thin films, the granules seemed to be lumped together.

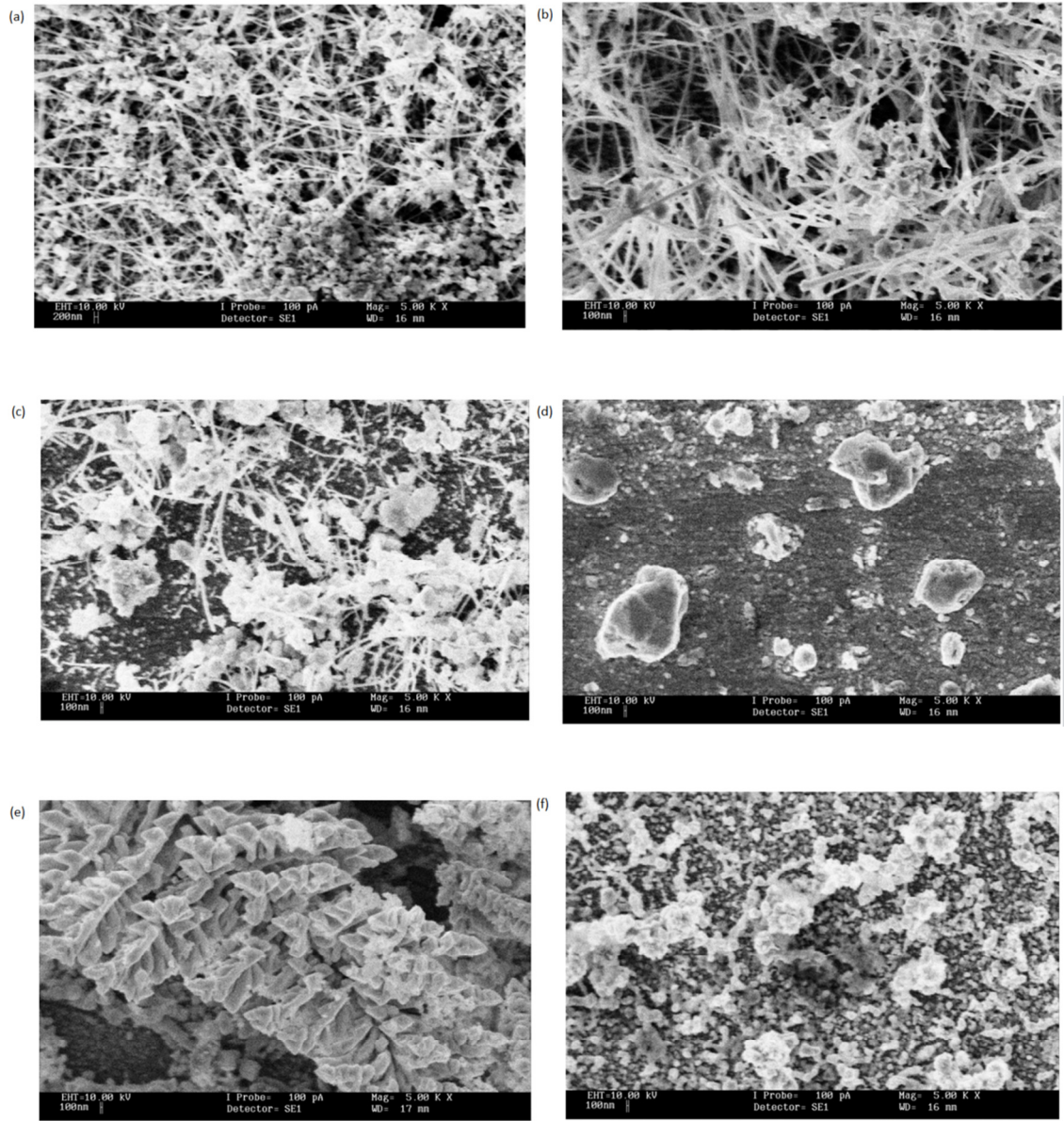


Figure 4.14: SEM characterization for electro-deposition of SnS on Copper Substrate at the potentials of (a) -0.15V, (b) -0.25V, (c) -0.35V, (d) -0.50V, (e) -1.00V and (f) -1.20V.

4.10 X-ray Diffraction (XRD) Characterization

The XRD results indicate that, the SnS thin film deposited on the copper substrate has the orthorhombic lattice. The XRD results attained is compared with the

JCPDS data with the JCP catalog number of [JCP2.2CA: 01-075-0925] (ICSD number: 030271). (XRD machine BRUKER model D5000 was used in this study).

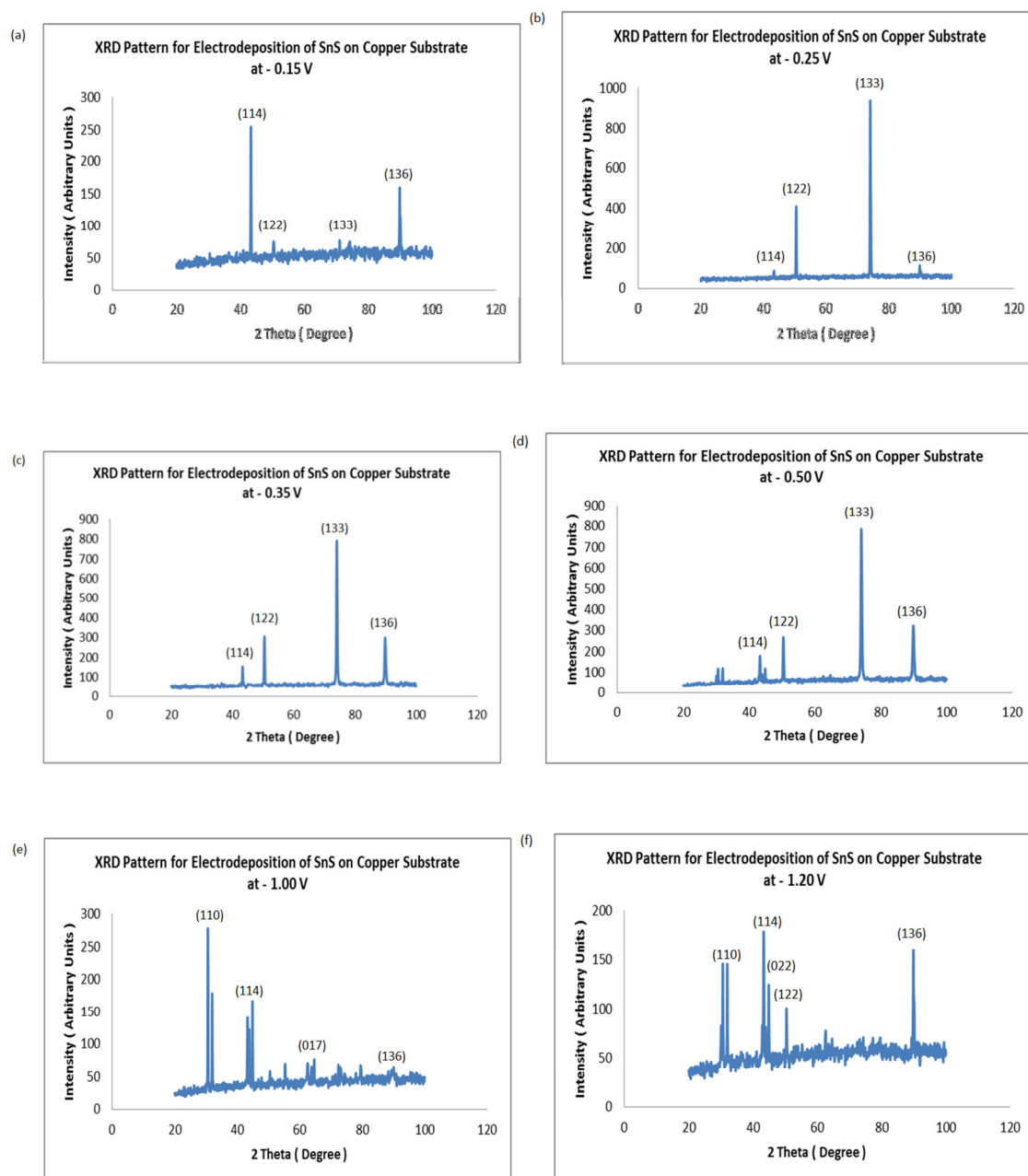


Figure 4.15: XRD characterization for electro-deposition of SnS on Copper Substrate at the potentials of (a) -0.15V, (b) -0.25V , (c) -0.35V, (d) -0.50V, (e) -1.00V and (f) -1.20V.

SnS thin film deposited on the copper substrate at the potential of -0.15V has the d-spacing value of 2.08960 Å at the strongest intensity. The Miller Indices value at the strongest intensity is (114). The incident angle for the radiation, θ at the strongest intensity is 21.6315°. The second strongest intensity happened at the d-spacing of 1.09008 Å. The Miller Indices value at the second strongest intensity is (136). The incident angle for the radiation, θ at the second strongest intensity is 44.963°. Therefore, the SnS thin film deposited on the copper substrate at the potential of -0.15V has the orthorhombic lattice.

SnS thin film deposited on the copper substrate at the potential of -0.25V has the d-spacing value of 1.27883 Å at the strongest intensity. The Miller Indices value at the strongest intensity is (133). The incident angle for the radiation, θ at the strongest intensity is 37.038°. The second strongest intensity happened at the d-spacing of 1.80903 Å. The Miller Indices value at the second strongest intensity is (122). The incident angle for the radiation, θ at the second strongest intensity is 25.202°. Therefore, the SnS thin film deposited on the copper substrate at the potential of -0.25V has the orthorhombic lattice.

SnS thin film deposited on the copper substrate at the potential of -0.35V has the d-spacing value of 1.80680 Å at the strongest intensity. The Miller Indices value at the strongest intensity is (122). The incident angle for the radiation, θ at the strongest intensity is 25.235°. The second strongest intensity happened at the d-spacing of 2.08729 Å. The Miller Indices value at the second strongest intensity is (114). The incident angle for the radiation, θ at the second strongest intensity is 21.6565°.

Therefore, the SnS thin film deposited on the copper substrate at the potential of -0.35V has the orthorhombic lattice.

SnS thin film deposited on the copper substrate at the potential of -0.50V has the d-spacing value of 1.27708 Å at the strongest intensity. The Miller Indices value at the strongest intensity is (133). The incident angle for the radiation, θ at the strongest intensity is 37.0975°. The second strongest intensity happened at the d-spacing of 1.09031 Å. The Miller Indices value at the second strongest intensity is (136). The incident angle for the radiation, θ at the second strongest intensity is 44.9505°. Therefore, the SnS thin film deposited on the copper substrate at the potential of -0.50V has the orthorhombic lattice.

SnS thin film deposited on the copper substrate at the potential of -1.00V has the d-spacing value of 2.92177 Å at the strongest intensity. The Miller Indices value at the strongest intensity is (110). The incident angle for the radiation, θ at the strongest intensity is 15.2865°. The second strongest intensity happened at the d-spacing of 2.02141 Å. The Miller Indices value at the second strongest intensity is (114). The incident angle for the radiation, θ at the second strongest intensity is 22.40°. Therefore, the SnS thin film deposited on the copper substrate at the potential of -1.00V has the orthorhombic lattice.

SnS thin film deposited on the copper substrate at the potential of -1.20V has the d-spacing value of 2.08784 Å at the strongest intensity. The Miller Indices value at

the strongest intensity is (114). The incident angle for the radiation, θ at the strongest intensity is 21.6505° . The second strongest intensity happened at the d-spacing of 1.08973 \AA . The Miller Indices value at the second strongest intensity is (136). The incident angle for the radiation, θ at the second strongest intensity is 44.981° . Therefore, the SnS thin film deposited on the copper substrate at the potential of -1.20V has the orthorhombic lattice.

4.11 Atomic Force Microscopy (AFM) Characterization

Atomic Force Microscopy was used to study the surface structure and morphology of researched thin films. AFM VEECO model D3000 was used in AFM characterization.

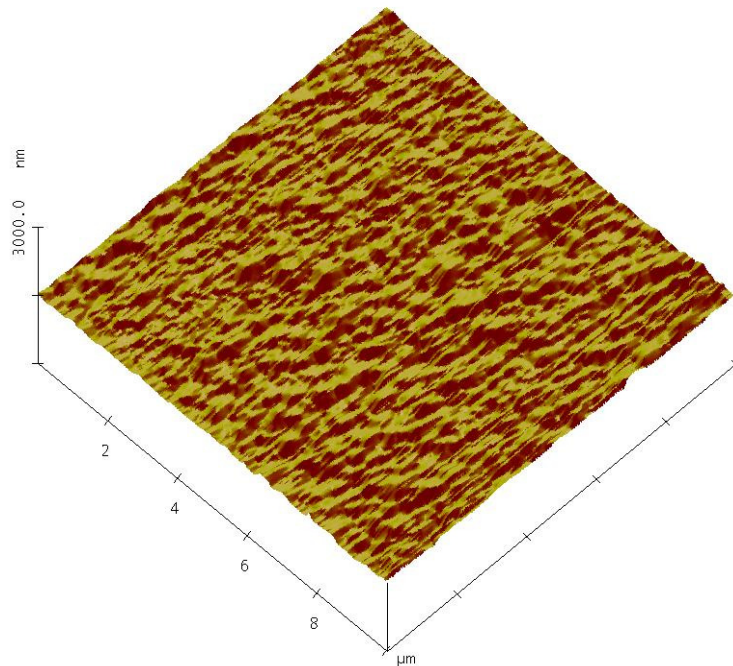


Figure 4.16 : AFM characterization for electro-deposition of SnS on Copper Substrate at the potential of -0.35 V .

The Figure 4.16 indicates the surface morphology characterized by the AFM at the height of 1500nm for the SnS thin film deposited on copper substrate at the potential of -0.35V. The scan size is 10.00 μm and the scan rate is 1.001 Hz. The grain size mean of the thin film is $4.07006 \times 10^5 \text{ nm}^2$. The grain size standard deviation is $1.874 \mu\text{m}^2$. Minimum grain size is 381.47 nm^2 and the maximum grain size is $17.012 \mu\text{m}^2$. The roughness analysis was conducted by using AFM for the surface area of $62.955 \mu\text{m}^2$. The Root Mean Square of the roughness is 24.568 nm. The mean roughness is 18.469 nm. The depth at maximum is 140.67 nm.

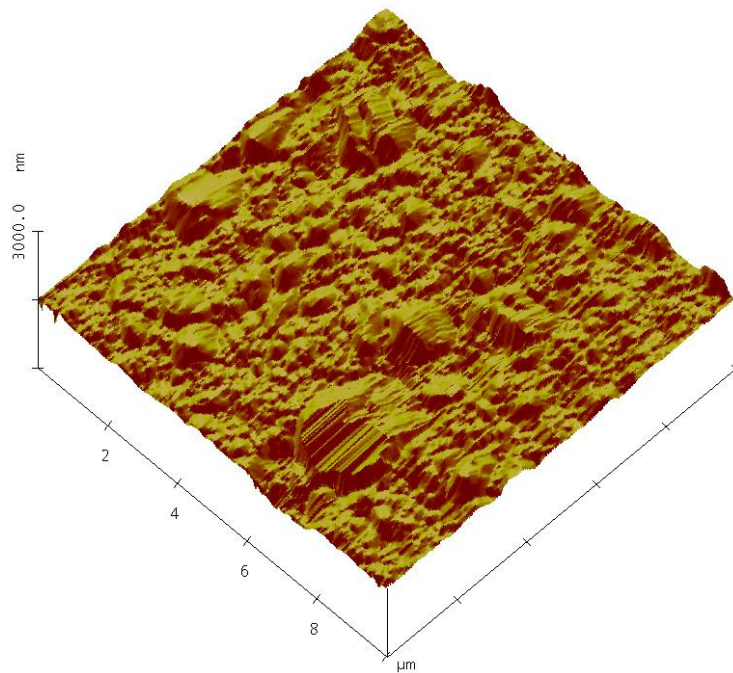


Figure 4.17 : AFM characterization for electro-deposition of SnS on Copper Substrate at the potential of -0.50 V.

The Figure 4.17 indicates the surface morphology characterized by the AFM for the SnS thin film deposited on copper substrate at the potential of -0.50V. The scan size is 10.00 μm and the scan rate is 1.001 Hz. The grain size mean of the thin film is $6.90041 \times 10^5 \text{ nm}^2$. The grain size standard deviation is $2.669 \mu\text{m}^2$. Minimum grain size is 381.47 nm^2 and the maximum grain size is $16.851 \mu\text{m}^2$. The roughness analysis was conducted by using AFM for the surface area of $25.762 \mu\text{m}^2$. The Root Mean Square of the roughness is 40.032 nm. The mean roughness is 29.119 nm. The depth at maximum is 319.84 nm.

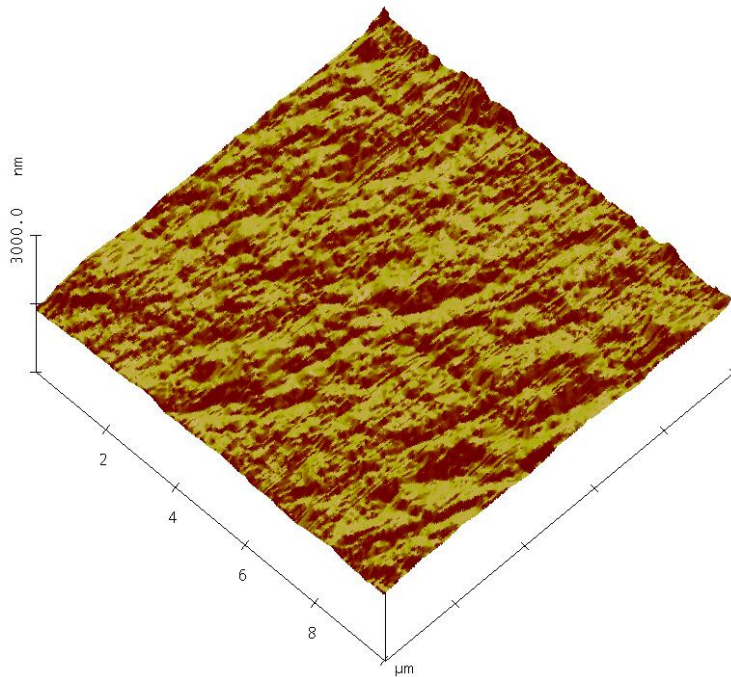


Figure 4.18 : AFM characterization for electro-deposition of SnS on Copper Substrate at the potential of -1.00 V.

The Figure 4.18 indicates the surface morphology characterized by the AFM for the SnS thin film deposited on copper substrate at the potential of -1.00V. The scan size is 10.00 μm and the scan rate is 1.001 Hz. The grain size mean of the thin film is $4.60568 \times 10^5 \text{ nm}^2$. The grain size standard deviation is $1.959 \mu\text{m}^2$. Minimum grain size is 381.47 nm^2 and the maximum grain size is $16.416 \mu\text{m}^2$. The roughness analysis was conducted by using AFM for the surface area of $71.169 \mu\text{m}^2$. The Root Mean Square of the roughness is 29.036 nm. The mean roughness is 22.723 nm. The depth at maximum is 178.58 nm.

4.12 Comparative Discussion :

R. Mariappana and T. Mahalingamb reported the direct band gap for the SnS thin film was 1.1 eV ^[42]. And, Y. Jayasree and U. Chalapathi reported the direct band gap for their researched SnS thin film was 1.55 eV. M. Calixto-Rodriguez and H. Martinez reported the direct band gap of SnS thin film was 1.30 eV. N. Koteswara Reddy and K.T. Ramakrishna Reddy reported that direct band gap for SnS thin film was 1.32 eV ^[43]. Whereas SnS₂ thin film direct band gap can reached 2.2 eV.

The band gap is the energy difference (in electron volts) between the valence band and the conduction band in semiconductors. This can referred as energy required to free an outer shell electron from its orbit about the nucleus to become a mobile charge carrier, able to move freely within the solid thin film.

The optical band gap, E_g , values are calculated by assuming a direct transition between the edges of the valence and the conduction bands, for which the variation of the absorption coefficient, α , with photon energy is given by

$$(\alpha h\nu)^n = A (h\nu - E_g) \quad (\text{Eq. 5})$$

Where A is a constant, and n describes transition process. A plot of $(\alpha h\nu)^n$ Vs $h\nu$ should be straight line with an intercept on the $h\nu$ axis equal to E_g .

For direct band-gap measurement, $n = 2$, therefore $(\alpha h\nu)^2 = A (h\nu - E_g)$

The band gap of the researched SnS thin film deposited at -0.35V was given in the graph shown below:

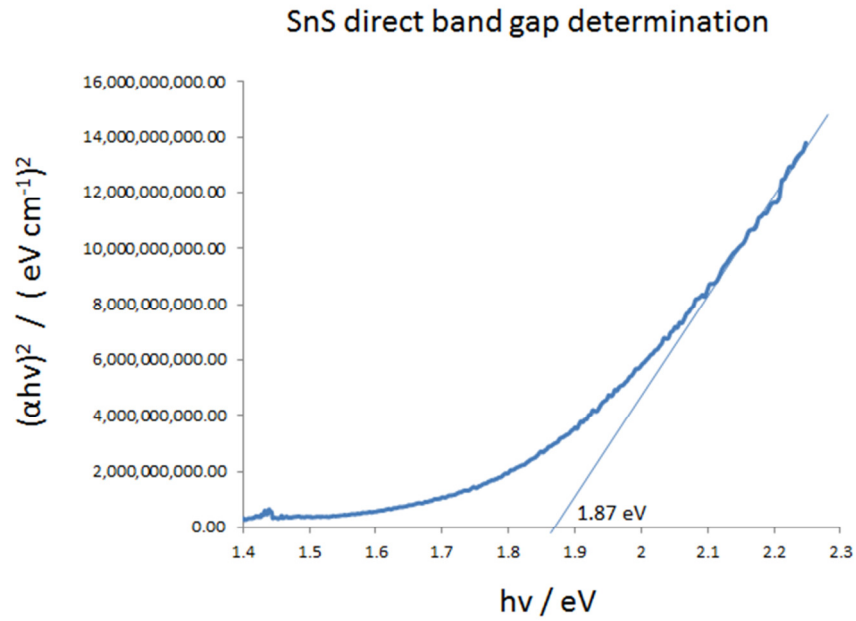


Figure 4.19: SnS direct band gap determination for deposition potential of -0.35V .

The result obtained for band gap measurement for SnS thin film deposited at -0.35V showed that it has the direct band gap value equal to 1.87 eV. (Hitachi U-300 UV-VIS-NIR spectrophotometer was used in this study)

Compared with the band gap result obtained with other scientists' band gap results, it was found that the value of direct band gap for the SnS thin film deposited at -0.35V was higher than the usual SnS band gap value which usually range from 1.00 eV ~ 1.30 eV. The band gap result of the researched SnS thin film was 1.80 eV, this proved that the SnS thin film deposited might contain derivatives of thin sulfide for example SnS₂ and Sn₂S₃.

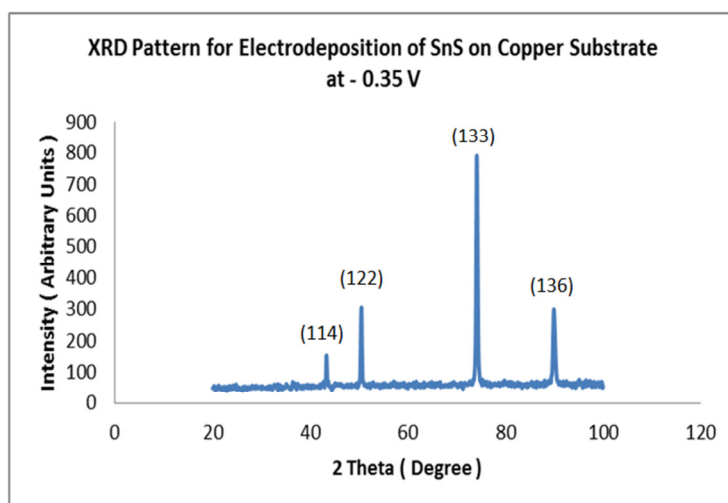


Figure 4.20 : XRD characterization for electro-deposition of SnS on Copper Substrate at the potential of -0.35 V.

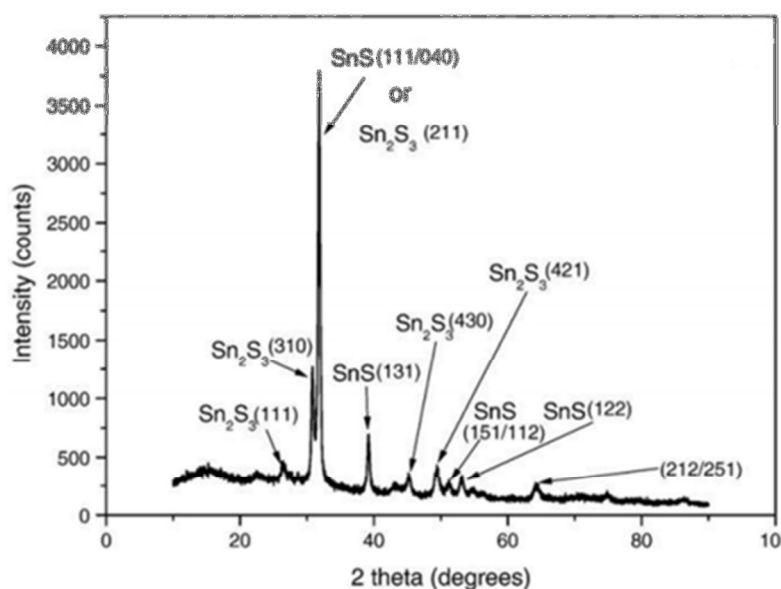


Figure 4.21 : Citation from Ogah E. Ogah and Guillaume Zoppi paper - XRD spectra of SnS layers deposited.

For comparative purpose, the XRD result for SnS deposition at -0.35V was compared with XRD spectra of SnS layers deposited gained from the research work of Ogah E. Ogah and Guillaume Zoppi ^[44]. It was found that, both of the XRD results had the Miller Indices value of (122) which showed that SnS was successfully deposited on the copper substrate at -0.35V. While the XRD result for SnS deposition at -0.35V has the Miller Indices value of (133) which is very close with Miller Indices value of (131) which is gained from the XRD spectra of SnS layers deposited gained from the research work of Ogah E. Ogah and Guillaume Zoppi. Again, it showed that, SnS was successfully deposited on the copper substrate at -0.35V. From Ogah E. Ogah and Guillaume Zoppi's XRD spectra of SnS layers deposited, they reported that, Sn₂S₃ has Miller Indices of (111) which is very close to the results obtained from this research which is (114), therefore, it showed that, Sn₂S₃ also most probably was deposited on the copper substrate at the potential of -0.35V.

Part IV: Results and Discussion for Electrodeposition of Tin Sulfoselenide from Tin (II) Methanesulfonate and Methane Sulfonic Acid Solution.

4.13 Cyclic Voltammetry Characterization for SnSSe Thin Films

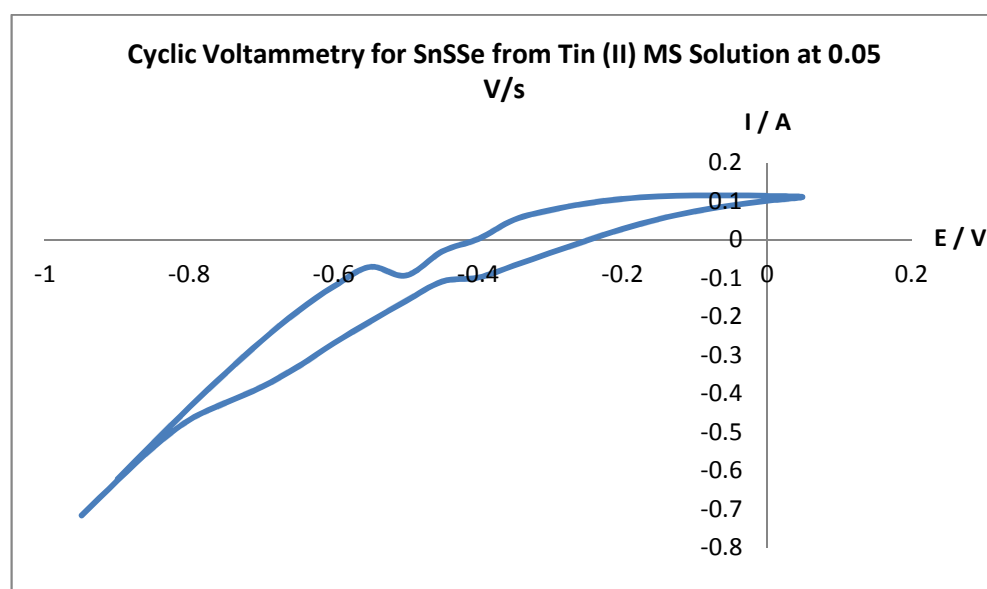
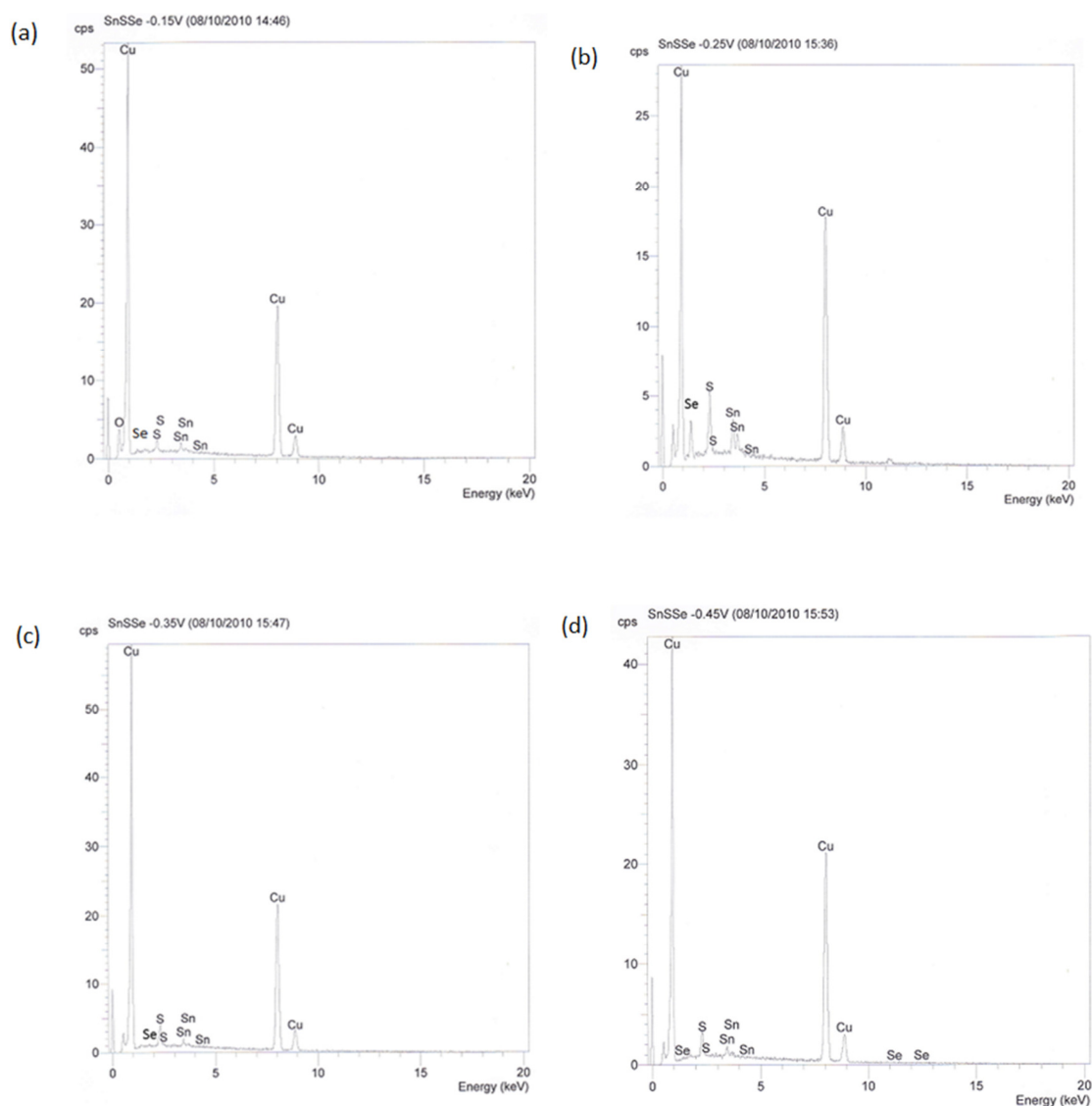


Figure 4.22 : The cyclic voltammogram for electro-deposition of SnSSe at the scan rate of 0.05 V/s.

Figure 4.22 shows the cyclic voltammogram of the solution containing 100ml of 0.01M Tin (II) Methane Sulfonate (50%w/v), 0.01M $\text{Na}_2\text{S}_2\text{O}_3$ and 0.01M Natrium Selenite (Na_2SeO_3) and 40ml Methane Sulfonic Acid ($\geq 99.5\%$). Reference electrode used was SCE electrode, counter electrode used is platinum wire, and copper substrate as the working electrode. The scan rate is 0.05 V/s.

From the cyclic voltammogram result, considering the negative potential region, the reduction potential peak to form SnSSe solid, E_{pc} is -0.45V, where the cathodic peak current, I_{pc} is -0.11A. The oxidation potential peak, E_{pa} is -0.55V, where the anodic peak current, I_{pa} is -0.07068A. The SnSSe thin films were deposited on the copper substrate under different potentials, they were -0.15V, -0.25V, -0.35V, -0.45V, -0.55V, -0.65V, -0.75V and -0.85V.

4.14 Energy Dispersive X-Ray (EDX) Characterization for SnSSe Thin Films



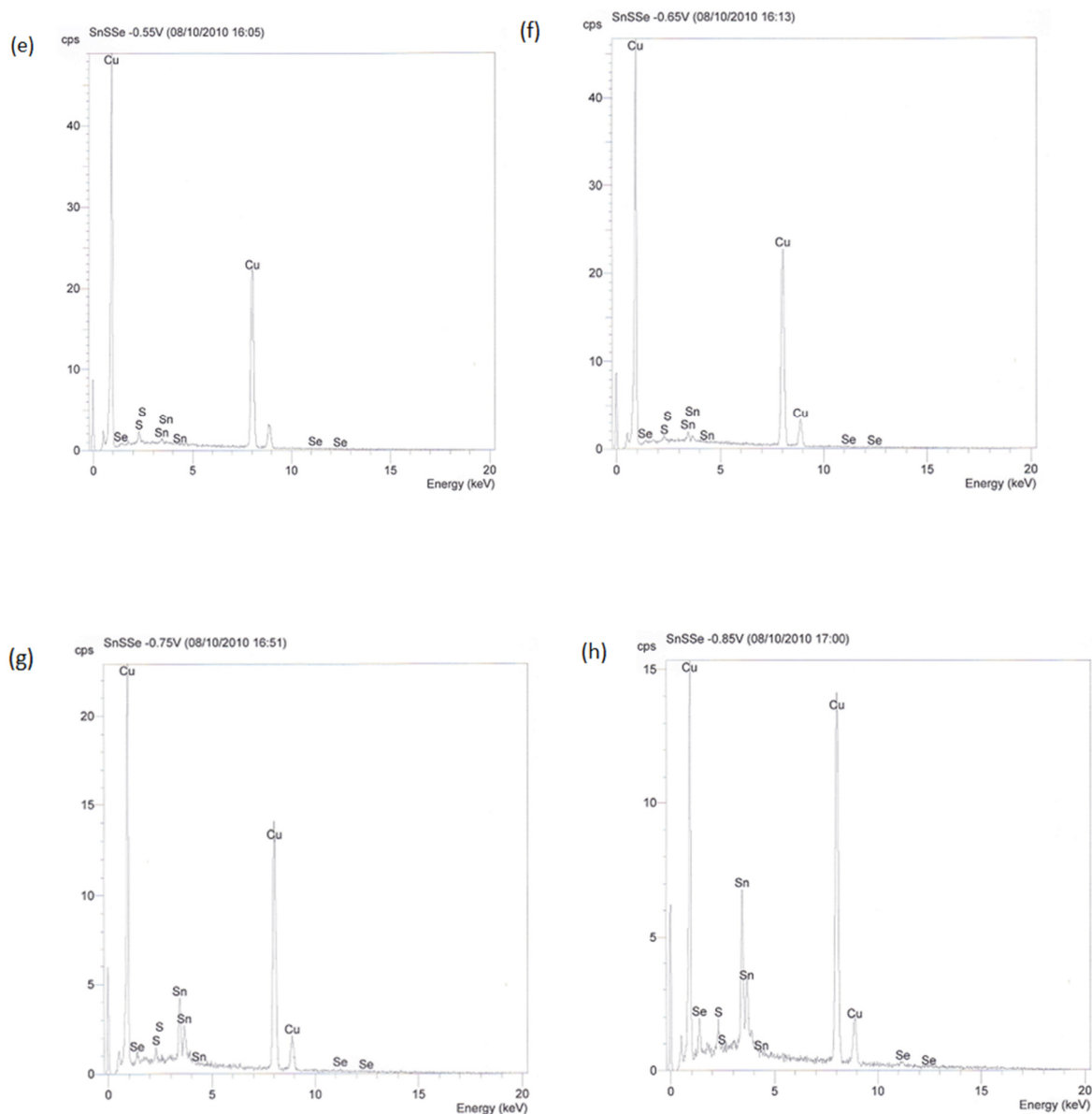


Figure 4.23: EDX characterization for electro-deposition of SnSSe on Copper Substrate at the potentials of (a) -0.15V, (b) -0.25V, (c) -0.35V, (d) -0.45V, (e) -0.55V and (f) -0.65V (g) -0.75V (h) -0.85V.

The EDX results shown in Figure 4.23 (a) proves that the SnSSe thin film can be deposited on the copper substrate at the potential of -0.15V by using tin (II) methanesulfonate solution containing natrium thiosulfate ($\text{Na}_2\text{S}_2\text{O}_3$) and natrium

selenite (Na_2SeO_3). The tin, sulfur and selenium are the elements deposited on the copper substrate from the tin (II) methanesulfonate solution containing natrium thiosulfate ($\text{Na}_2\text{S}_2\text{O}_3$) and natrium selenite (Na_2SeO_3) at the potential of -0.15V . The element weight percentage is shown in the ratio of Sn : S : Se equals to 62.86 : 23.45 : 13.69 . In term of element weight percentage, the SnSSe thin fim deposited at the potential of -0.15V containing 62.86% of Sn, 23.45% of S and 13.69% of Se . Therefore, this EDX result proves that SnSSe thin film can be deposited at the potential of -0.15V .

The EDX results shown in Figure 4.23 (b) proves that the SnSSe thin film can be deposited on the copper substrate at the potential of -0.25V by using tin (II) methanesulfonate solution containing natrium thiosulfate ($\text{Na}_2\text{S}_2\text{O}_3$) and natrium selenite (Na_2SeO_3). The tin, sulfur and selenium elements are the elements deposited on the copper substrate from the tin (II) methanesulfonate solution containing natrium thiosulfate ($\text{Na}_2\text{S}_2\text{O}_3$) and natrium selenite (Na_2SeO_3) at the potential of -0.25V . The element weight percentage is shown in the ratio of Sn : S : Se equals to 48.13 : 24.80 : 27.07 . In term of element weight percentage, the SnSSe thin fim deposited at the potential of -0.25V containing 48.13% of Sn, 24.80% of S and 27.07% of Se . Therefore, this EDX result proves that SnSSe thin film can be deposited at the potential of -0.25V .

The EDX results shown in Figure 4.23 (c) proves that the SnSSe thin film can be deposited on the copper substrate at the potential of -0.35V by using tin (II) methanesulfonate solution containing natrium thiosulfate ($\text{Na}_2\text{S}_2\text{O}_3$) and natrium selenite (Na_2SeO_3). The tin, sulfur and selenium elements are the elements deposited on the copper substrate from the tin (II) methanesulfonate solution containing natrium

thiosulfate ($\text{Na}_2\text{S}_2\text{O}_3$) and natrium selenite (Na_2SeO_3) at the potential of -0.35V . The element weight percentage is shown in the ratio of Sn : S : Se equals to 48.95 : 42.42 : 8.62 . In term of element weight percentage, the SnSSe thin fim deposited at the potential of -0.35V containing 48.95% of Sn, 42.42% of S and 8.62% of Se. Therefore, this EDX result proves that SnSSe thin film can be deposited at the potential of -0.35V . However, because of the element percentage for the Se element are too low compared to Sn and S elements, therefore, the deposition of SnSSe thin film at the potential of -0.35V is not ideal.

The EDX results shown in Figure 4.23 (d) proves that the SnSSe thin film can be deposited on the copper substrate at the potential of -0.45V by using tin (II) methanesulfonate solution containing natrium thiosulfate ($\text{Na}_2\text{S}_2\text{O}_3$) and natrium selenite (Na_2SeO_3). The tin, sulfur and selenium elements are the elements deposited on the copper substrate from the tin (II) methanesulfonate solution containing natrium thiosulfate ($\text{Na}_2\text{S}_2\text{O}_3$) and natrium selenite (Na_2SeO_3) at the potential of -0.45V . The element weight percentage is shown in the ratio of Sn : S : Se equals to 53.75 : 41.16 : 5.09 . In term of element weight percentage, the SnSSe thin fim deposited at the potential of -0.45V containing 53.75% of Sn, 41.16% of S and 5.09% of Se. Therefore, this EDX result proves that SnSSe thin film can be deposited at the potential of -0.45V . However, because of the element percentage for the Se element are too low compared to Sn and S elements, therefore, the deposition of SnSSe thin film at the potential of -0.45V is not ideal.

The EDX results shown in Figure 4.23 (e) proves that the SnSSe thin film can be deposited on the copper substrate at the potential of -0.55V by using tin (II) methanesulfonate solution containing natrium thiosulfate ($\text{Na}_2\text{S}_2\text{O}_3$) and natrium selenite (Na_2SeO_3). The tin, sulfur and selenium elements are the elements deposited on the copper substrate from the tin (II) methanesulfonate solution containing natrium thiosulfate ($\text{Na}_2\text{S}_2\text{O}_3$) and natrium selenite (Na_2SeO_3) at the potential of -0.55V. The element weight percentage is shown in the ratio of Sn : S : Se equals to 49.16 : 36.42 : 14.42 . In term of element weight percentage, the SnSSe thin fim deposited at the potential of -0.55V containing 49.16% of Sn, 36.42% of S and 14.42% of Se. Therefore, this EDX result proves that SnSSe thin film can be deposited at the potential of -0.55V.

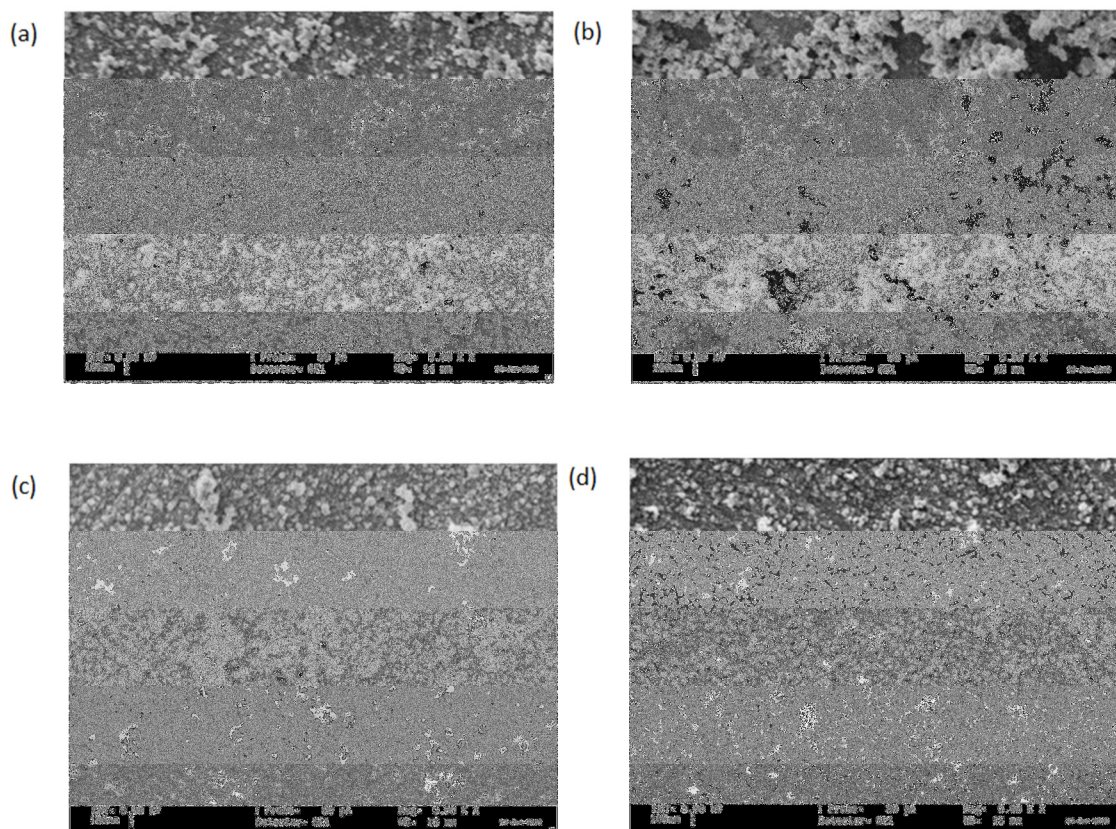
The EDX results shown in Figure 4.23 (f) proves that the SnSSe thin film can be deposited on the copper substrate at the potential of -0.65V by using tin (II) methanesulfonate solution containing natrium thiosulfate ($\text{Na}_2\text{S}_2\text{O}_3$) and natrium selenite (Na_2SeO_3). The tin, sulfur and selenium elements are the elements deposited on the copper substrate from the tin (II) methanesulfonate solution containing natrium thiosulfate ($\text{Na}_2\text{S}_2\text{O}_3$) and natrium selenite (Na_2SeO_3) at the potential of -0.65V. The element weight percentage is shown in the ratio of Sn : S : Se equals to 71.79 : 10.95 : 17.26 . In term of element weight percentage, the SnSSe thin fim deposited at the potential of -0.65V containing 71.79% of Sn, 10.95% of S and 17.26% of Se. Therefore, this EDX result proves that SnSSe thin film can be deposited at the potential of -0.65V.

The EDX results shown in Figure 4.23 (g) proves that the SnSSe thin film can be deposited on the copper substrate at the potential of -0.75V by using tin (II) methanesulfonate solution containing natrium thiosulfate ($\text{Na}_2\text{S}_2\text{O}_3$) and natrium selenite (Na_2SeO_3). The tin, sulfur and selenium elements are the elements deposited on the copper substrate from the tin (II) methanesulfonate solution containing natrium thiosulfate ($\text{Na}_2\text{S}_2\text{O}_3$) and natrium selenite (Na_2SeO_3) at the potential of -0.75V. The element weight percentage is shown in the ratio of Sn : S : Se equals to 85.23 : 4.67 : 10.10 . In term of element weight percentage, the SnSSe thin fim deposited at the potential of -0.75V containing 85.23% of Sn, 4.67% of S and 10.10% of Se. Therefore, this EDX result proves that SnSSe thin film can be deposited at the potential of -0.75V.

The EDX results shown in Figure 4.23 (h) proves that the SnSSe thin film can be deposited on the copper substrate at the potential of -0.85V by using tin (II) methanesulfonate solution containing natrium thiosulfate ($\text{Na}_2\text{S}_2\text{O}_3$) and natrium selenite (Na_2SeO_3). The tin, sulfur and selenium elements are the elements deposited on the copper substrate from the tin (II) methanesulfonate solution containing natrium thiosulfate ($\text{Na}_2\text{S}_2\text{O}_3$) and natrium selenite (Na_2SeO_3) at the potential of -0.85V. The element weight percentage is shown in the ratio of Sn : S : Se equals to 84.07 : 3.61 : 12.32 . In term of element weight percentage, the SnSSe thin fim deposited at the potential of -0.85V containing 84.07% of Sn, 3.61% of S and 12.32% of Se. Therefore, this EDX result proves that SnSSe thin film can be deposited at the potential of -0.85V.

4.15 Scanning Electron Microscopy (SEM) Characterization for SnSSe Thin Films

The below SEM images indicated that, at the deposition potential of -0.15V, there are many small granules on the surface of the thin films. At the deposition potential of -0.25V, the surface of the thin films has granules where the small granules lumped together. At the deposition potentials of -0.35V and -0.45V are distributed on the surface of the thin films. Whereas, at the deposition potentials of -0.55V and -0.65V, many small granules on the layer growth of the surface of the thin films. At the deposition potentials of -0.75V and -0.85V, the surface of the thin films are fully covered by the small granules.



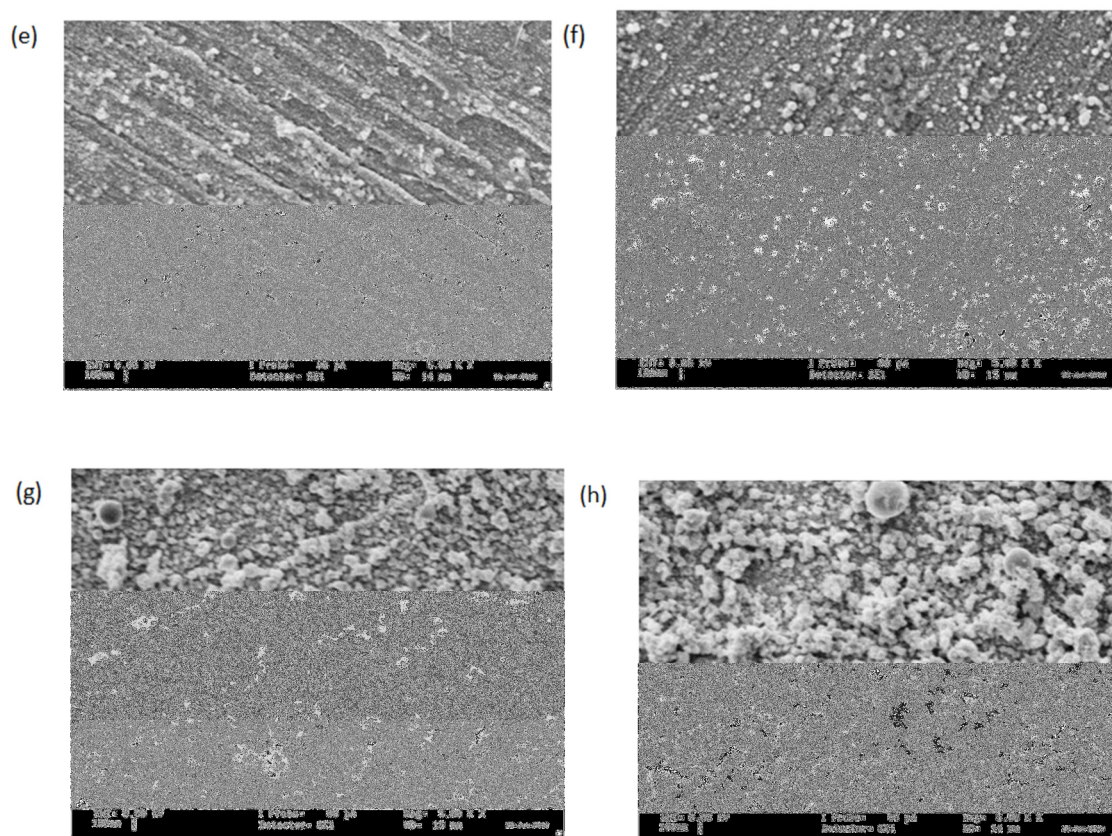


Figure 4.24: SEM characterization for electro-deposition of SnSSe on Copper Substrate at the potentials of (a) -0.15V, (b) -0.25V, (c) -0.35V, (d) -0.45V, (e) -0.55V, (f) -0.65V, (g) -0.75V and (h) -0.85V.

4.16 X-ray Diffraction (XRD) Characterization for SnSSe Thin Films

The XRD results indicate that, the SnSSe thin film deposited on the copper substrate has the orthorhombic lattice. The XRD results attained is compared with the JCPDS data with the JCP catalog number of [JCP2.2CA: 00-048-1225] of SnSSe.

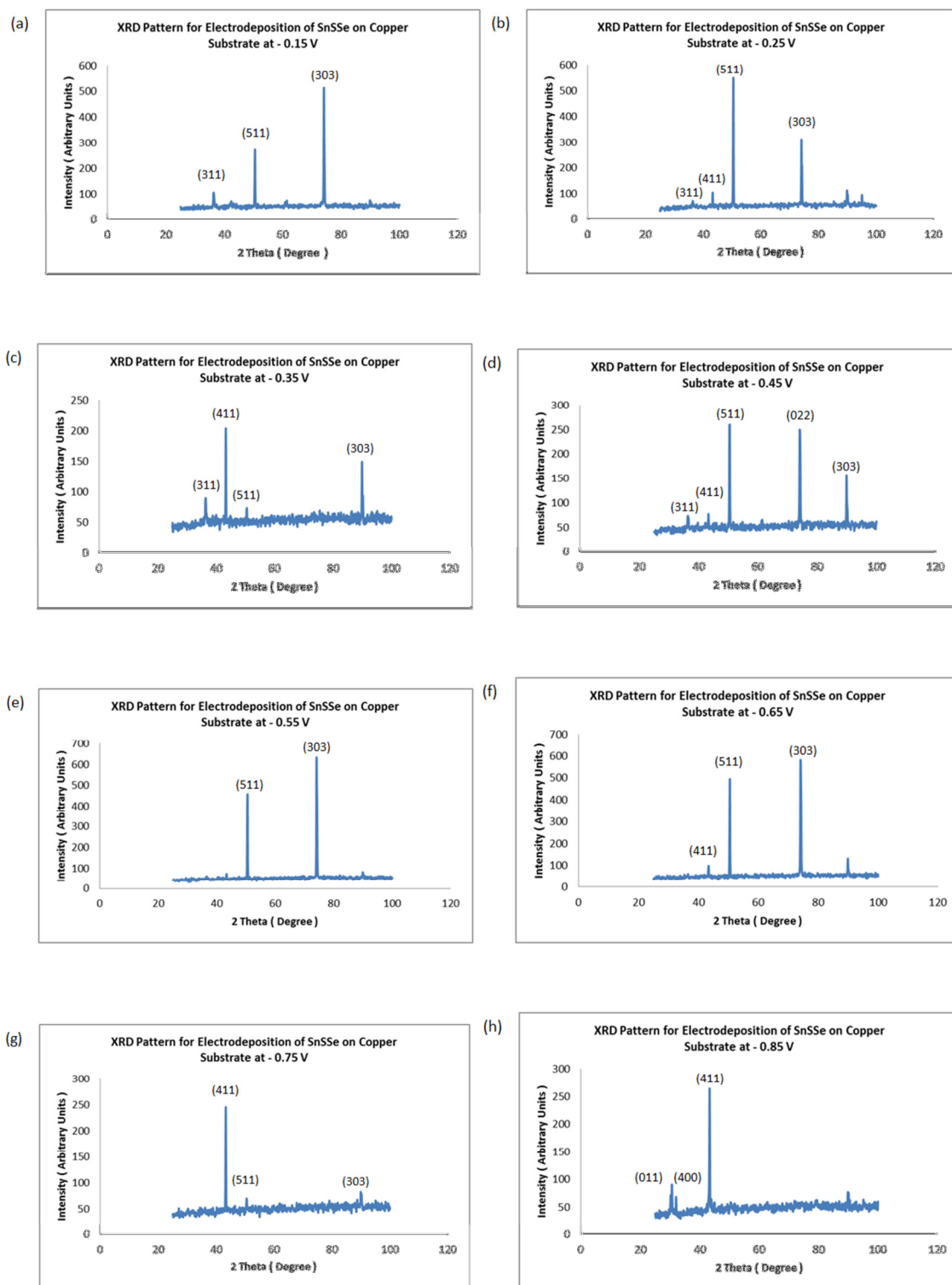


Figure 4.25: XRD characterization for electro-deposition of SnSSe on Copper Substrate at the potentials of (a) -0.15V, (b) -0.25V, (c) -0.35V, (d) -0.45V, (e) -0.55V, (f) -0.65V, (g) -0.75V and (h) -0.85V.

Figure 4.25 (a) indicates that the SnSSe thin film deposited on the copper substrate at the potential of -0.15V has the d-spacing value of 1.27683 Å at the strongest intensity. The Miller Indices value at the strongest intensity is (303). The incident angle for the radiation, θ at the strongest intensity is 37.106°. The second strongest intensity happened at the d-spacing of 1.80899 Å. The Miller Indices value at the second strongest intensity is (511). The incident angle for the radiation, θ at the second strongest intensity is 25.2025°. Therefore, the SnSSe thin film deposited on the copper substrate at the potential of -0.15V has the orthorhombic lattice.

Figure 4.25 (b) indicates that the SnSSe thin film deposited on the copper substrate at the potential of -0.25V has the d-spacing value of 1.80924 Å at the strongest intensity. The Miller Indices value at the strongest intensity is (511). The incident angle for the radiation, θ at the strongest intensity is 25.1985°. The second strongest intensity happened at the d-spacing of 1.27678 Å. The Miller Indices value at the second strongest intensity is (303). The incident angle for the radiation, θ at the second strongest intensity is 37.1075°. Therefore, the SnSSe thin film deposited on the copper substrate at the potential of -0.25V has the orthorhombic lattice.

Figure 4.25 (c) indicates that the SnSSe thin film deposited on the copper substrate at the potential of -0.35V has the d-spacing value of 2.08901 Å at the strongest intensity. The Miller Indices value at the strongest intensity is (411). The incident angle for the radiation, θ at the strongest intensity is 21.638°. The second strongest intensity happened at the d-spacing of 1.08994 Å. The Miller Indices value at the second strongest intensity is (303). The incident angle for the radiation, θ at the second strongest intensity

is 44.97° . Therefore, the SnSSe thin film deposited on the copper substrate at the potential of -0.35V has the orthorhombic lattice.

Figure 4.25 (d) indicates that the SnSSe thin film deposited on the copper substrate at the potential of -0.45V has the d-spacing value of 1.80958 \AA at the strongest intensity. The Miller Indices value at the strongest intensity is (511). The incident angle for the radiation, θ at the strongest intensity is 25.1935° . The second strongest intensity happened at the d-spacing of 1.27803 \AA . The Miller Indices value at the second strongest intensity is (303). The incident angle for the radiation, θ at the second strongest intensity is 37.0655° . Therefore, the SnSSe thin film deposited on the copper substrate at the potential of -0.45V has the orthorhombic lattice.

Figure 4.25 (e) indicates that the SnSSe thin film deposited on the copper substrate at the potential of -0.55V has the d-spacing value of 1.27802 \AA at the strongest intensity. The Miller Indices value at the strongest intensity is (303). The incident angle for the radiation, θ at the strongest intensity is 37.0655° . The second strongest intensity happened at the d-spacing of 1.80986 \AA . The Miller Indices value at the second strongest intensity is (511). The incident angle for the radiation, θ at the second strongest intensity is 25.1895° . Therefore, the SnSSe thin film deposited on the copper substrate at the potential of -0.55V has the orthorhombic lattice.

Figure 4.25 (f) indicates that the SnSSe thin film deposited on the copper substrate at the potential of -0.65V has the d-spacing value of 1.27831 \AA at the strongest

intensity. The Miller Indice value at the strongest intensity is (303). The incident angle for the radiation, θ at the strongest intensity is 37.0555° . The second strongest intensity happened at the d-spacing of 1.80833 \AA . The Miller Indice value at the second strongest intensity is (511). The incident angle for the radiation, θ at the second strongest intensity is 25.2125° . Therefore, the SnSSe thin film deposited on the copper substrate at the potential of -0.65V has the orthorhombic lattice.

Figure 4.25 (g) indicates that the SnSSe thin film deposited on the copper substrate at the potential of -0.75V has the d-spacing value of 2.08624 \AA at the strongest intensity. The Miller Indice value at the strongest intensity is (411). The incident angle for the radiation, θ at the strongest intensity is 21.668° . The second strongest intensity happened at the d-spacing of 1.08828 \AA . The Miller Indice value at the second strongest intensity is (303). The incident angle for the radiation, θ at the second strongest intensity is 45.0575° . Therefore, the SnSSe thin film deposited on the copper substrate at the potential of -0.75V has the orthorhombic lattice.

Figure 4.25 (h) indicates that the SnSSe thin film deposited on the copper substrate at the potential of -0.85V has the d-spacing value of 2.08854 \AA at the strongest intensity. The Miller Indice value at the strongest intensity is (411). The incident angle for the radiation, θ at the strongest intensity is 21.643° . The second strongest intensity happened at the d-spacing of 2.91471 \AA . The Miller Indice value at the second strongest intensity is (011). The incident angle for the radiation, θ at the second strongest intensity is 15.324° . Therefore, the SnSSe thin film deposited on the copper substrate at the potential of -0.85V has the orthorhombic lattice.

4.17 Atomic Force Microscopy (AFM) Characterization of SnSSe Thin Films

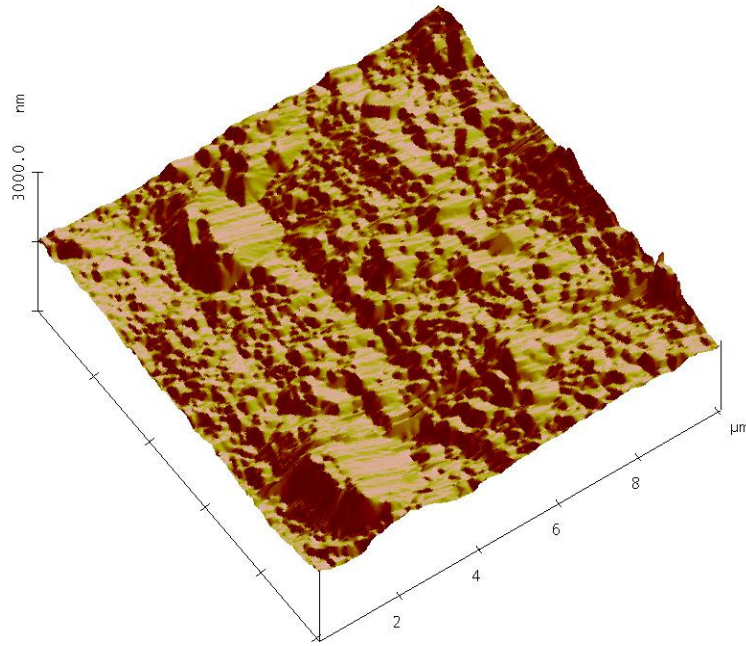


Figure 4.26 : AFM characterization for electro-deposition of SnSSe on Copper Substrate at the potential of -0.15 V.

The Figure 4.26 indicates the surface morphology characterized by the AFM for the SnSSe thin film deposited on copper substrate at the potential of -0.15V. The scan size is 10.00 μm and the scan rate is 0.5003 Hz. The grain size mean of the thin film is $1.340 \times 10^3 \text{ nm}^2$. The grain size standard deviation is $4.476 \mu\text{m}^2$. Minimum grain size is 762.94 nm^2 and the maximum grain size is $22.932 \mu\text{m}^2$. The roughness analysis was conducted by using AFM for the surface area of $111.07 \mu\text{m}^2$. The Root Mean Square of the roughness is 105.98 nm. The mean roughness is 76.442 nm. The depth at maximum is 505.46 nm.

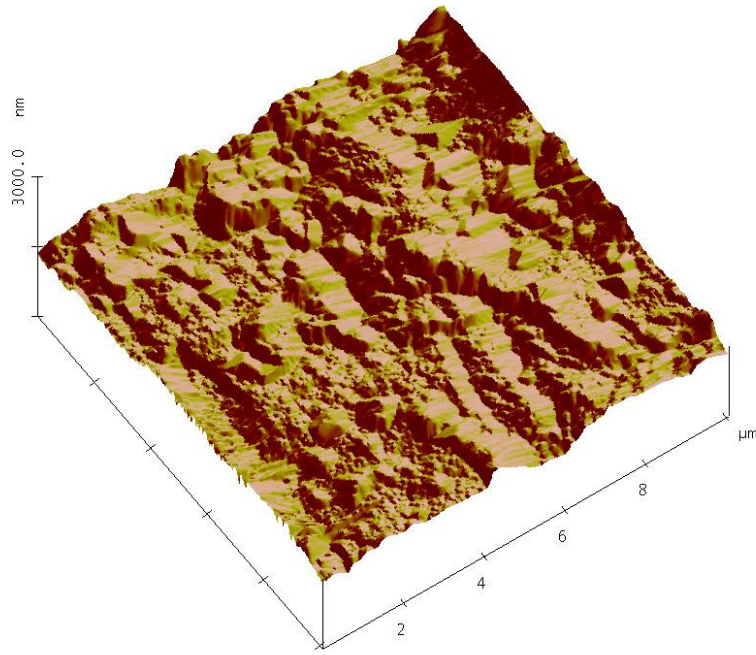


Figure 4.27 : AFM characterization for electro-deposition of SnSSe on Copper Substrate at the potential of -0.25 V.

The Figure 4.27 indicates the surface morphology characterized by the AFM for the SnSSe thin film deposited on copper substrate at the potential of -0.25V. The scan size is 10.00 μm and the scan rate is 0.5003 Hz. The grain size mean of the thin film is $1.319 \times 10^3 \text{ nm}^2$. The grain size standard deviation is $6.506 \mu\text{m}^2$. Minimum grain size is 381.47 nm^2 and the maximum grain size is $39.689 \mu\text{m}^2$. The roughness analysis was conducted by using AFM for the surface area of $117.14 \mu\text{m}^2$. The Root Mean Square of the roughness is 105.99 nm. The mean roughness is 82.040 nm. The depth at maximum is 448.46 nm.

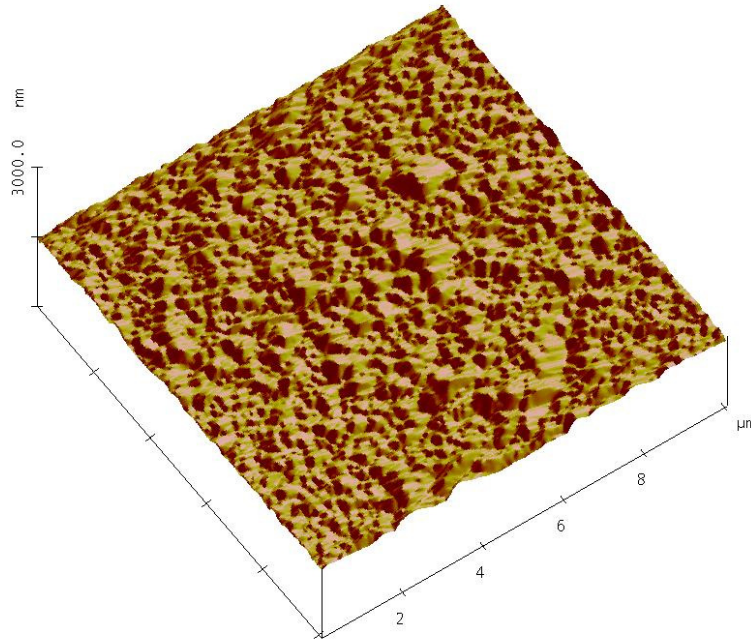


Figure 4.28 : AFM characterization for electro-deposition of SnSSe on Copper Substrate at the potential of -0.35 V.

The Figure 4.28 indicates the surface morphology characterized by the AFM for the SnSSe thin film deposited on copper substrate at the potential of -0.35V. The scan size is 10.00 μm and the scan rate is 0.5003 Hz. The grain size mean of the thin film is $5.29210 \times 10^5 \text{ nm}^2$. The grain size standard deviation is $2.542 \mu\text{m}^2$. Minimum grain size is 381.47 nm^2 and the maximum grain size is $22.707 \mu\text{m}^2$. The roughness analysis was conducted by using AFM for the surface area of $106.96 \mu\text{m}^2$. The Root Mean Square of the roughness is 33.380 nm. The mean roughness is 24.979 nm. The depth at maximum is 225.87 nm.

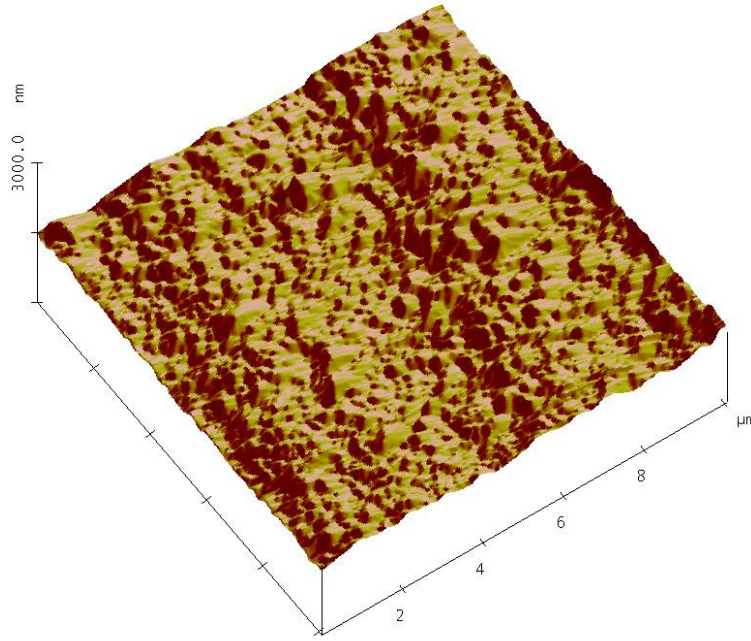


Figure 4.29 : AFM characterization for electro-deposition of SnSSe on Copper Substrate at the potential of -0.45 V.

The Figure 4.29 indicates the surface morphology characterized by the AFM for the SnSSe thin film deposited on copper substrate at the potential of -0.45V. The scan size is 10.00 μm and the scan rate is 0.5003 Hz. The grain size mean of the thin film is $9.31042 \times 10^5 \text{ nm}^2$. The grain size standard deviation is $4.546 \mu\text{m}^2$. Minimum grain size is 381.47 nm^2 and the maximum grain size is $26.942 \mu\text{m}^2$. The roughness analysis was conducted by using AFM for the surface area of $110.80 \mu\text{m}^2$. The Root Mean Square of the roughness is 75.462 nm. The mean roughness is 60.596 nm. The depth at maximum is 363.82 nm.

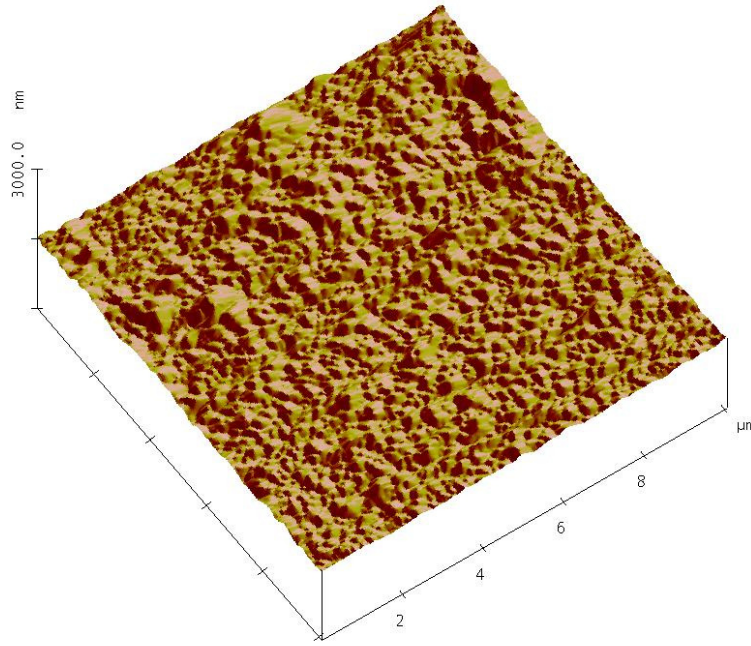


Figure 4.30 : AFM characterization for electro-deposition of SnSSe on Copper Substrate at the potential of -0.55 V.

The Figure 4.30 indicates the surface morphology characterized by the AFM for the SnSSe thin film deposited on copper substrate at the potential of -0.55V. The scan size is 10.00 μm and the scan rate is 0.5003 Hz. The grain size mean of the thin film is $5.23690 \times 10^5 \text{ nm}^2$. The grain size standard deviation is $2.813 \mu\text{m}^2$. Minimum grain size is 381.47 nm^2 and the maximum grain size is $19.785 \mu\text{m}^2$. The roughness analysis was conducted by using AFM for the surface area of $107.30 \mu\text{m}^2$. The Root Mean Square of the roughness is 38.519 nm. The mean roughness is 28.513 nm. The depth at maximum is 254.73 nm.

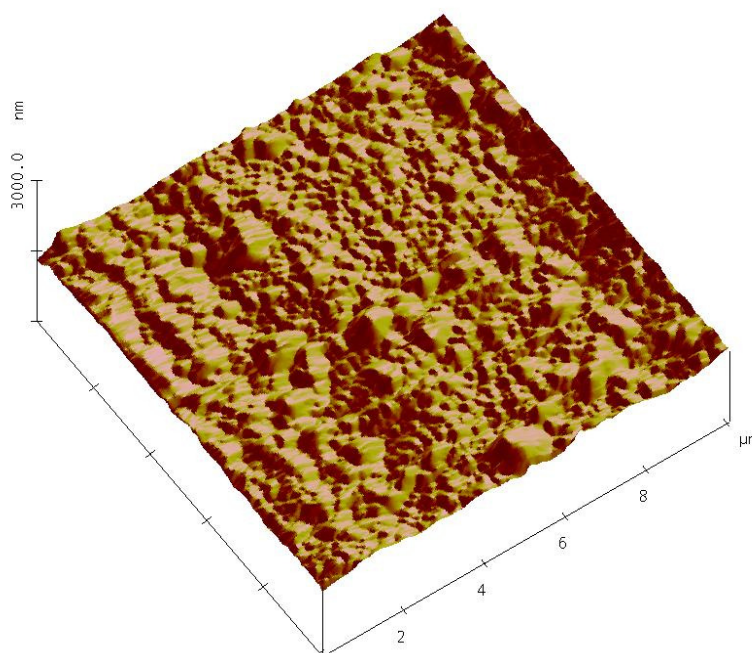


Figure 4.31 : AFM characterization for electro-deposition of SnSSe on Copper Substrate at the potential of -0.65 V.

The Figure 4.31 indicates the surface morphology characterized by the AFM for the SnSSe thin film deposited on copper substrate at the potential of -0.65V. The scan size is 10.00 μm and the scan rate is 0.5003 Hz. The grain size mean of the thin film is $1.131 \times 10^3 \text{ nm}^2$. The grain size standard deviation is $6.842 \mu\text{m}^2$. Minimum grain size is 381.47 nm^2 and the maximum grain size is $45.462 \mu\text{m}^2$. The roughness analysis was conducted by using AFM for the surface area of $106.44 \mu\text{m}^2$. The Root Mean Square of the roughness is 52.783 nm. The mean roughness is 39.623 nm. The depth at maximum is 293.46 nm.

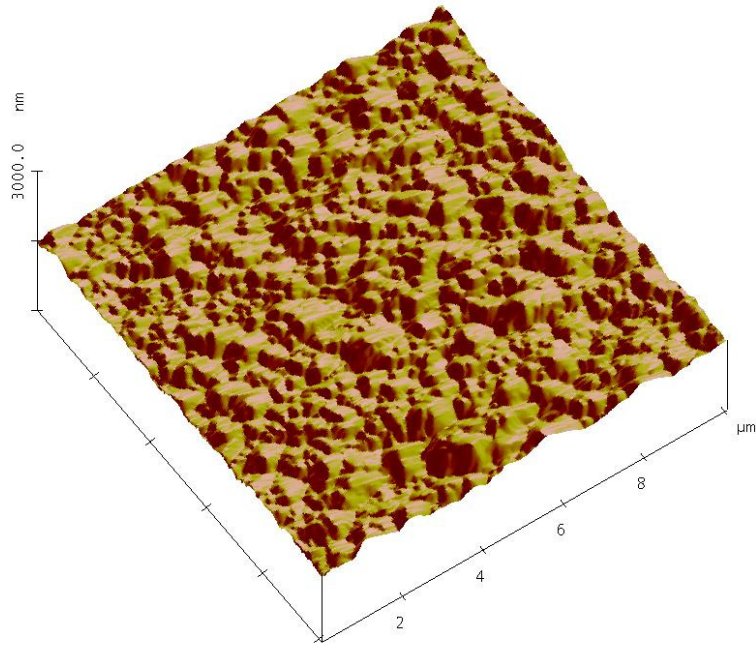


Figure 4.32 : AFM characterization for electro-deposition of SnSSe on Copper Substrate at the potential of -0.75 V.

The Figure 4.32 indicates the surface morphology characterized by the AFM for the SnSSe thin film deposited on copper substrate at the potential of -0.75V. The scan size is 10.00 μm and the scan rate is 0.5003 Hz. The grain size mean of the thin film is $5.78956 \times 10^5 \text{ nm}^2$. The grain size standard deviation is $1.231 \mu\text{m}^2$. Minimum grain size is 381.47 nm^2 and the maximum grain size is $5.009 \mu\text{m}^2$. The roughness analysis was conducted by using AFM for the surface area of $111.16 \mu\text{m}^2$. The Root Mean Square of the roughness is 61.344 nm. The mean roughness is 48.208 nm. The depth at maximum is 392.10 nm.

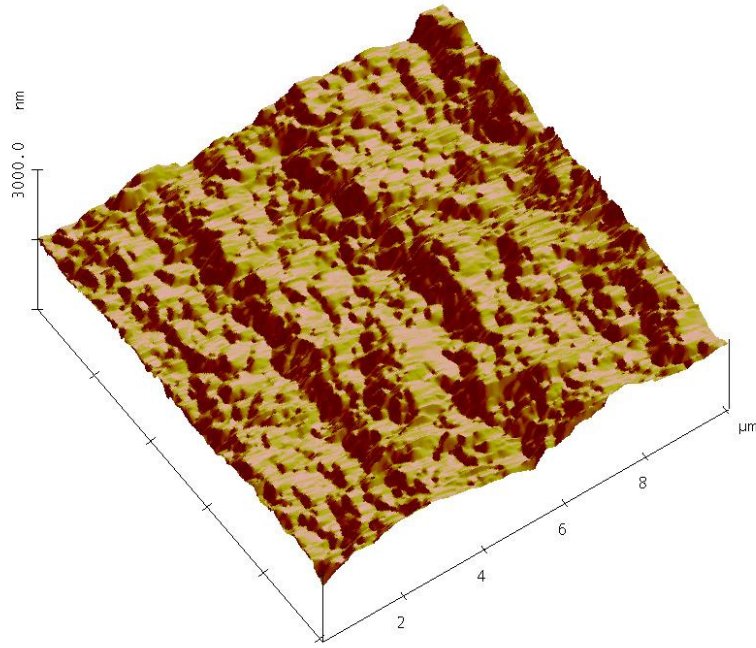


Figure 4.33 : AFM characterization for electro-deposition of SnSSe on Copper Substrate at the potential of -0.85 V.

The Figure 4.33 indicates the surface morphology characterized by the AFM for the SnSSe thin film deposited on copper substrate at the potential of -0.85V. The scan size is 10.00 μm and the scan rate is 0.5003 Hz. The grain size mean of the thin film is $8.90687 \times 10^5 \text{ nm}^2$. The grain size standard deviation is $2.673 \mu\text{m}^2$. Minimum grain size is 381.47 nm^2 and the maximum grain size is $15.329 \mu\text{m}^2$. The roughness analysis was conducted by using AFM for the surface area of $113.87 \mu\text{m}^2$. The Root Mean Square of the roughness is 89.744 nm. The mean roughness is 72.526 nm. The depth at maximum is 275.74 nm.

Chapter 5: Conclusion

5.1 Conclusion

In this research, it is concluded that, tin and tin chalcogenides such as tin sulfide and tin sulfo-selenide thin films can be electrochemically deposited on copper substrate by using tin (II) methanesulfonate and methane sulfonic acid mixture of solution. The electrodeposition of tin using tin (II) methane sulfonate salt in a solvent mixture of water and air stable ionic liquid 1-butyl-1 methyl-pyrrolidinium tri-fluoro-methane sulfonate and MSA showed that the electro-reduction was diffusion controlled. From the experiments of cyclic voltammetry and chronoamperometry, the diffusion coefficient is $2.2 \times 10^{-7} \text{ cm}^2 \text{ s}^{-1}$ and $2.5 \times 10^{-7} \text{ cm}^2 \text{ s}^{-1}$, respectively. The values of the diffusion coefficient in ionic liquids are smaller due to the larger viscosity of the ionic liquid and size of the dynamic radius in the solution.

The electrodeposition of tin in the mixture of water and air stable ionic liquid 1-butyl-1 methyl-pyrrolidinium trifluoro-methane sulfonate and methane sulfonic acid (MSA) based tin methanesulfonate salts showed promising results in this study with current efficiency as high as 99%. The deposit morphology of the mixture BMPOTF and MSA based tin coated substrates were observed by using EDX and SEM, where dense, fine and polygonal grain structures were obtained. In this study, it was convinced that water and air stable ionic liquids have a huge potential in the additive-free electrodeposition of metals, especially when there is very small hydrogen gas evolution, even though mixed with the methane sulfonic acid (MSA) based tin salt.

References :

- (1) C.T.J. Low, F.C. Walsh. (2008). *Electrochim. Acta*, 33: 16, 5280-5286.
- (2) M.J. Deng, I.W. Sun, P.Y. Chen, J.K. Chang, W.T. Tsai. (2008). 53:19, 5812-5818.
- (3) S. Zein El Abedin, E.M. Moustafa, R. Hempelmann, H. Natter, F. Endres. (2005). *Electrochem. Comm.*, 7: 11, 1111-1116.
- (4) Noguchi H., A. Setiyadi, H. Tanamura, T. Nagatomo, O. Omoto. (1994). *Solar Energy Materials and Solar Cells*, 35, 325–331.
- (5) C.L. Hussey, X.H. Xe (1993), *J. Electrochem. Soc.*, 140:3, 618-626.
- (6) W.Z. Yang, H. Chang, Y.M. Tang, J.T. Wang, Y.X. Shi. (2008). *J. App. Electrochem.*, 38, 537-542.
- (7) N. Tachikawa, N. Serizawa, Y. Katayama, T. Miura. (2008). *Electrochim. Acta.*, 53, 6530-6534.
- (8) J.F. Huang and I.W. Sun. (2003). *J. Electrochem. Soc.*, vol. 150 (6), pp. E229–E306.
- (9) J.S. Wilkes and M.J. Zaworotko. (1992). *J. Chem. Soc., Chem. Comm.*, 13, 965–67.
- (10) B. Thangaraju, P. Kaliannan. (2000). *Journal of Physics D: Applied Physics*, 33, 1054–1059.
- (11) W.J. Basirun, D. Pletcher, and A. Saraby Reintjes. (1996). *J. App. Electrochem.*, 26, 873–80.
- (12) W.J. Basirun, D. Pletcher. (1998). *J. App. Electrochem.*, 28, 167–72.
- (13) M. Ebadi, W.J. Basirun, Y. Alias. (2009). *Asian J. Chem.*, 21 (8), 6343–53.
- (14) M. Ebadi, W.J. Basirun, Y. Alias. (2009). *Asian J. Chem.*, vol. 21 (9), 7354–62.

- (15) M. Ebadi, W.J. Basirun, Y. Alias, M.R. Mahmoudian. (2010). Chem. Central. J., 4, 14.
- (16) M.Ebadi,W.J.Basirun, Y.Alias. (2010). J.Chem. Sci, 122 (2), 1–7. B. M. Basol. (1988). Solar Cells, 2, 369.
- (17) Y. Wang, N. J. Herron. (1991). Phys. Chem., 95, 525.
- (18) M. G. Bawendi, M. L. Steigerwald, L. E. Brus. (1990). Ann. Rev. Phys. Chem., 41, 477.
- (19) M. L. Steigerwald, L. E. Brus. (1988). Ann. Rev. Mater. Sci., 19, 471.
- (20) C. B. Murray, C. R. Kagan, and M. G. Bawendi. (1995). Science, 270, 1335.
- (21) C. Natarajan, G. Nogami, M. Sharon (1995) Thin Solid Films, 261, 44-51.
- (22) R.N. Bhargava, D. Gallagher, X. Hong, A. Nurmikko. (1994). Phys. Rev. Lett., 72 , 416.
- (23) A.V. Firth, D. J. Cole-Hamilton, J.W. Allens. (1999). Appl. Phys. Letter., 75, 3120.
- (24) S.N. Sarangi, S. N. Sahu. (2004). Physica, 23, 159-167.
- (25) M. Bouroushian, J. Charoud-Got, Z. Loizos, N. Spyrellis, G. Maurin. (2001). Thin Solid Films, 381, 39-47.
- (26) M. Bouroushian, Z. Loizos, N. Spyrellis, G. Maurin. (1993). Thin Solid Films, 229, 101.
- (27) Z. Loizos, N. Spyrellis, G. Maurin, D. Pottier. (1989). J. Electroanal. Chem., 269, 399.
- (28) Z. Loizos, N. Spyrellis, G. Maurin, D. Pottier. (1991). Surf. Coat Technol. 45, 273.
- (29) Z. Loizos, N. Spyrellis, G. Maurin. (1991). Thin Solid Films, 204, 139.
- (30) Wasa, K., Bull. (1995). Matter. Res., 18, 937.

- (31) M. Ichimura, K. Takeuchi. (2000). Thin Solid Films, 361-362, 98-101.
- (32) Robert W. Miles, Ogah E. Ogah. (2009). Thin Solid Films, 517, 4702-4705.
- (33) Tanusevski, D. Poelman. (2003). Sol. Energy Mater. Sol. Cells, 80, 297.
- (34) Ogah E. Ogah, Guillaume Zoppi, Ian Forbes, R.W. Miles. (2009). Thin Solid Films, 517, 2485.
- (35) S.Y. Cheng, Y.J. He, G.N. Chen, Eun-Chel Cho, G. Conibeer. (2008). Surf. Coat. Technol., 202, 6070.
- (36) Ghazali, Z.Zainal, M.Z.Hussein, A.Kassim. (1998). Solar Energy Mater. Solar Cells, 55, 237.
- (37) M.M. El-Nahass, H.M. Zeyada, M.S. Aziz, N.A. El-Ghamaz. (2002). Opt. Mater., 20, 159.
- (38) Ortiz, J.C. Alonso, M. Garcia, J. Toriz. (1996). Semicond. Sci. Technol., 11, 243.
- (39) K.T. Ramakrishna Reddy, P. Purandar Reddy, R.W. Miles, P.K. Datta. (2001). Opt. Mater. ,17, 295.
- (40) R. Mariappana, T. Mahalingamb. (2011). Optik, volume 122, 24, 2216–2219.
- (41) N. Koteswara Reddy, K. T. Ramakrishna Reddy. (2005). Physica B, 368, 25-31.Ogah E.
- (42) Ogah, Guillaume Zoppi. (2009) Thin Solid Films, 517, 2485-2488.
- (43) N.K. Reddy, K.T.R. Reddy. (1998). Thin Solid Films 325, 4.
- (44) N.K. Reddy, K.T.R. Reddy. (2007). Mater. Chem. Phys. 102, 13.
- (45) M. Gunasekaran, M. Ichimura. (2007). Sol. Energy Mater. Sol. Cells 91, 774.
- (46) S. Cheng, Y. Chen, C. Huang, G. Chen. (2006). Thin Solid Films 500, 96.
- (47) K.T. Ramakrishna Reddy, P. Purandhara Reddy. (2002). Mater. Lett. 56, 108.
- (48) M.M. El-Nahass, H.M. Zeyada, M.S. Aziz. (2002). Opt. Mater. 20, 159.
- (49) M.T.S. Nair, P.K. Nair. (1991). Semicond. Sci. Technol. 6, 132.

- (50) Ghazali, Z. Zainal, M.Z. Hussein, A. Kasssim. (1998). Sol. Energy Mater. Sol. Cells, 55, 237.
- (51) N. Sato, M. Ichimura, E. Arai, Y. Yamazaki. (2005). Sol. Energy Mater. Sol. Cells, 85, 153.
- (52) H. Nozaki, M. Onoda, M. Sekita, K. Kosuda, T. Wada. (2005). J. Solid State Chem., 178, 245.
- (53) J.H. Lee, H.Y. Lee, J.H. Kim, Y.K. Park. (2000). J. Appl. Phys., 39, 1669.
- (54) Pejova, I. Grozdanov, A. Tanusevski. (2004). Mater. Chem. Phys., 83, 245.
- (55) Wangperawong, J.S. King, S.M. Herron, B.P. Tran, K. Pangan-Okimoto, S.F. Bent. (2011). Thin Solid Films, 519, 2488.
- (56) M.M. El. Nahass, H.M. Zeyada, M.S. Aziz, N.A. El-Ghamaz. (2002). Opt. Mater., 20, 159.
- (57) K.Hartman, J.L. Johnson, M.I. Bertoni, D. Recht, M.J. Aziz, M.A. Scarpulla, T. Buonassisi. (2010). Thin Solid Films 519, 7421.
- (58) N.K. Reddy, K.T.R. Reddy. (1998). Thin Solid Films, 4, 325.
- (59) Thangaraju, P. Kaliannan. (2000). J. Phys. D Appl. Phys., 33, 1054.
- (60) H. Ben Haj Salah, H. Bouzouita, B. Rezig. (2005). Thin Solid Films 480-481, 439.
- (61) M. Calixto-Rodriguez, H. Martinez, A. Sanchez-Juarez, J. Campos-Alvarez. (2009). Thin Solid Films, 17, 2497.
- (62) M. Ichimura, K. Takeuchi, Y. Ono, E. Arai. (2000). Thin Solid Films, 98, 361–362.
- (63) K. Takeuchi, M. Ichimura, E. Arai, Y. Yamazaki. (2003). Sol. Energy Mater. Sol. Cells, 75, 427.
- (64) Ortiz, J.C. Alonso, M. Garcia, J. Toriz. (1996). Semicond. Sci. Technol., 11, 243.

- (65) K.T. Ramakrishna Reddy, P. Purandar Reddy, R.W. Miles, P.K. Datta. (2001).
Opt. Mater., 17, 295.
- (66) Thangaraju, P. Kaliannan. (2000). J. Phys., D, Appl. Phys. 33, 1054.
- (67) P.K. Nair, M.T.S. Nair, R.A. Zingaro, E.A. Meyers. (1994). Thin Solid Films, 85,
239.
- (68) M.T.S. Nair, C. Lopéz-Mata, O. GomezDaza, P.K. Nair. (2003). Semicond. Sci.
Technol., 18, 755.
- (69) Hidenori Noguchi, Agus Setitadi, Hiromasa Tanamura, Takao Nagatomo,
Osamu Omoto. (1994). Sol. Energy Mater. Sol. Cells, 35, 325.
- (70) Subramanian, C. Sanjeeviraja, M. Jayachandran. (2003). Sol. Energy Mater. Sol.
Cells, 79, 57.
- (71) M.T.S. Nair, P.K. Nair, R.A. Zingaro, E.A. Meyers. (1994). J. Appl. Phys., 75,
1557.
- (72) P.K. Nair, V.M. García, A.M. Fernández, H.S. Ruiz, M.T.S. Nair. (1991). J.
Phys., D 24, 441.
- (73) R.H. Misho, W.A. Murad. (1992). Sol. Energy Mater. Sol. Cells, 27, 335.
- (74) Thangaraju, P. Kaliannan. (2000). J. Phys. D: Appl. Phys., 33, 1054.
- (75) M.M. El-Nahass, H.M. Zeyada, M.S. Aziz. (2002). Opt. Mater., 20, 159.
- (76) Tanusevski. (2003). Semicond. Sci. Technol., 18, 501.
- (77) M.T.S. Nair, P.K. Nair. (1991). Semicond. Sci. Technol., 6, 132.
- (78) K. Takeuchi, M. Ichimura, E. Arai. (2003). Sol. Energy Mater. Sol. Cells 75,
427.
- (79) J.P. Singh, R.K. Bedi. (1991). Thin Solid Films, 9, 199.
- (80) M. Radot (1977). Rev. Phys. Appl., 18, 345.
- (81) H. Zhu, D. Yang, Y. Ji, H. Zhang, X. Shen. (2005). J. Mater. Sci. 40, 591.

- (82) An, K. Tang, G. Shen. (2002). *J. Cryst. Growth* 244, 333.
- (83) H. Hu, B. Yang, J. Zeng, Y. Qian. (2004). *Mater. Chem. Phys.*, 86, 233.
- (84) Y. Liu, D. Hou, G. Wang. (2003). *Chem. Phys. Lett.*, 379, 67.
- (85) G. Shen, D. Chen, K. Tang. (2003). *Inorg. Chem. Commun.*, 6, 178.
- (86) Ray Sehhar, K. Karanjai Malay, D. Das Gupta. (1999). *Thin Solid Films*, 72, 350.
- (87) J.B. Johson, H. Jones, B.S. Latham. (1999). *Semicond. Sci. Technol.*, 14, 501.
- (88) Avellaneda, G. Delgado, M.T.S. Nair. (2007). *Thin Solid Films* 515, 5771.
- (89) S. Cheng, Y. Chen, Y. He, G. Chen. (2007). *Mater. Lett.*, 61, 1408.
- (90) Y. Li, J.P. Tu, X.H. Huang. (2007). *Electrochem. Commun.*, 9, 49.
- (91) S.Y. Cheng, G.N. Chen, Y.Q. Chen, C.C. Huang. (2006). *Opt. Mater.*, 29, 439.
- (92) W. Albers, C. Hass, H.J. Vink, J.D. Wasscher. (1996). *J. Appl. Phys. Suppl.*, 32, 2220.
- (93) M. Parenteau, C. Carbone. (1990). *Phys. Rev. B*, 41, 5227.
- (94) G. Said, P.A. Lee. (1973). *Phys. Status Solidi, A Appl. Res.*, 15, 99.
- (95) J. George, C.K. Valsala Kumari. (1983). *J. Cryst. Growth*, 63, 233.
- (96) K. Kourtakis, J. DiCarlo, R. Kershaw, K. Dwight. (1988). *J. Solid State Chem.*, 76, 186.
- (97) P. Pramanik, P.K. Basu, S. Biswas. (1987). *Thin Solid Films*, 150, 269.
- (98) G.H. Yue, P.X. Yan, J. Wang. (2005). *Journal of Crystal Growth*, 274, 464.
- (99) Devika M, Reddy NK, Ramesh K. (2006). *Appl. Surf. Sci.*, 253, 1673-1676.
- (100) Wiedemeier H, Csillag FJ. (1979). *Thermochimica Acta*, 34, 257-265.

Appendices

Electrodeposition of tin using tin(II) methanesulfonate from a mixture of ionic liquid and methane sulfonic acid

Yang Kok Kee ^{1,a}, Wan Jeffrey Basirun ^{1,b}, Koay Hun Lee ^{2,c}

¹ Department of Chemistry, Faculty of Science, University of Malaya, 50603 Kuala Lumpur, Malaysia.

² Malaysia University of Science and Technology, Department of Material Science and Engineering, GL33, Ground Floor, Block C, Kelana Square, No.17, Jalan SS7/26, Kelana Jaya, 47301 Petaling Jaya, Selangor, Malaysia.

^a kk.yang80@gmail.com, ^b jeff@um.edu.my, ^c koayhunlee@gmail.com

Key words: Electrodeposition, Tin, Ionic liquids

Abstract

The electrodeposition of tin from Tin (II) Methane Sulfonate (MSA) with varying concentration in air and water stable 1-Butyl-1-Methylpyrrolidinium Trifluoro-Methanesulfonate, (BMPOTF) ionic liquid at room temperature was studied. Cyclic Voltammetry served to characterize the electrochemical behavior of tin reduction and oxidation. The diffusion coefficient of stannous ions in the mixture of BMPOTF ionic liquid and MSA based electrolyte obtained via Randles-Sevcik was approximately $2.11 \times 10^{-7} \text{ cm}^2/\text{s}$. Electroplating on copper panel was conducted under different current densities to determine BMPOTF based tin plating solution current efficiency. Mixture of BMPOTF and MSA based tin plating solution gave current efficiency as high as 99.9%. The deposit morphology of the mixture BMPOTF and MSA based tin coated substrates was observed by using EDX and SEM. A dense, fine and polygonal grain structure was obtained.

1. Introduction

Tin and its alloys can be electrodeposited from various electrolytes including aqueous fluoroborate, sulfate and methane sulfonate solutions. The sulfate electrolyte is generally adopted as a first choice of plating electrolyte due to its low cost and long history. The fluoroborate bath is used when high current density is required. The methanesulfonate-based electrolyte is favored for its environmental benefits and it facilitates higher stannous ion saturation solubility with a low oxidation rate to stannic ions [1].

However, hydrogen evolution reaction often occurs in the aqueous based electrolyte electrodeposition resulting in profound effect on current efficiency and quality of the tin deposits. As a result, different additives may be needed to suppress such difficulties. In contrast, a fundamental advantage of using ionic liquid electrolytes in electroplating is that, since these are non-aqueous solutions, there is negligible hydrogen evolution during electroplating and the coatings possess the much superior mechanical properties of the pure metal. Hence essentially crack-free, more corrosion-resistant deposits are possible. This may allow thinner deposits to be used, thus reducing overall material and power consumption [2].

Electrodeposition in ionic liquids was rarely studied in the past. In 1992, Wilkes and Zaworotko reported the first air and moisture stable imidazolium based ionic liquid with either tetrafluoroborate or hexafluorophosphate as anions. Then, several, liquids consisting of 1-ethyl-3-methylimidazolium, 1,2-dimethyl-3-propylimidazolium, or 1-butyl-1-methyl-pyrrolidinium cations with various anions, such as tetrafluoroborate (BF_4^-), tri-fluoro-methanesulfonate (CF_3SO_3^-), bis (trifluoromethanesulfonyl)imide [$(\text{CF}_3\text{SO}_2)_2\text{N}^-$] & tris (tri fluoro methanesulfonyl)methide [$(\text{CF}_3\text{SO}_2)_3\text{C}^-$], were found and received much attention because of low reactivity against moisture [3-4].

Few studies were reported on the electrodeposition of Tin (II) in ionic liquids. The first was done by Hussey and Xe [5] in an AlCl_3 mixed in 1-Methyl-3-Ethyl Imidazolium chloride melt. W. Yang *et al.* [6] has done Tin and Antimony electrodeposition in 1-ethyl-3-methylimidazolium tetrafluoroborate, and N. Tachikawa *et al.* [7] has done electrodeposition of Tin (II) in a hydrophobic ionic liquid, 1-*n*-butyl-1-methylpyrrolidinium bis (trifluoromethylsulfonyl) imide.

In view of the advantages of the air and water stable ionic liquids, we report here the results on the Tin electrodeposition from a mixture of an ionic liquid, 1-Butyl-1-methyl-pyrrolidinium trifluoro-methanesulfonate, (BMPOTF) with Tin (II) Methane Sulfonate in Methane Sulfonic Acid (MSA).

2. Experimental

The electrochemical behavior of tin reduction and oxidation was studied in the water and air stable ionic liquid 1-Butyl-1 methyl-pyrrolidinium trifluoro- methanesulfonate, (BMPOTF) which was purchased from Merck. The experiments were carried out using a conventional 3-electrode cell. The working electrode was a copper rod with diameter of 4 mm and exposed area of 0.1257 cm². Before each experiment, the copper rod was prepared as follows: wet grinding with SiC type abrasive paper grade 100, 1000 and 1200 to a mirror finish. Cleaning 10 minutes in ethanol and then de-scaled with 10% Methane Sulfonic Acid (10%) and final rinsing in de-ionized water. The counter electrode was a platinum wire with 4 cm length and 0.1 mm diameter. The working electrode potentials reported herein were measured versus a Ag/AgCl reference electrode. Table 1 and Table 2 gives the content of the Tin (II) methanesulfonate solution and the content of the ionic liquid.

For the electroplating experiments, copper panels with dimension 2 cm x 2 cm were used as the substrate for tin electrodeposition. Before each experiment, the pre-treatment of the copper panels were as follows: Cleaning 10 minutes in ethanol and then de-scaled with 10% Methane Sulfonic Acid (10%) and final rinsing in de-ionized water. Precautionary measures were taken to eliminate oxygen from the system by bubbling high purity nitrogen through the solution prior to the experiments for 3 minutes.

The electrochemical experiments were carried out using an Autolab PGSTAT 30 Potentiostat/Galvanostat. All experiments were conducted at room temperature, 29 ± 1 °C in a mixture of BMPOTF ionic liquid and MSA based tin methane sulfonate salts. Tin Methane Sulfonate, (CH₃SO₃)₂Sn was added in the desired amounts. No organic additives were mixed in the solutions in this study. The electrolyte volume for the mixture was fixed at 15 mL in these experiments. Scanning Electron Microscopy (SEM) was model Philips XL 30 and Energy Dispersive X-Ray Analysis (EDX) was using EDAX Analyzer Genesis was used in the surface studies of these deposits.

Table 1: Component of Tin Methane Sulfonate

Component	Percent (%)
Stannous Methane Sulfonate, (CH ₃ SO ₃) ₂ Sn	55
Water, H ₂ O	30
Methane Sulfonic Acid, CH ₃ SO ₃ H	15

Table 2: Component of Ionic Liquid liquid: 1-Butyl-1 methyl-pyrrolidinium trifluoro-methanesulfonate, (BMPOTF)

Component	Percent (%)
Assay (electrophoresis)	≥98
Water, H ₂ O	≤1
Halides	≤0.1

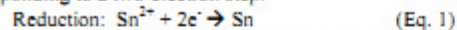
3. Results and discussion

3.1 Voltammetry

Figure 1 shows the voltametric response for BMPOTF with different tin concentration. Cyclic voltammetry experiments were swept from 0 to -1.0 V vs. Ag/AgCl, then the sweep direction was reversed. The potential sweep rate was remained at 0.05 V/s throughout the experiments. Increasing Tin (II) concentration produces a stronger reduction and oxidation peak. A single reduction and oxidation peak were observed in the cyclic voltammetry of Tin deposition and

dissolution at a copper substrate, where these peaks were absent when done with only the ionic liquid without the $(\text{CH}_3\text{SO}_3)_2\text{Sn}$ in MSA.

The forward sweep from 0 to -1V vs. Ag/AgCl shows a reduction peak for tin deposition corresponding to a two-electron step:



On reversing the potential sweep from -1.0V to 0V vs. Ag/AgCl, a single stripping peak was observed confirming the two-electron oxidation of metallic to stannous ions via the reverse reaction:

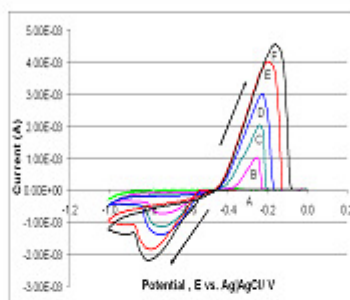
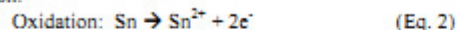


Fig. 1 Cyclic voltammogram at 0.05 V/s for solution $X \text{ M } (\text{CH}_3\text{SO}_3)_2\text{Sn}$, A=0M, B=0.1M, C=0.2M, D=0.3M, E=0.4M, F=0.5M

The relation between the peak current density, J_p and the concentration of the electroactive species in solution can be given by the Randles-Sevcik equation:

$$J_p = 2.69 \times 10^5 Z^{1.5} D^{0.5} \nu^{0.5} c \quad (\text{Eq. 3})$$

Where J_p is the peak current density, Z is the number of electrons involved in the electrode process, D is the diffusion coefficient of stannous ions, ν is the potential sweep rate and c is the concentration of stannous ions.

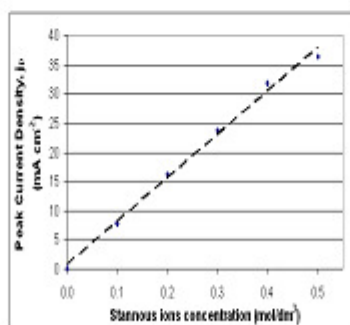


Fig. 2: Effect of Sn^{2+} concentration on peak current density

From the graph in Fig. 2, the diffusion coefficient of stannous ions in BMPOTF ionic liquid is approximately $2.11 \times 10^{-7} \text{ cm}^2 \text{ s}^{-1}$. Table 3 gives the diffusion coefficients of Tin (II) in various types of ionic liquids.

Table 3: Tin (II) diffusion coefficient from literature

Solvent	Ref.	Tin (II) Dif. coefficient $D/\text{cm}^2 \text{ s}^{-1}$
Aqueous	[1]	6.5×10^{-6}
1-ethyl-3-methylimidazolium tetrafluoroborate	[6]	6.1×10^{-7}
1- <i>n</i> -butyl-1-methylpyrrolidinium bis (trifluoromethylsulfonyl) imide	[7]	1.0×10^{-7}
AlCl_3 with 1-Methyl-3-Ethyl Imidazolium chloride	[5]	5.3×10^{-7}
1-Butyl-1-Methylpyrrolidinium Trifluoro-Methanesulfonate	This work	2.11×10^{-7}

The dependency of the Diffusion coefficient to the viscosity and the radius of the diffusing species can be explained by the Stoke-Einstein equation, $D = kT / 6 \pi \eta r$ where k = Boltzmann constant, T = Kelvin temperature, η = viscosity of the solvent, r = dynamic radius of the diffusing species. Hussey *et. al.* [9] found that the Tin(II) exists as SnCl_4^{2-} in AlCl_3 with 1-Methyl-3-Ethyl Imidazolium chloride ionic liquid and the low values of the diffusion coefficient was due to the increased viscosity of the ionic liquid. They also suggest that there is some degree of association between the Tin(II) with chloroaluminate ions such as AlCl_4^- and Al_2Cl_7^- , which contribute to the low value of the diffusion coefficient [5].

W. Yang *et. al.* [6] used tetrafluoroborate, BF_4^- based ionic liquid, where the diffusion coefficient was higher than calculated from the chloroaluminate ionic liquid by Hussey. From the Stoke-Einstein equation, it can be seen that the smaller Tin(II) tetrafluoroborate species will contribute to a slightly higher diffusion coefficient value for the Tin(II) species.

Studies using trifluoromethylsulfonyl imide ionic liquids from Tachikawa *et. al.* [7] and this work using trifluoromethylsulfonate ionic liquid gave smaller diffusion coefficient for the Tin(II) species. It can be suggested that the complexation between the Tin (II) with trifluoromethylsulfonate and trifluoromethylsulfonyl imide, which is larger than the chloride ion and the tetrafluoroborate ion, has increased the radius of the Tin(II) species in solution. This contributes to the lower diffusion coefficient compared to the chloride and tetrafluoroborate based ionic liquids in the works of Hussey and Tachikawa.

3.2 Electroplating Experiments

Electroplating on macroelectrodes were carried out to estimate the plating current efficiency and hydrogen evolution reaction for the mixture of 1-Butyl-1-methyl-pyrrolidinium trifluoromethane sulfonate (BMPOTF) with Methane Sulfonic Acid and tin methane sulfonate salts. Table 4 presents the results of current efficiencies from electroplating experiments using Tin (II) solution in ionic liquid at different current densities and Tin (II) concentrations.

Scanning electron microscopy (SEM) and Energy Dispersive X-ray spectroscopy (EDX) were used to examine the surface morphology and analyze the elemental compositions of the electrodeposits. Table 4 shows the current efficiencies obtained from experiments using current densities from 1 A dm^{-2} (ASD) to 7 ASD for various concentrations of Tin (II) from 0.1 M to 0.5 M in ionic liquids solutions.

Table 4: Current efficiency obtained at different Sn^{2+} concentration

Current Density, (A/dm^2)	Stannous Ions, concentration, (mol/dm^3)				
	0.1	0.2	0.3	0.4	0.5
1.0	99.58	99.58	98.90	98.23	94.84
2.0	99.92	98.23	98.23	97.89	87.73
3.0	99.81	96.42	98.00	97.78	81.07
4.0	99.24	98.74	97.89	97.04	72.65
5.0	99.58	98.63	97.01	96.87	66.25
6.0	99.70	97.66	96.87	95.97	61.65
7.0	98.71	97.55	96.29	94.55	58.26

From the results, increasing current densities for higher concentrations of Tin(II) such as 0.4 and 0.5 M gave decreasing current efficiencies for Tin deposition. At these conditions, the hydrogen evolution reaction becomes prominent and decreases the current efficiency for the Tin deposition. The deposits became dull and less reflecting in appearance, owing to the porous nature of the surface as can be seen in Figure 3.

Scanning Electron Microscopy (SEM) from Figures 3 at 3500X magnification reveal that the deposits became less compact, less dense and more porous for higher current densities and higher concentrations of Tin(II). This can be also seen in the EDX results in Figures 4. The copper element was present in the EDX spectrum at the tin plated surface when analyzed under 20 keV EDX as shown in Figure 4.b. The higher current densities of 7 A dm^{-2} for 0.5 M of Tin (II) shows copper peaks from the copper substrate, because of the porous nature of the deposits.

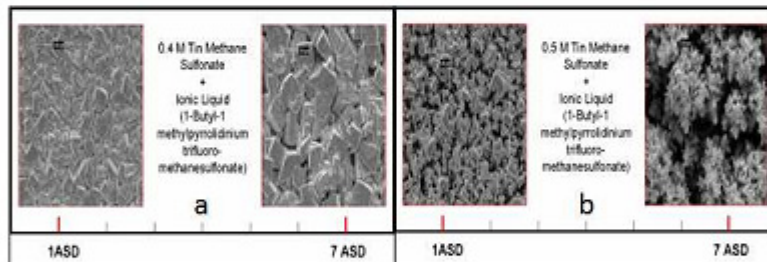


Figure 3 Electrodeposits from a: 0.4 M Tin (II) methanesulfonate and BMPOTF using 1 and 7 A dm^{-2} (ASD) b: 0.5 M Tin (II) methanesulfonate and BMPOTF using 1 and 7 A dm^{-2} (ASD)

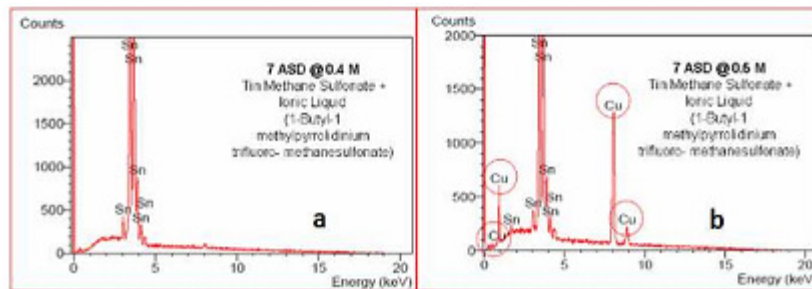


Figure 4: EDX spectrum for Tin electrodeposit using 7 A dm^{-2} (ASD) at a: 0.4 M and b: 0.5 M Tin(II) methanesulfonate and BMPOTF

5 CONCLUSIONS

The electrodeposition of tin in the mixture of water and air stable ionic liquid- 1-Butyl-1-methyl-pyrrolidinium trifluoro- methane sulfonate and Methane Sulfonic Acid (MSA) based Tin Methane Sulfonate salts shows promising results in this study with current efficiency as high as 99%. The deposit morphology of the mixture BMPOTF and MSA based tin coated substrates were observed by using EDX and SEM, where dense, fine and polygonal grain structures were obtained. In this study, we are convinced that water and air stable ionic liquids have a huge potential in the additive free electrodeposition of metals, especially there is very less hydrogen evolution even though mixed with the Methane Sulfonic Acid (MSA) based Tin salt.

6 REFERENCES

- [1] C.T.J. Low, F.C. Walsh, The stability of an acidic tin methanesulfonate electrolyte in the presence of a hydroquinone antioxidant, *Electrochim. Acta.*, 33: 16 (2008), 5280-5286.
- [2] M.J. Deng, I.W. Sun, P.Y. Chen, J.K. Chang, W.T. Tsai, Electrodeposition behavior of nickel in the water-and-air stable 1-ethyl-3-methylimidazolium- dicyanamide room-temperature ionic liquid, *Electrochim. Acta.*, 53:19 (2008), 5812-5818.
- [3] S. Zein El Abedin, E.M. Moustafa, R. Hempelmann, H. Natter, F. Endres, Additive free electrodeposition of nanocrystalline aluminum in a water and air stable ionic liquid, *Electrochem. Comm.*, 7: 11, (2005), 1111-1116.
- [4] A. P. Abbott, I. Dalrymple, F. Endres, D. R. MacFarlane, *Electrodeposition from Ionic Liquids*, A. P. Abbott, D. R. MacFarlane (Eds.), (Wiley-VCH, 2008, 1-12).
- [5] C.L. Hussey, X.H. Xe, The electrochemistry of Tin in the Aluminum Chloride-1-Methyl-3-ethylimidazolium chloride molten salt, *J. Electrochem. Soc.*, 140:3 (1993), 618-626.
- [6] W.Z. Yang, H. Chang, Y.M. Tang, J.T. Wang, Y.X. Shi, Electrodeposition of Tin and Antimony in 1-ethyl-3-methylimidazolium tetrafluoroborate ionic liquids, *J. App. Electrochem.*, 38, (2008), 537-542.
- [7] N. Tachikawa, N. Serizawa, Y. Katayama, T. Miura, Electrodeposition of Sn (II)/ Sn in a hydrophobic room-temperature ionic liquid, *Electrochim. Acta.*, 53, (2008), 6530-6534.

Advances in Materials and Processing Technologies II

doi:10.4028/www.scientific.net/AMR.264-265

Electrodeposition of Tin Using Tin(II) Methanesulfonate from a Mixture of Ionic Liquid and Methane Sulfonic Acid

doi:10.4028/www.scientific.net/AMR.264-265.1462

Diffusion Coefficient of Tin(II) Methanesulfonate in Ionic Liquid and Methane Sulfonic Acid (MSA) Solvent

KOK KEE YANG, M.R. MAHMOUDIAN, MEHDI EBADI, HUN LEE KOAY,
and WAN JEFFREY BASIRUN

Voltammetry and chronoamperometry for the electrodeposition of tin from Tin(II) methane sulfonate mixed with ionic liquid and methane sulfonic acid at room temperature was studied. Cyclic voltammetry shows redox waves of Tin(II), which proves that the electrodeposition of tin from Tin(II) methane sulfonate is a diffusion-controlled process. The diffusion coefficient of Tin(II) ions in the solvent mixture showed good agreement from both voltammetry and chronoamperometry results. The diffusion coefficient of Tin(II) in the mixture was much smaller than in aqueous solution, and it depends on the anion of the ionic liquid.

DOI: 10.1007/s11663-011-9560-z

© The Minerals, Metals & Materials Society and ASM International 2011

I. INTRODUCTION

TIN and alloys of tin has been electrodeposited from electrolytes of Tin(II) salts such as the fluoroborate and sulfate. Both the anions have certain advantages over the other, but a new Tin(II) salt, which is based on methanesulfonate anion, is gathering interest because of its environmental low toxicity and its low oxidation rate to stannic ions.^[1] The use of ionic liquid in smaller laboratory-scale electrodeposition was proven to be an effective solvent to reduce the effect of hydrogen evolution reaction; thus, essentially it is crack free and better quality. In addition, reduced overall material and power consumption were reported.^[2]

Wilkes and Zaworotko^[3] reported the first moisture-stable, imidazolium-based ionic liquid with tetrafluoroborate or hexafluorophosphate as anions. Later, several ionic liquids based on 1-ethyl-3-methylimidazolium, 1,2-dimethyl-3-propylimidazolium, or 1-butyl-1-methylpyrrolidinium cations with tetrafluoroborate (BF_4^-), tri-fluoro-methanesulfonate (CF_3SO_3^-), bis (trifluoromethanesulfonyl)imide [$(\text{CF}_3\text{SO}_2)_2\text{N}^-$], and tris (tri fluoro methanesulfonyl) methide [$(\text{CF}_3\text{SO}_2)_3\text{C}^-$] anions received much attention because of low reactivity against moisture.^[4,5]

Among the studies carried out on the electrodeposition of Tin(II) in ionic liquids includes the publication by Hussey and Xe,^[6] who used AlCl_3 mixed in a 1-methyl-3-ethyl imidazolium chloride melt. Later, Yang *et al.*^[7] reported the alloy electrodeposition of tin and antimony in 1-ethyl-3-methylimidazolium

tetrafluoroborate, and Tachikawa *et al.*^[8] reported the electrodeposition of Tin(II) using a hydrophobic ionic liquid, 1-*n*-butyl-1-methylpyrrolidinium bis (trifluoromethylsulfonyl) imide.

In view of the advantages of the air and water stable ionic liquids, we report the voltammetry and chronoamperometry of tin electrodeposition from a mixture of an ionic liquid, 1-butyl-1-methyl-pyrrolidinium trifluoro- methanesulfonate (BMPOTF) with Tin(II) methane sulfonate in methane sulfonic acid (MSA).

II. EXPERIMENTAL

The water and air stable ionic liquid BMPOTF (>98 pct purity) and tin methanesulfonate ($\text{CH}_3\text{SO}_3\text{Sn}$) were purchased from Merck (Whitehouse Station, NJ). The experiments were carried out using a conventional three-electrode cell. The working electrode was a copper rod with diameter of 4 mm with an exposed area of 0.1257 cm^2 . Before each experiment, the copper rod subjected to wet grinding with a SiC-type abrasive paper grade 100, 1000, and 1200 to obtain a smooth finish, followed by cleaning for 10 minutes in ethanol and then descaling with 10-pct MSA (10 pct) and final rinsing in deionized water. The counterelectrode was a platinum wire with 4 cm length and 0.1 mm diameter. The working electrode potentials reported herein were measured vs a saturated Ag/AgCl reference electrode. Oxygen was eliminated from the system by bubbling nitrogen gas through the solution for 3 minutes prior to each experiment. The weight percentage composition of the Tin(II) methane sulfonate used in this study is given in Table I.

All experiments were conducted at room temperature, $302 \text{ K} \pm 1 \text{ K}$ ($29^\circ\text{C} \pm 1^\circ\text{C}$) in a mixture of BMPOTF ionic liquid and MSA where tin methane sulfonate ($\text{CH}_3\text{SO}_3\text{Sn}$) was diluted, in the desired amounts with pure MSA and ionic liquid with a ratio of 1:1, to obtain finally a solution of 0.1 M to 0.5 M Tin(II) methane

KOK KEE YANG, M.Sc. Student, M.R. MAHMOUDIAN and MEHDI EBADI, PhD Students, and WAN JEFFREY BASIRUN, Academic/Researcher, are with the Department of Chemistry, University of Malaya, Kuala Lumpur 50603, Malaysia. Contact e-mail: wjeffreyb@yahoo.com HUN LEE KOAY, PhD Student, is with the Department of Material Science and Engineering, Malaysia University of Science and Technology, 47301 Petaling Jaya, Selangor, Malaysia.

Manuscript submitted March 4, 2011.

Article published online August 10, 2011.

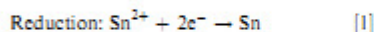
sulfonate. The electrochemical experiments were carried out using an Autolab PGSTAT 30 Potentiostat/Galvanostat (Eco Chemie, Utrecht, Netherlands). No organic additives were mixed in the solutions in this study. The scanning electron microscope (SEM) used in the surface studies of these deposits was Philips XL 30 (Philips, Amsterdam, The Netherlands), and the energy dispersive X-ray analysis (EDX) machine used was the EDAX Analyzer Genesis (EDAX Inc., Mahwah, NJ).

III. RESULTS AND DISCUSSION

A. Voltammetry

Figure 1 is the cyclic voltammetry of $(\text{CH}_3\text{SO}_3)_2\text{Sn}$ in a mixture in BMPOTF and MSA solvent with different tin concentrations. The cyclic voltammograms were swept from 0 to -1.0 V vs Ag/AgCl at a potential sweep rate of 0.05 V s^{-1} throughout the experiments. The increase of Tin(II) concentration produces a stronger reduction and oxidation peak. A single reduction and oxidation peak were observed in the cyclic voltammetry of Tin(II) deposition and dissolution at a copper substrate, where these peaks were absent when done with the ionic liquid and MSA solvent without the $(\text{CH}_3\text{SO}_3)_2\text{Sn}$.

The forward scan from -0.5 V to -1.0 V vs Ag-AgCl shows a reduction peak for Tin(II) deposition corresponding to a two-electron step



With the reverse potential sweep from -0.5 V to 0.0 V vs Ag-AgCl, a single stripping peak was observed confirming the two-electron oxidation of metallic to stannous ions via the reverse reaction

Table I. Composition of Tin(II) Methane Sulfonate		
Component	Weight Percent (pct)	
Tin(II) methane sulfonate, $(\text{CH}_3\text{SO}_3)_2\text{Sn}$	55	
Water, H_2O	30	
Methane sulfonic acid, $\text{CH}_3\text{SO}_3\text{H}$	15	

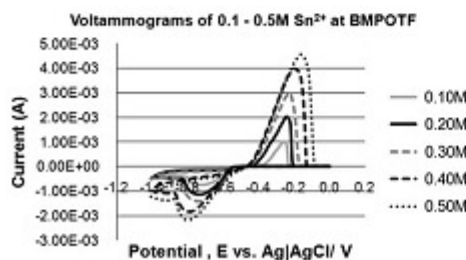
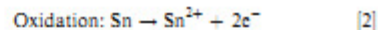


Fig. 1—Cyclic voltammogram at 0.05 V s^{-1} for solution of $(\text{CH}_3\text{SO}_3)_2\text{Sn}$.



The relation between the peak current density J_p and the concentration of the electroactive species in solution can be given by the Randles-Sevcik equation^[9]

$$J_p = 2.69 \times 10^5 Z^{1/2} D^{1/2} v^{1/2} c \quad [3]$$

where J_p is the peak current density, Z is the number of electrons involved in the electrode process, D is the diffusion coefficient of stannous ions, v is the potential sweep rate, and c is the concentration of Tin(II) ions.

From the graph in Figure 2, the diffusion coefficient of stannous ions in BMPOTF ionic liquid is approximately $2.2 \times 10^{-7} \text{ cm}^2 \text{ s}^{-1}$.

B. Chronoamperometry

Figure 3 shows chronoamperometry of current I/A vs time/s, stepped at -0.9 V for 0.1 M to 0.5 M of Tin(II). For chronoamperometry, the relation between the current I/A and the time/s can be given by the Cottrell equation^[9]

$$I = \frac{nFA D^{1/2} c}{\pi^{1/2} t^{1/2}} \quad [4]$$

where n is the number of electrons involved in the electrode process, A is the area of electrode, D is the diffusion coefficient of Tin(II) ions, F is the Faraday constant, t is the time in s, and c is the concentration of Tin(II) ions.

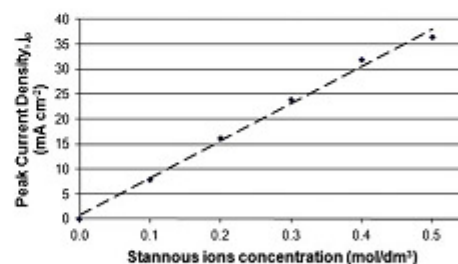


Fig. 2—Effect of Tin(II) concentration on peak current density.

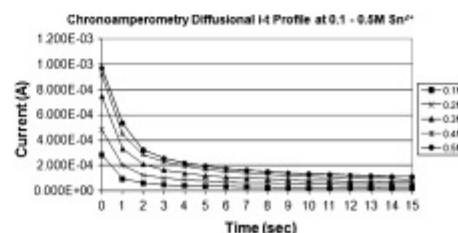


Fig. 3—Chronoamperometry of current I/A vs time/s, stepped at -0.9 V vs Ag/AgCl at various concentrations.

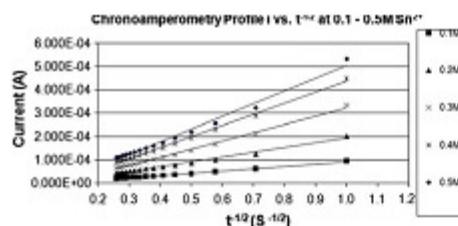


Fig. 4—Cottrell plots, I/A vs $t^{1/2}$ for chronoamperometry in Fig. 3, stepped to -0.9 V vs Ag/AgCl.

The results in Figure 2 show clearly that the electroreduction of Tin(II) in the mixture of ionic liquid and MSA solvent is diffusion controlled, which permits the Diffusion constant to be calculated from Cottrell plots in Figure 4. The average diffusion coefficient calculated for all concentration used within 0.1 to 0.5 M was $2.5 \times 10^{-7} \text{ cm}^2 \text{ s}^{-1}$ and is comparable with the voltammetry experiments in Section III-C.

C. Diffusion Coefficients

There are not many reports about Tin(II) diffusion in ionic liquids, and Table II gives the diffusion coefficients of Tin(II) in various types of ionic liquids.

The relation of the diffusion coefficient with the viscosity and the dynamic radius of the diffusing species can be explained by the Stoke-Einstein equation

$$D = \frac{KT}{6\pi\eta r}$$

where K is the Boltzmann constant, T is Kelvin temperature, η is viscosity of the solvent, and r is the dynamic radius of the diffusing species.

Hussey and Xe^[6] found that the Tin(II) exists as SnCl_4^{2-} in AlCl_3 with 1-methyl-3-ethyl imidazolium chloride ionic liquid, and the lesser values of the diffusion coefficient compared with aqueous solvent was a result of the increased viscosity of the ionic liquid. They also suggest that there is some degree of association between the Tin(II) with chloroaluminate ions such as AlCl_4^- and Al_2Cl_7^- , which contribute to the low value of the diffusion coefficient. In addition, the dynamic radius of the Tin(II) in AlCl_3 with 1-methyl-3-ethyl imidazolium chloride ionic liquid is larger than the dynamic radius of the Tin(II) ions in aqueous solution, and it decreases the diffusion coefficient according to the Stoke-Einstein equation.

Yang *et al.*^[7] used tetrafluoroborate, BF_4^- -based ionic liquid, where the diffusion coefficient was higher than calculated from the chloroaluminate ionic liquid by Hussey and Xe^[6]. It can be observed that the smaller Tin(II) tetrafluoroborate species will contribute to a slightly higher diffusion coefficient value for the Tin(II) species.

Studies using trifluoromethylsulfonyl imide ionic liquids from Tachikawa *et al.*^[8] and this work using trifluoromethylsulfonate ionic liquid gave a smaller

diffusion coefficient for the Tin(II) species. It can be suggested that the complexation between the Tin(II) with trifluoromethylsulfonate and trifluoromethylsulfonyl imide, which is larger than the chloride ion and the tetrafluoroborate ion, has increased the radius of the Tin(II) species in solution. This contributes to the lower diffusion coefficient compared with the chloride and tetrafluoroborate based ionic liquids from the works of Hussey and Xe^[6] and Yang *et al.*^[7] It can also be said that the diffusion coefficient from this work using trifluoromethylsulfonate ionic liquid has a greater value compared with the trifluoromethylsulfonyl imide,^[8] which is in accordance with larger dynamic radius of the trifluoromethylsulfonyl imide ionic liquid compared with the trifluoromethylsulfonate ionic liquid.

From Table II, the electroreduction of Tin(II) from aqueous solution gave a higher diffusion coefficient^[1] than all other diffusion coefficients in the ionic liquid solution. The complexation of the Tin(II) ion in aqueous solution involves the smaller water molecules compared with the larger anions in the ionic liquids. In addition, the viscosity of aqueous solutions is lower than the viscosity of ionic liquids. Table II provides a decreasing diffusion coefficient with increasing complex anion size when descending the table, which suggests that some level of complexation between the anion of the ionic liquid and the Tin(II) has taken place during electrodeposition.

D. Bulk Electrodeposition

Electroplating on copper surface (2 cm \times 2 cm) was carried out to estimate the plating current efficiency for tin electrodeposition from Tin(II) methanesulfonate dissolved in BMPOTF with MSA as the solvent.

Scanning electron microscopy and EDX were used to examine the surface morphology and analyze the elemental compositions of the electrodeposits. The current efficiency is defined as the proportion of the current that is used in the specified reaction: The unused portion in this process is considered a waste. Thus, the current efficiency for metal deposition ϕ is defined as the ratio of the experimental mass of electrodeposition to the theoretical mass of electrodeposition. Thus,

$$\phi(\text{pct}) = \frac{\text{Mass}(\text{experimental})}{\text{Mass}(\text{theoretical})} \times 100 \quad [5]$$

The efficiencies are not always 100 pct as hydrogen evolution, oxygen reduction, and solvent decomposition can occur at the cathode.^[6,9] The Faraday's law

$$Q = I \times t \quad [6]$$

$$m = \frac{QM}{Fn} \quad [7]$$

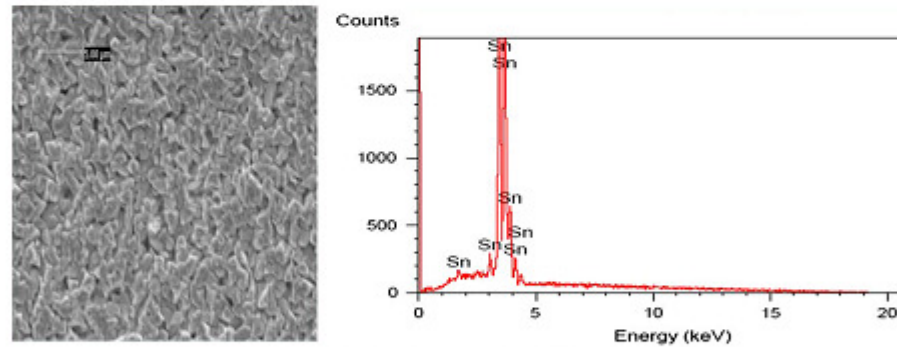
where m is the theoretical mass of the substance produced at the electrode (in grams), Q is the total electric charge that passed through the solution (in coulombs), n is the number of the electron transferred in the electron transfer step, $F = 96,485 \text{ C mol}^{-1}$ is

Table II. Comparison of Tin(II) Diffusion Coefficients

Reference	Solvent	Complexing Anion	Tin(II) Diffusion Coefficient ($D/\text{cm}^2 \text{ s}^{-1}$)
1	Aqueous	Water	6.5×10^{-6}
6	1-ethyl-3-methylimidazolium tetrafluoroborate	BF_4^-	6.1×10^{-7}
8	AlCl_3 with 1-methyl-3-ethyl imidazolium chloride	Predominantly Cl^- with AlCl_4^-	5.3×10^{-7}
2	ZnCl_2 with 1-methyl-3-ethyl imidazolium chloride	Predominantly Cl^- with ZnCl_4^{2-}	4.6×10^{-7}
This work	1-butyl-1-methylpyrrolidinium trifluoro-methanesulfonate	CF_3SO_3^-	2.3×10^{-7}
7	1-n-butyl-1-methylpyrrolidinium bis (trifluoromethylsulfonyl) imide	$[(\text{CF}_3\text{SO}_2)_2\text{N}]^-$	1.0×10^{-7}

Table III. Current Efficiency of Tin Electrodeposition Obtained at Different Tin(II) Concentration

Current Density (A dm^{-2})	Tin(II) Concentration (M)				
	0.1	0.2	0.3	0.4	0.5
1.0	99.58	99.58	98.90	98.23	94.84
2.0	99.92	98.23	98.23	97.89	87.73
3.0	99.81	96.42	98.00	97.78	81.07
4.0	99.24	98.74	97.89	97.04	72.65
5.0	99.58	98.63	97.01	96.87	66.25
6.0	99.70	97.66	96.87	95.97	61.65
7.0	98.71	97.55	96.29	94.55	58.26

0.1 M Tin Methane Sulfonate + Ionic Liquid, 1 A dm^{-2} Fig. 5—SEM (3500 times magnification) and EDX spectrum of tin electrodeposited from 0.1 M Tin(II) methane sulfonate solution at 1 A dm^{-2} .

Faraday's constant, and M is the molar mass of tin (g mol^{-1}).

Table III shows the current efficiencies obtained from experiments using current densities from 1 A dm^{-2} (ASD) to 7 ASD for various concentrations of Tin(II) from 0.1 M to 0.5 M in ionic liquids solutions.

From the results, increasing current densities for higher concentrations of Tin(II) such as 0.4 M and 0.5 M gave decreasing current efficiencies for tin deposition. From the solution preparation, 0.5 M has the highest water content, and at these conditions, the

hydrogen evolution reaction from the presence of water becomes prominent and decreases the current efficiency for the tin deposition. The deposits became dull and less reflecting in appearance because of the porous nature of the surface as can be observed in Figure 8.

Scanning electron microscopy from Figures 5 through 8 at 3500 times magnification reveal that the deposits became less compact, less dense, and more porous for higher current densities and higher concentrations of Tin(II). The poor quality of deposits with increasing amount of Tin(II) concentration is expected as higher

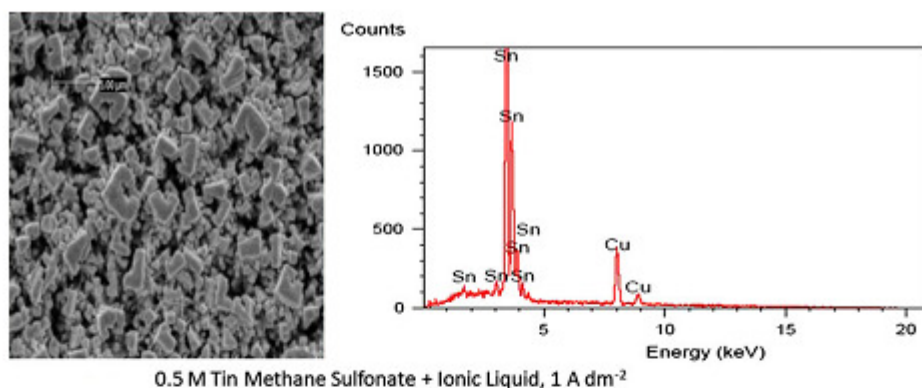


Fig. 6—SEM (3500 times magnification) and EDX spectrum of tin electrodeposited from 0.5 M Tin(II) methane sulfonate solution at 1 A dm⁻².

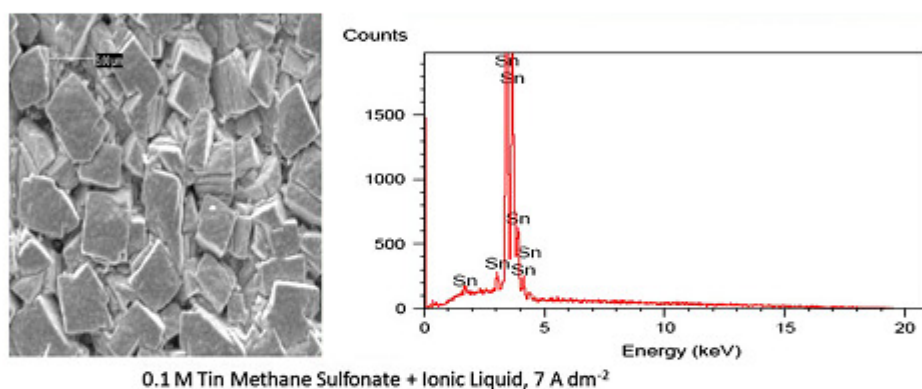


Fig. 7—SEM (3500 times magnification) and EDX spectrum of tin electrodeposited from 0.1 M Tin(II) methane sulfonate solution at 7 A dm⁻².

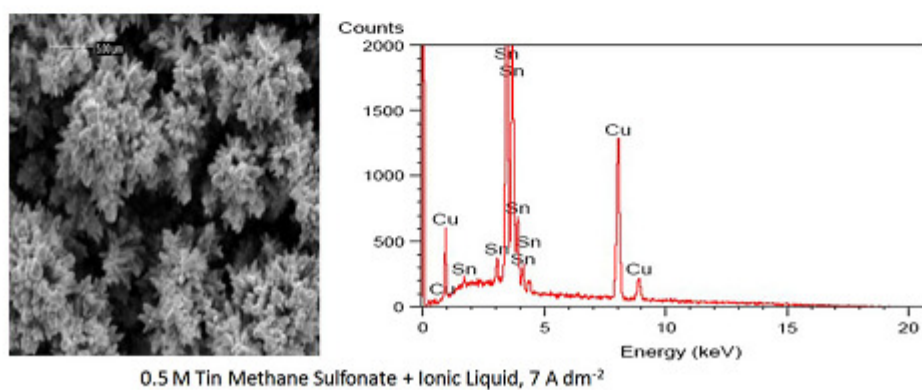


Fig. 8—SEM (3500 times magnification) and EDX spectrum of tin electrodeposited from 0.5 M Tin(II) methane sulfonate solution at 7 A dm⁻².

concentrations of Tin(II) prepared from the stock solution contained slightly more percentage of water compared with lower Tin(II) concentrations, thus facilitating the hydrogen evolution process. As for the poor quality of deposit with increasing current density, the increase in current density will result in the increase toward negative potentials where the hydrogen evolution reaction and solvent decomposition are more dominant than metal electrodeposition. This behavior is quite similar with previous works involving platinum,^[10,11] nickel^[12,13] and Nickel-Cobalt alloy.^[14,15] The poor quality and porous nature of the deposits can be also observed in the EDX results in Figures 6 and 8. The copper element was present in the EDX spectrum at the tin-plated surface when analyzed under 20 keV EDX as shown in Figures 6 and 8 when done with higher current densities of 7 A dm⁻² and higher Tin(II) concentration of 0.5 M of Tin(II), which shows copper peaks from the copper substrate, because of the porous nature of the deposits.

IV. CONCLUSIONS

The electrodeposition of tin using Tin(II) methane sulfonate salt in the solvent mixture of water and air stable ionic liquid 1-butyl-1-methyl-pyrrolidinium trifluoromethane sulfonate and MSA showed that the electroreduction is diffusion controlled. From the experiments of cyclic voltammetry and chronoamperometry, the diffusion coefficient was found to have a value of $2.2 \times 10^{-7} \text{ cm}^2 \text{ s}^{-1}$ and $2.5 \times 10^{-7} \text{ cm}^2 \text{ s}^{-1}$, respectively. The values of the diffusion coefficient in ionic liquids are smaller because of the viscosity of the ionic

liquid and the larger size of the dynamic radius in the solution.

REFERENCES

1. C.T.J. Low and F.C. Walsh: *Electrochim. Acta*, 2008, vol. 53 (16), pp. 5280-86.
2. J.F. Huang and I.W. Sun: *J. Electrochem. Soc.*, 2003, vol. 150 (6), pp. E229-E306.
3. J.S. Wilkes and M.J. Zaworotko: *J. Chem. Soc., Chem. Comm.*, 1992, (13), pp. 965-67.
4. S. Zein El Abedin, E.M. Moustafa, R. Hempelmann, H. Natter, and F. Endres: *Electrochem. Comm.*, 2005, vol. 7 (11), pp. 1111-16.
5. A.P. Abbott, I. Dalrymple, F. Endres, and D.R. MacFarlane: *Electrodeposition from Ionic Liquids*, 1st ed., A.P. Abbott and D.R. MacFarlane, eds., Wiley-VCH, Weinheim, Germany, 2008, pp. 1-12.
6. C.L. Hussey and X.H. Xe: *J. Electrochem. Soc.*, 1993, vol. 140 (3), pp. 618-26.
7. W.Z. Yang, H. Chang, Y.M. Tang, J.T. Wang, and Y.X. Shi: *J. App. Electrochem.*, 2008, vol. 38, pp. 537-42.
8. N. Tachikawa, N. Serizawa, Y. Katayama, and T. Miura: *Electrochim. Acta*, 2008, vol. 53, pp. 6530-34.
9. A.J. Bard and L.R. Faulkner: *Electrochemical Methods: Fundamentals and Applications*, 2nd ed., Wiley, New York, NY, 2000, pp. 163, 231.
10. W.J. Basirun, D. Pletcher, and A. Saraby Reintjes: *J. App. Electrochem.*, 1996, vol. 26, pp. 873-80.
11. W.J. Basirun and D. Pletcher: *J. App. Electrochem.*, 1998, vol. 28, pp. 167-72.
12. M. Ebadi, W.J. Basirun, and Y. Alias: *Asian J. Chem.*, 2009, vol. 21 (8), pp. 6343-53.
13. M. Ebadi, W.J. Basirun, and Y. Alias: *Asian J. Chem.*, 2009, vol. 21 (9), pp. 7354-62.
14. M. Ebadi, W.J. Basirun, Y. Alias, and M.R. Mahmoudian: *Chem. Central. J.*, 2010, vol. 4, p. 14.
15. M. Ebadi, W.J. Basirun, and Y. Alias: *J. Chem. Sci.*, 2010, vol. 122 (2), pp. 1-7.